Major Styles of Mineralization and Hydrothermal Alteration and Related Solid- and Aqueous-Phase Geochemical Signatures

By Dana J. Bove, M. Alisa Mast, J. Bradley Dalton, Winfield G. Wright, and Douglas B. Yager

Chapter E3 of
Integrated Investigations of Environmental Effects of Historical Mining in the Animas River Watershed, San Juan County, Colorado
Edited by Stanley E. Church, Paul von Guerard, and Susan E. Finger

Professional Paper 1651

U.S. Department of the Interior
U.S. Geological Survey

Contents

Figures

Tables

Chapter E3
Major Styles of Mineralization and Hydrothermal Alteration and Related Solid- and Aqueous-Phase Geochemical Signatures

By Dana J. Bove, M. Alisa Mast, J. Bradley Dalton, Winfield G. Wright, and Douglas B. Yager

Abstract

The Animas River watershed study area was subdivided into five discrete areas that represent the major styles and ages of mineralization and alteration in this area: (1) Mount Moly area—26–25 Ma molybdenum–copper porphyry mineralization, (2) Red Mountains and (3) Ohio Peak–Anvil Mountain areas (OPAM)—sites of 23-Ma acid-sulfate mineralization, (4) Eureka Graben and (5) South Silverton areas—18–10 Ma northeast- and northwest-trending polymetallic veins, respectively. Each of these five areas was affected by calcite-rich, regional propylitic alteration that predated the mineralizing episodes by 5–15 million years.

Combined geologic and aqueous geochemical studies within these five areas have led to a better understanding of the major sources of anthropogenic and natural acidity and metals in the watershed. Detailed geologic mapping has shown how the degree of bedrock alteration controls the variability of water composition within each of these mineralized source areas. Aqueous geochemical signatures, quite distinctive in some of these areas, can generally be explained by the varying geologic and mineralogic characteristics. Some of the more diagnostic geochemical signatures have been useful in our identifying the origin of unidentified discharge distal to these sources.

Introduction

The Animas River watershed study area is characterized by several highly contrasting styles and ages of mineralization and related hydrothermal alteration. As suggested in Plumlee and others (1999), the geology and mineralogy of each of these types of mineralized or altered rocks can exert an important and predictable control on the environmental signatures that result from mining as well as on the signatures of natural processes. Important geologic features, such as the acid-producing or acid-neutralizing potential of minerals in deposits and related alteration assemblages, influence the chemical response of the deposits to weathering. The mineralogy and trace-element compositions of the deposits and the altered wallrocks also importantly affect the chemical and physical response to weathering and environmental dispersion (Plumlee and Logsdon, 1999; Plumlee, 1999; Plumlee and others, 1999). That such effects occur is confirmed by integrated geologic and aqueous geochemical studies conducted in other parts of the San Juan Mountains (Miller and McHugh, 1994; Bove and others, 1996; Kirkham and others, 1995; Miller, 1999; Bove and Knepper, 2000), which document how different lithologies or types of mineralization and related zoned alteration sequences produce relatively distinct aqueous geochemical signatures. These studies were grounded in an understanding of the geologic setting, structural controls, mineralogy and geochemistry of the deposits and mine wastes, and the character of the hydrothermal alteration zones. Thus, using these studies as a model, we chose a number of subbasins representative of the major styles and ages of mineralization in the study area for integrated geologic and aqueous geochemical studies.

Details of the ore deposits and mineralization history were obtained from many excellent sources covering this classic area (for example, Ransome, 1901; Kelley, 1946; Varnes, 1963; Burbank and Luedke, 1969; Casadevall and Ohmoto, 1977; Langston, 1978; Ringrose, 1982). Although information regarding the distribution of hydrothermal alteration assemblages is available in some areas (Burbank and Luedke, 1969; Fisher and Leedy, 1973; Casadevall and Ohmoto, 1977), the level of detail was generally insufficient to clarify specific water-rock interactions. For this reason, we carefully mapped alteration assemblages and important structural features in several key mineralized areas by field and by remote methods (Airborne Visible/Infrared Imaging Spectrometer or AVIRIS; Dalton and others, this volume, Chapter E2); a detailed hydrothermal alteration map was also compiled for the entire watershed. Mineralogic and geochemical data from altered rocks, mineralized samples, and mine dumps were compiled to characterize the signatures of source material and to assess the dispersion of associated elements into surface water.

The aqueous geochemical data utilized in this report are part of a broader study (Mast and others, this volume, Chapter E7) that characterized the water quality from non-anthropogenic sources in the entire study area. As part of that study, 221 streams and water from mines were sampled from 1995 to 1999 in the Animas River watershed study area (Mast and others, this volume; Mast, Evans, and others, 2000).

The structure of this report reflects two of the major objectives of this study: (1) to provide the framework for our understanding of the complex character of mineralization, hydrothermal alteration, and mining activity in the study area, and (2) utilization of this framework data, wherever possible, to examine the chemical and physical responses to weathering of these variably altered and mineralized rocks and multiple types of mineral deposits. Some of the most detailed investigations for this study were conducted in the Red Mountains and OPAM acid-sulfate areas (fig. 1), where contributions of acidity and metals to the watershed from both mined and unmined sources are substantial. Although our work in these areas focused on water-quality issues, it has also led to a better understanding of the genesis, character, and geometry of these massive and complex acid-sulfate systems.

The integration of the geologic studies with results of the aqueous geochemical data has produced these results:

- Definition of geochemical signatures of both solid and aqueous phases within the major mineralized areas in the watershed
- Understanding of the relationship between specific alteration assemblages, other structural and mineralogic features, and local water chemistry
- Effective comparison of the compositional signatures of mining versus non-mining-related water within each mineralized area
- Better overall understanding of the types of geologic and hydrothermal systems in the watershed
- Source of information for geoenvironmental comparison to other large acid-sulfate systems of different genesis and climatic setting.

Methods

The boundaries of the five mineralized areas discussed in this report (fig. 1) were delineated based on the distribution and zoning of hydrothermally altered rock, the age and type of mineralization and hydrothermal alteration, and trends or patterns of veins and faults. These areas were differentiated in order to characterize and contrast the geochemical signatures of solids and waters in a variety of mineralized areas. In this report, we assigned various geochemical data to one of the mineralized areas if they were collected within the boundary of that area.

Hydrothermal alteration assemblage maps were compiled from the following sources: (1) detailed field mapping (1:12,000 scale) and associated X-ray diffraction (XRD) analysis, (2) mineral maps by remote spectroscopy (AVIRIS) (Dalton and others, this volume), and (3) mapping by aerial photography at a scale of 1:24,000. Mapping by Ringrose (1982) was also used in this compilation. Field and remote spectroscopic identification of mineral phases was confirmed by whole rock XRD. XRD studies of more than 200 samples were performed using standard clay XRD techniques (Moore and Reynolds, 1989). These results are in the relational database (Sole and others, this volume, Chapter G). We obtained major- and minor-element analyses of discrete mineral phases using a JEOL 8900 electron microprobe at the U.S. Geological Survey (USGS), Denver, Colo. Sample analysis was performed on polished thin sections with machine conditions of 15 kV accelerating voltage with a 15–20 μm (micrometer) beam width. The analyses were corrected using on-line ZAF correction procedures (Goldstein and others, 1992). Replicate analyses of secondary standards indicated a relative analytical precision of better than ±1 percent (1 σ) for major elements. For trace elements, analytical error is less than that for counting statistics where counting error is equal to one sigma or ± the square root of *n*.

One hundred twenty-six samples of variably altered rock and mineralized material were analyzed for 40 elements by inductively coupled plasma–atomic emission spectroscopy (ICP-AES) using the procedures of Briggs (1996). In addition, 25 rock samples and several mineral separates were analyzed by inductively coupled plasma–mass spectroscopy (ICP-MS) (Lamothe and others, 1999) at USGS laboratories in Denver, Colo. These analytical results are in the relational database (Sole and others, this volume). Analytical data for samples of waste rock from mine dumps discussed in this report were part of a larger data set presented by Fey and others (2000); analytical methods and sampling procedures are discussed in that report, and the data and field relationships are discussed in Nash and Fey (this volume, Chapter E6). All rock and mine dump geochemical data collected by the USGS during the course of the study (Sole and others, this volume) were included in this report. However, mill tailings were excluded from the mine dump data set. Several additional geochemical data sets with well-documented methodologies were also used in this study. These data include 12 outcrop samples (Ringrose, 1982), 153 drill core splits (McCusker, 1982), and 15 mine dump composites (McCusker, 1983) from the Mount Moly area (fig. 1), and 82 surface rock samples (Langston, 1978) from the Eureka Graben area (fig. 1). Two of these non-USGS data sets contain mostly metals concentration data; analyses of major elements were generally not conducted. Where both major ion and metal concentration data are available, they will be evaluated in the related discussions. We grouped rock geochemical data according to alteration assemblage on the basis of field mapping and mineralogical descriptions.

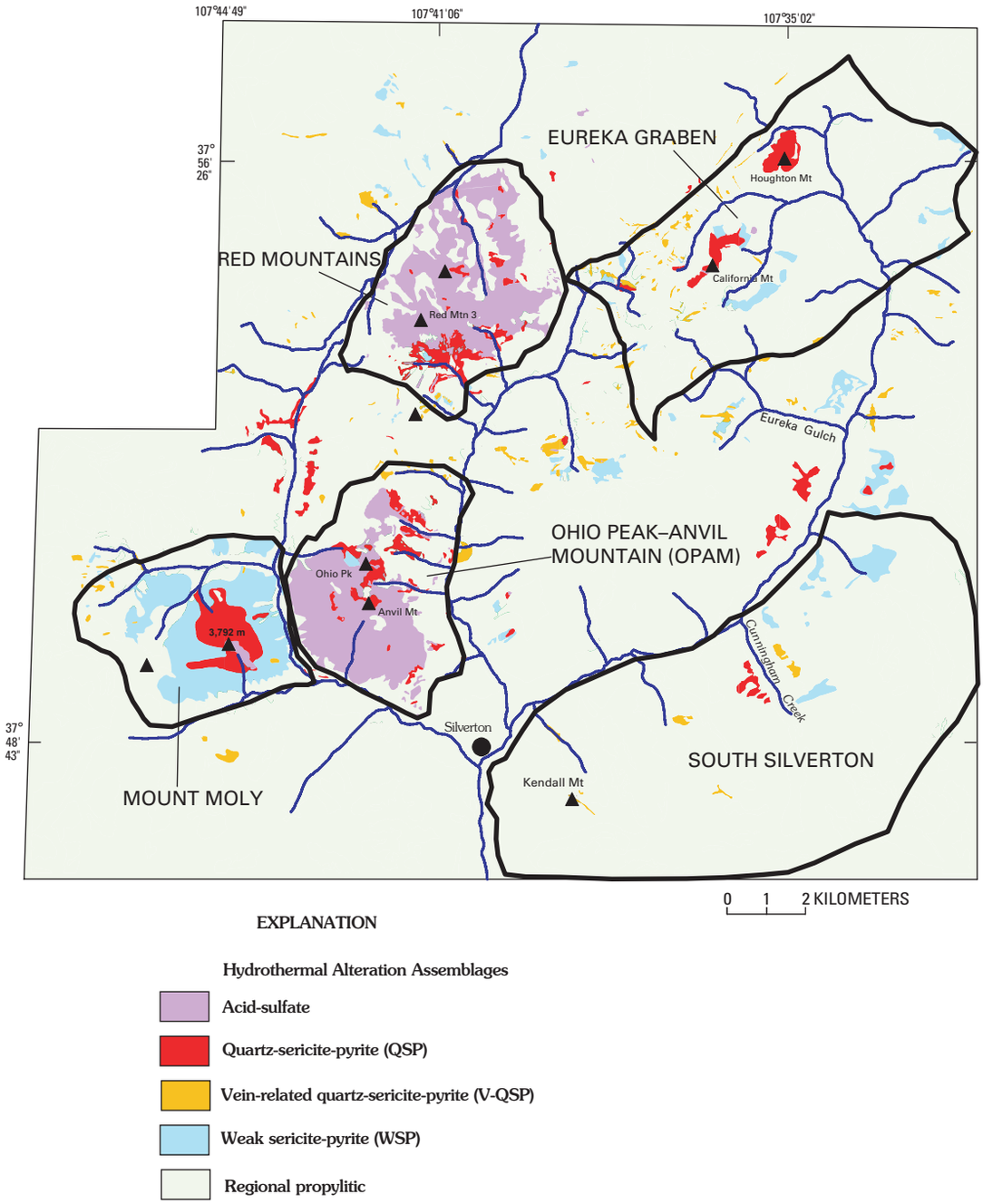

Figure 1. Five areas that represent major styles and ages of mineralization and alteration in the study area. Generalized map of hydrothermal alteration assemblages is superimposed. Solid triangle, prominent peak. Mount Moly is an informal name used herein to identify the area centered on peak 3,792 m.

Minerals analyzed for stable isotopes were separated by various physical and chemical methods and analyzed in the USGS laboratory of R.O. Rye in Denver, Colo. Analytical methods used in these various analyses are described in Wasserman and others (1992).

Water-quality data were collected from 75 mine and 146 "background" sites during summer low-flow conditions (Mast and others, this volume). The term "background" as used in this report refers to sites where dissolved constituents in surface water are derived from weathering processes rather than mining-related sources. Classification of waters into mining-affected and background categories was based on criteria discussed in Mast and others (this volume). According to this classification scheme, mining-affected sites fall under categories III and IV, whereas background sites are classified as category I or II. Background sites were also grouped by the dominant alteration type upstream of the sampling site ("end-member waters") on the basis of alteration mapping

of the watershed. Samples from localities draining mixtures of alteration types ("mixed waters") were not included in the statistical tabulations of these end-member waters. In addition, sites that drain end-member alteration assemblages but that are also downstream of large mineralized or vein structures (unmined), were also placed into separate groups. The locations of streams, springs, and mine sites, along with related chemical results, are in the database (Sole and others, this volume); sampling and analytical methods appear in Mast and others (this volume). All geochemical data, with the exception of water-quality data from the Red Mountains area (fig. 1), fall within the boundaries of the Animas River watershed study area (fig. 2 in von Guerard and others, this volume, Chapter B). Ten mine and background water samples included in the Red Mountains data set (30 total samples) were collected less than 0.5 km outside the study area (Bove and Knepper, 2001; Neubert, 2000). These data were included to better represent the geochemical signature of waters draining acid-sulfate altered rock, which underlies a large percentage of the Red Mountains mineralized area. Only three such waters were located and sampled within the study area by the USGS during the course of this study (Mast, Evans, and others, 2000).

Statistical comparison of water and solids geochemical data was performed using the nonparametric Wilcoxon Signed-Ranks tests. Concentrations or abundances were considered statistically different if values of α were ≤ 0.01.

Outline of Major Styles and Ages of Mineralization and Hydrothermal Alteration within the Animas River Watershed Study Area

Most mineralization as well as associated hydrothermal alteration in the study area was temporally and genetically associated with three major episodes of high-level magmatism between about 27 and 10 Ma (Bove and others, 2001). These events postdated the collapse of the San Juan, Uncompahgre, and Silverton calderas (28–27 Ma) (see Yager and Bove, this volume, Chapter E1, pl. 1) by about 5–15 Ma (Lipman and others, 1976; Bove and others, 2001; Yager and Bove, this volume). Caldera collapse and resurgent doming created a favorable structural environment for later mineralization and hydrothermal activity. In general, deuteric activity was temporally associated with caldera development and caused regional propylitization, which characterizes a major portion of the study area. Rocks affected by this alteration type contain abundant calcite, epidote, and chlorite, which contribute to the intrinsic acid-neutralizing capacity of this alteration assemblage (Desborough and others, 1998; Bove and others, 2000).

Because of the large size of the study area, we have delineated five major areas that represent the major styles and ages of mineralization and alteration as just outlined. As shown in figure 1, these areas include (1) Mount Moly[1]—26–25 Ma molybdenum-copper porphyry mineralization, (2) Red Mountains—23 Ma acid-sulfate system, (3) Ohio Peak–Anvil Mountain—23 Ma acid-sulfate mineralization, (4) Eureka Graben—northeast-trending polymetallic veins (<18 Ma), and (5) South Silverton—north- to northwest-trending polymetallic veins (<18 Ma). Owing to the widespread nature of the earlier formed regional propylitic event, we discuss the characteristics of this related assemblage as it occurs throughout the entire study area.

The earliest important mineralizing and related hydrothermal event, at about 26–25 Ma, was related to a large swarm of calc-alkaline intrusions emplaced over a broad region of the western San Juan Mountains (Bove and others, 2001). The Mount Moly area, centered around peak 3,792 m between South and Middle Forks Mineral Creek (fig. 1) is the only known mineralized hydrothermal system of this type and age in the study area.

Remnants of two large acid-sulfate systems are centered in the Red Mountains and Ohio Peak–Anvil Mountain (OPAM) areas (fig. 1). The Red Mountains system encompasses a roughly 22 km^2 area that was host to economically important silver-copper-lead breccia-pipe and fault-hosted mineralization (Burbank and Luedke, 1969; Bove and others, 2000). The OPAM system (21 km^2), although similar in size and genesis, was generally devoid of economically important mineralization, as shown by the paucity of mines in the area (Church, Mast, and others, this volume, Chapter E5). Both of these altered and mineralized systems formed at 23 Ma and are genetically linked to high-level dacite porphyry intrusions.

Economically important, post-18 Ma vein mineralization in the western San Juan Mountains is closely associated with intrusion of high-silica alkali rhyolite (Lipman and others, 1973; Bartos, 1993). Veins are mostly a polymetallic variety (silver, lead, zinc, copper, ±gold) and formed as fracture- or fissure-fillings. The veins within the San Juan and inner nested Silverton calderas are either concentric or radial to the ring fracture zone, as in the South Silverton area (fig. 1) or trend parallel to graben faults related to resurgent doming of the San Juan–Uncompahgre calderas (for example, the Eureka Graben area) (Burbank and Luedke, 1969). Zones of hydrothermally altered rock related to the veins consist of narrow envelopes that are superimposed over regional propylitically altered rock (Ransome, 1901; Burbank and Luedke, 1969).

Because these five major mineralized areas cover only a portion of the study area, some mineralized features or mineral occurrences are not addressed in this report. However, many of these details can be found in other chapters of this volume, or within the wealth of previously published literature pertaining to the study area.

[1]Mount Moly is the informal name for the peak labeled in figure 1 as 3,792 m. Its use in this report is confined to giving a name to the altered and mineralized area around that peak and does not indicate a formal geographic name for peak 3,792 m.

Pre-Ore Regional Propylitic Alteration Assemblage

Nearly all the rocks in the study area were affected by low-grade regional metamorphism or propylitization resulting from thermal events related to the San Juan–Uncompahgre and later Silverton calderas. The timing of this alteration event is roughly constrained to about 28.2–27.5 Ma—the ages of these respective calderas—and preceded most ore mineralization by 5–15 Ma (Lipman and others, 1976; Bove and others, 2001). The propylitic mineral assemblage contains varying amounts of chlorite, epidote, calcite, and illite, in the presence of fresh to weakly altered primary feldspar crystals. Mass balance studies indicate that elements within the protolith were mostly conserved during the propylitic event with only minor additions of carbon dioxide and water (Burbank and Luedke, 1969; Fisher and Leedy, 1973). However, the common presence of epidote, calcite, and chlorite within fractures indicates that some of the major base chemical elements were locally redistributed.

Field mapping in conjunction with AVIRIS mineral maps (Dalton and others, this volume) indicates that the propylitic alteration assemblage can be broadly differentiated into two major subgroups: (1) chlorite-epidote-calcite dominant (CEC), and (2) chlorite-illite-calcite dominant (CIC). Mapped distributions of these assemblages reflect several important variables including degree of alteration, nature and composition of protolith, and stratigraphic position or relative depth of burial.

CEC Group

Rocks of the CEC propylitic assemblage are characteristically green to pistachio green in color due to the presence of epidote and chlorite. Plagioclase phenocrysts, most notably the calcic cores, show significant replacement by mixtures of epidote, chlorite, calcite, and illite, whereas the groundmass is altered to fine aggregates of these secondary minerals. The appearance of epidote denotes a higher degree of alteration, although calcite instead of epidote can predominate within these altered grains. As shown in table 1, percentages of epidote, chlorite, and calcite within the CEC group vary significantly: total abundances range from about 30 to more than 50 volume percent of the rock. Limited point count studies suggest that although calcite and epidote coexist in some rocks, these minerals more typically occur to the exclusion of one another. Calcite and chlorite can be quite abundant in these rocks (table 1); however, chlorite is almost everywhere present, whereas calcite is locally absent. Percentages of illite, although not determined quantitatively, are estimated to range as high as 10–20 volume percent in some samples. Chemical compositions of these mineral phases are in table 2.

The degree or intensity of propylitic alteration, as noted by systematic variations in the propylitic mineral assemblage, was strongly influenced by lithologic characteristics. For example, lavas of the Burns Member of the Silverton Volcanics were generally affected by a much higher degree of propylitic alteration than were lavas and volcaniclastics of the overlying Henson Member. (For maps showing contacts between Burns and Henson Members, see Burbank and Luedke, 1964; Luedke and Burbank, 1989; Luedke and Burbank, 2000.) This difference in alteration intensity is well illustrated north of the Animas River in the vicinity of Boulder Gulch (fig. 2), where the strong CEC signature of the underlying Burns Member contrasts sharply with the weakly altered (epidote-poor) Henson Member. The lack of epidote in the Henson Member probably represents an incipient phase of the CEC propylitic assemblage. This assemblage is marked by relatively fresh plagioclase, chlorite-illite-leucoxene-altered ferromagnesian minerals, and hematite along microfractures and disseminated after primary opaque grains. A decrease in overall permeability in the upper Henson Member is probably an important factor that influenced this general upward transition from stronger to weaker propylitic assemblages. Such permeability contrasts are documented by studies in the Prospect Gulch area (D.J. Bove and others, unpub. data, 2002) and around the Sunnyside vein system (Langston, 1978), where the movement of hypogene hydrothermal fluids was also similarly restricted at the Burns Member–Henson Member interface. There are many exceptions, however, to this generalized alteration pattern, and localized zones of strongly CEC-altered rock extend into the upper Henson Member. These irregularities likely correspond to areas of increased fracture density or local changes in lithology, which would have effectively increased permeability to propylitic-altering fluids (Bove and others, 2000).

Table 1. Point count data in volume percent for propylitic samples.

[All samples with exception of ODY9735 (CIC group) from CEC group; 500 points counted for each sample]

Sample No.	Epidote	Chlorite	Calcite
HDY9840	2.8	26.3	9.5
IDB7297	26.4	13.5	0
IDB6597	27.6	6.7	0
ODY9735	0	45.6	0.4
ODY9801A	17	25.2	19.2
ODY9801B	18.6	11.3	18.2
ODY9802	13.5	35.3	0.3
SDB34	5.4	35.5	0.7
SDB35A	0.2	21.1	33.7
SDY9752	1.4	33.5	16.9
SDY9754	0.2	32.1	15.8
SDY9626	0	11.9	37
SDY9767	0	8.6	50.6
SDY9837	27	46.9	0.3
SJ98740	41.7	12.7	7.9
SJ9848	21.8	19.4	0

Table 2. Analytical data for various mineral species; values in percent.

[n.d., not determined]

Element	plag[1]	chlorite[1]	diopside[1]	illite[2]	epidote[1]	pyrite[3]	pyrite[4]	alunite[5]	gypsum[6]	calcite[7]	calcite[8]
Na_2O	11.20	0.01	0.37	0.10	0.01	0.00	0.00	4.41	0.01	0.03	0.01
MgO	0.00	18.46	15.26	1.38	0.00	0.00	0.00	0.00	0.02	0.03	0.10
Al_2O_3	19.87	19.76	0.81	33.00	24.13	0.00	0.00	39.03	0.02	0.02	0.04
SiO_2	67.37	28.09	53.36	48.90	37.47	0.00	0.00	0.00	0.00	0.00	0.00
TiO_2	0.01	0.13	0.19	0.33	0.08	0.00	0.00	0.00	0.00	0.00	0.00
FeO	0.11	21.03	8.37	<0.08	10.61	46.40	n.d.	51.60	0.08	0.09	0.04
MnO	0.00	0.73	0.54	0.00	0.75	0.00	0.00	0.00	0.01	0.30	1.42
K_2O	0.19	0.09	0.00	9.32	0.00	0.00	0.00	4.26	0.00	0.00	0.00
CaO	0.81	0.08	21.87	<0.03	21.97	0.00	0.00	0.00	32.20	57.40	57.40
BaO	0.01	0.00	0.02	0.00	0.00	0.00	0.00	0.00	0.00	0.00	0.00
S	0.00	0.00	0.00	0.00	0.00	53.51	n.d.	0.00	0.00	0.00	0.00
SO_2	0.00	0.00	0.00	0.00	0.00	n.d.	n.d.	0.00	0.00	0.00	0.00
Cu	0.00	0.00	0.00	0.00	0.00	0.02	<.01	0.00	0.00	0.00	0.00
Pb	0.00	0.00	0.00	0.00	0.00	0.00	0.04	0.00	0.00	0.00	0.00
Zn	0.00	0.00	0.00	0.00	0.00	0.04	0.05	0.00	0.00	0.00	0.00
As	0.00	0.00	0.00	0.00	0.00	0.01	<.01	0.00	0.00	0.00	0.00
Co	0.00	0.00	0.00	0.00	0.00	0.06	<.01	0.00	0.00	0.00	0.00
Sr	n.d.	n.d.	n.d.	n.d.	n.d.	n.d.	n.d.	n.d.	0.30	0.04	0.25
H_2O	n.d.	n.d.	n.d.	n.d.	n.d.	n.d.	n.d.	13.35	n.d.	n.d.	n.d.

[1]Albitized plagioclase from Mount Moly and OPAM areas; chlorite, epidote, and diopside from miscellaneous locations; all by electron microprobe; this study.

[2]Red Mountains and Eureka Graben areas (Eberl and others, 1987).

[3]Disseminated pyrite from Prospect Gulch, electron microprobe; this study.

[4]Disseminated pyrite, Mount Moly area by ICP-MS; this study.

[5]Alunite from National Belle (Hurlburt, 1894).

[6]Gypsum near Paradise mine (AMLI # 168); ICP-AES, this study.

[7]Calcite from regional propylitic assemblage; ICP-AES, this study.

[8]Sparry calcite from vein, South Silverton area, ICP-AES, this study.

CIC Group

Mapping by AVIRIS remote sensing (Dalton and others, this volume) has been very useful in differentiation of propylitically altered rocks dominated by combinations of illite and chlorite (CIC group) versus the CEC mineral assemblage. However, field studies have shown that the CIC group as mapped by AVIRIS actually represents two notably different types and styles of alteration: (1) superimposition of the regional propylitic assemblage by a later calcite-poor, weak "hydrothermal" mineral assemblage, and (2) an epidote-poor, calcite-rich assemblage formed during the regional propylitic event (chlorite-illite-calcite, CIC). Illite predominates over chlorite within rocks superimposed by the weak sericite[2]-pyrite "hydrothermal" alteration suite (illite-chlorite-pyrite with metastable feldspars). Epidote is generally subordinate or absent in this assemblage. In contrast, chlorite, which formed mostly during the regional propylitic event, is typically metastable, showing partial replacement by illite. Further discussion of the hydrothermal "weak sericite-pyrite" suite is found in later sections on hydrothermal alteration assemblages.

The regional CIC propylitic assemblage is especially characteristic of the San Juan Formation west of Mineral Creek (fig. 3*A*), and within the Eureka Member of the Sapinero Mesa Tuff (Eureka Tuff) in the southeast and east portions of the study area (fig. 3*B*). The San Juan Formation west of Mineral Creek is notably epidote poor and illite rich. Plagioclase within these intermediate-composition rocks is generally altered to a mixture of illite, calcite, and lesser chlorite, whereas biotite, pyroxene, and hornblende are mostly altered to leucoxene and illite. Matrix and pumice within a nearby ash-flow unit, however, are typically chloritic-altered, and plagioclase phenocrysts are weakly altered to illite, chlorite, and calcite. These rocks are locally weakly silicified and contain as much as 1 volume percent pyrite owing to the high density of the northwest-trending veins cutting this region. Calcite is still mostly stable within these altered zones.

[2]Petrographic term used for fine-grained, highly birefringent muscovite (Srodon and Eberl, 1984). Used interchangeably with illite in this report.

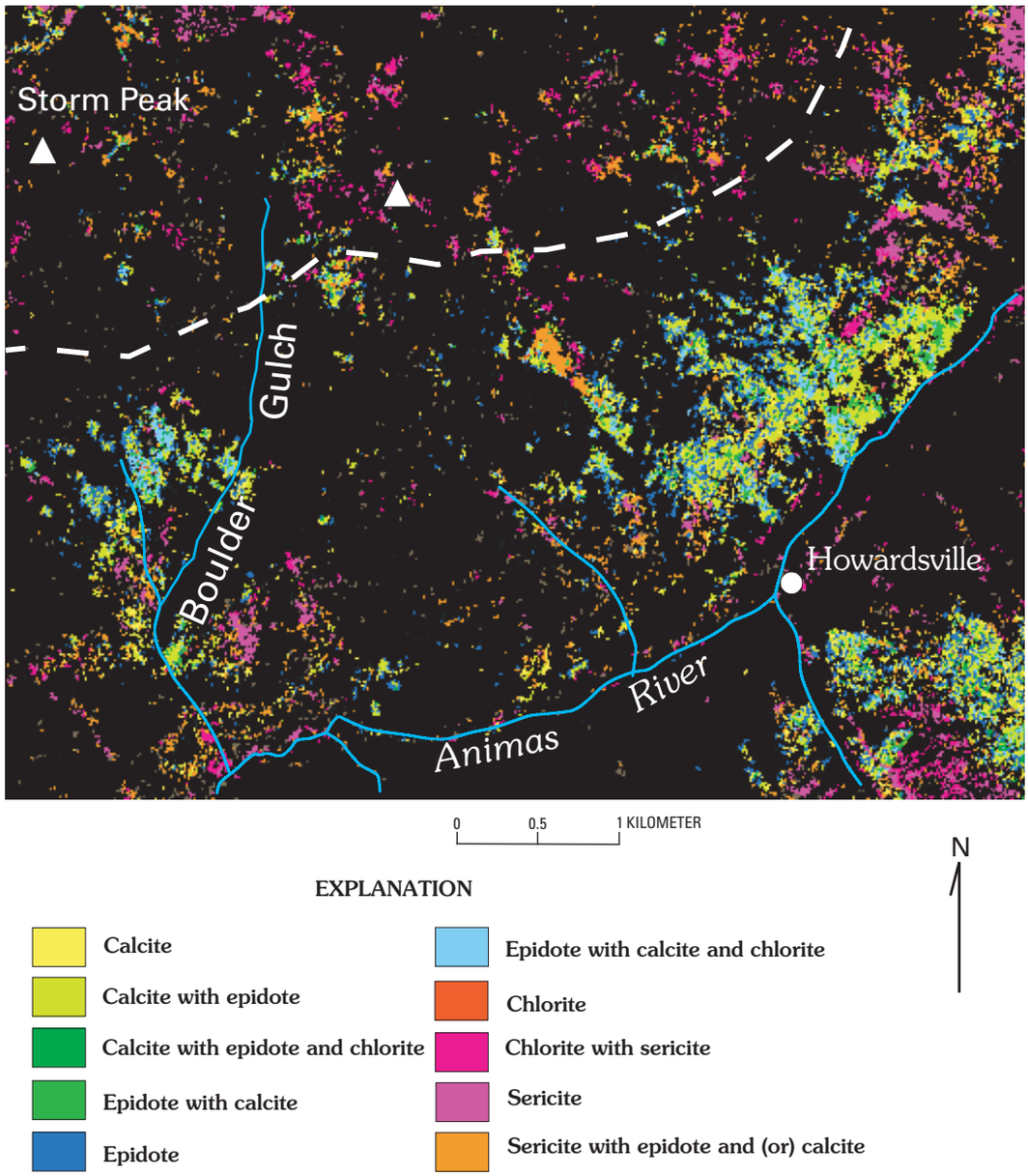

Figure 2. Propylitic assemblage minerals as mapped by AVIRIS (Dalton and others, this volume) in Boulder Gulch–Howardsville area. Burns Member is generally present south of white dashed line and has undergone relatively more intense propylitic alteration with abundant epidote. Henson Member is north of dashed line and is typically less altered. White triangle, peak.

A distinct contrast between CIC-altered Sapinero Mesa Tuff (Eureka and Picayune Megabreccia Members) and overlying CEC-altered Burns Member lavas is observed in the area west of Niagara Gulch (fig. 3*B*). The CIC-altered tuffs are characterized by waxy, light-green, illite-altered pumice, whereas the groundmass is conspicuously whitish green due to replacement by chlorite, illite, and calcite. Plagioclase phenocrysts are variably altered to illite, with lesser chlorite, and calcite. Biotite phenocrysts are typically replaced by chlorite and fine opaque minerals.

There are notable exceptions to these simple lithology-specific associations. For example, immediately south of Silverton (outside the boundary of the Silverton caldera but within the San Juan caldera), both the Eureka and Picayune Megabreccia Members and overlying Burns Member are altered to the CEC assemblage (fig. 3*C*). Similarly, near Animas Forks (Yager and Bove, this volume, pl. 1), exposures of both the Picayune Megabreccia Member and the Burns lavas are distinctly CEC-altered. However, this assemblage changes upward into the CIC suite at about 3,750 m elevation, which dominates

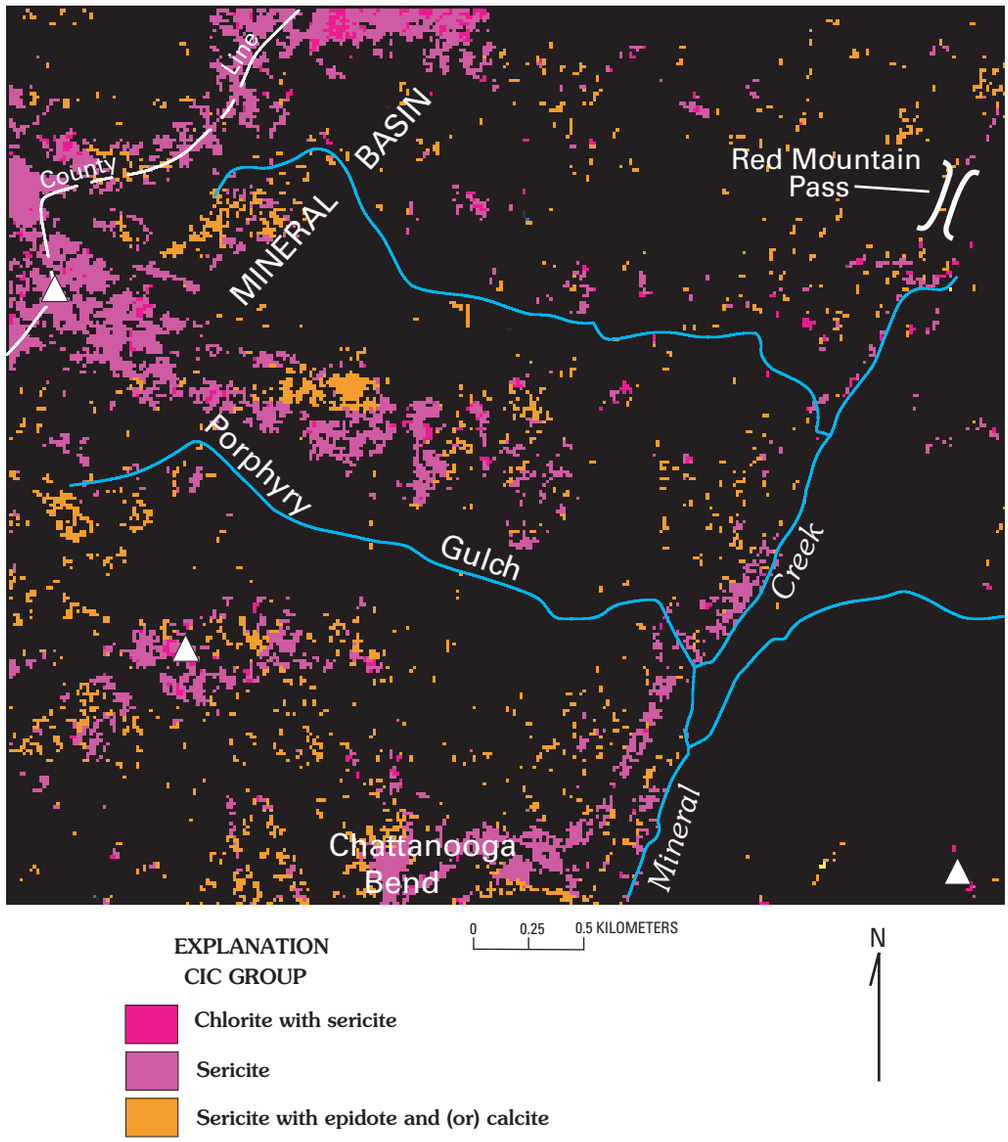

Figure 3 (above and following pages). AVIRIS mapping images, showing *A*, dominance of CIC propylitic assemblage in volcanic sequence west of Mineral Creek. White triangle, peak. *B*, Propylitic assemblage minerals in the Niagara Gulch area, showing alteration changes specific to lithologies. CEC-altered Burns Member lavas (Tsb) overlie the CIC-altered Sapinero Mesa Tuff (Eureka and Picayune Megabreccia Members; Tse). Both rock types have undergone moderate to intense propylitization. *C*, Alteration assemblage minerals in Kendall Mountain area, immediately south of Silverton. Both the Eureka and Picayune Megabreccia Members (Tse) and overlying Burns Member (Tsb) are altered to the CEC assemblage.

in all lithologies westward toward Cinnamon Pass. A similar trend towards CIC dominance with higher elevation is observed in the Burns lavas west of Denver Lake (3,660 m), up to an elevation of 3,960 m near Engineer Pass (in Ouray County just north of the area of pl. 1).

Thus, from these examples, style of propylitic alteration appears to be correlated with lithology as well as with topographic elevation. The difference in alteration patterns within the Sapinero Mesa members at Silverton (CEC; for example, figs. 2 and 3*C*) and west of Eureka (CIC; for example, fig. 3*B*) could be explained by their relative topographic elevations or depth of burial following asymmetric collapse of the Silverton caldera (Yager and Bove, this volume) within the earlier subsided San Juan caldera. Rocks were most deeply buried near the southwest margin of the Silverton caldera, where subsidence reached a maximum of about 600 m (Varnes, 1963; Lipman and others, 1973). In contrast, near the Silverton caldera's hinged eastern margin, caldera subsidence was

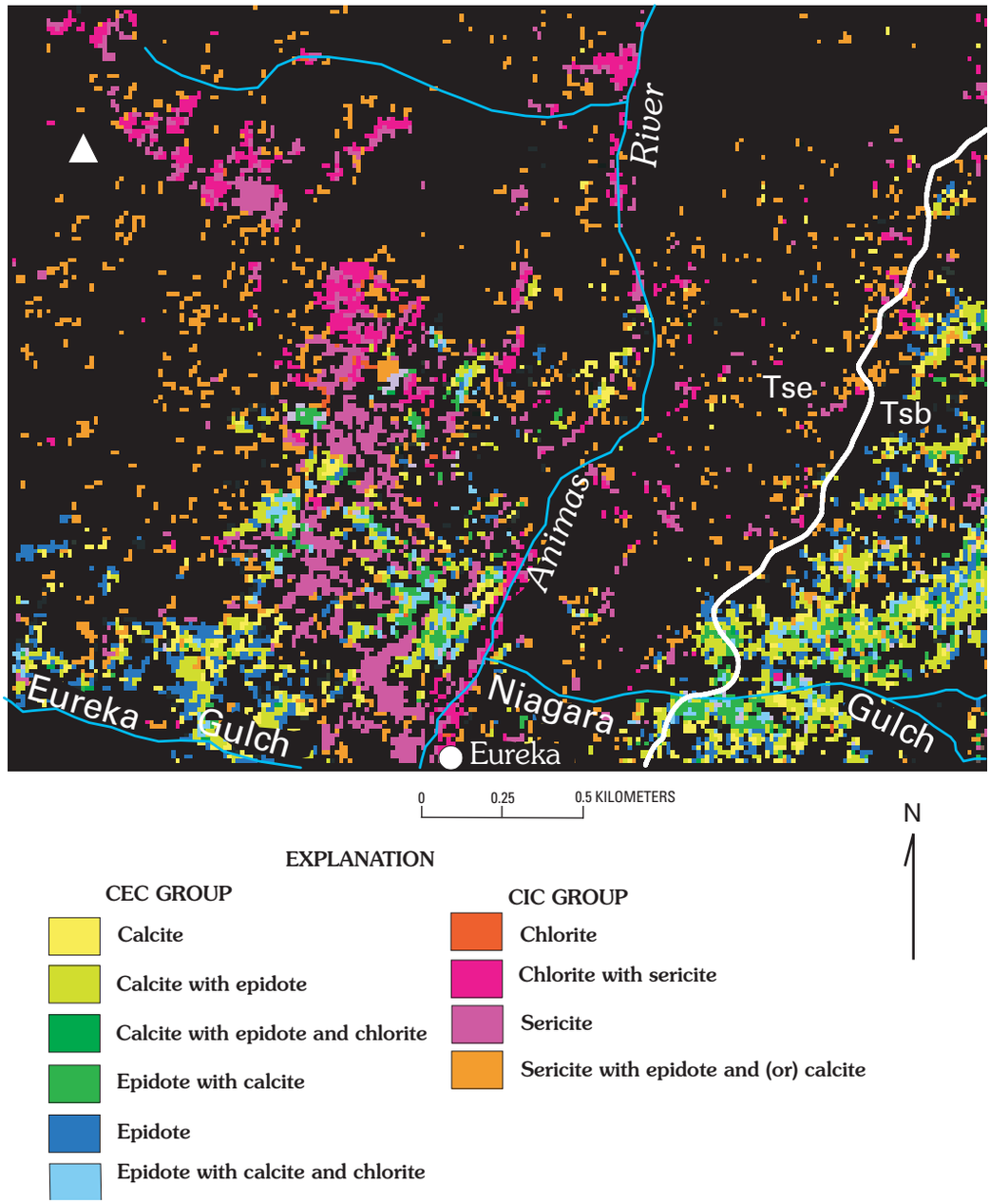

Figure 3—Continued. AVIRIS mapping images. *B*, Propylitic assemblage minerals in the Niagara Gulch area, showing alteration changes specific to lithologies. CEC-altered Burns Member lavas (Tsb) overlie the CIC-altered Sapinero Mesa Tuff (Eureka and Picayune Megabreccia Members; Tse). Both rock types have undergone moderate to intense propylitization. Solid white line is geologic contact between units Tse and Tsb. White triangle, peak.

minimal to nonexistent. The correlation of the CEC-dominant assemblage in the most deeply subsided areas of the caldera and changes from CEC to CIC alteration with increasing topographic elevation are consistent with mineral zoning patterns that can develop with the establishment of temperature gradients. These temperature gradients and the resultant mineral zoning patterns (for example, increasing epidote abundance with higher temperature) probably reflect differential burial depths during the regional propylitic event (Sillitoe, 1984).

Geochemistry of Propylitically Altered Rocks

Geochemical data from 72 propylitically altered rocks from the Mount Moly, combined Red Mountains–OPAM, and Eureka Graben areas (fig. 1) are summarized in table 3 and figure 4. Comparisons of data from these areas show the abundances of manganese, lead, zinc, and copper to be analytically indistinguishable, with the exception of slightly lower concentrations of lead and zinc in the Eureka Graben

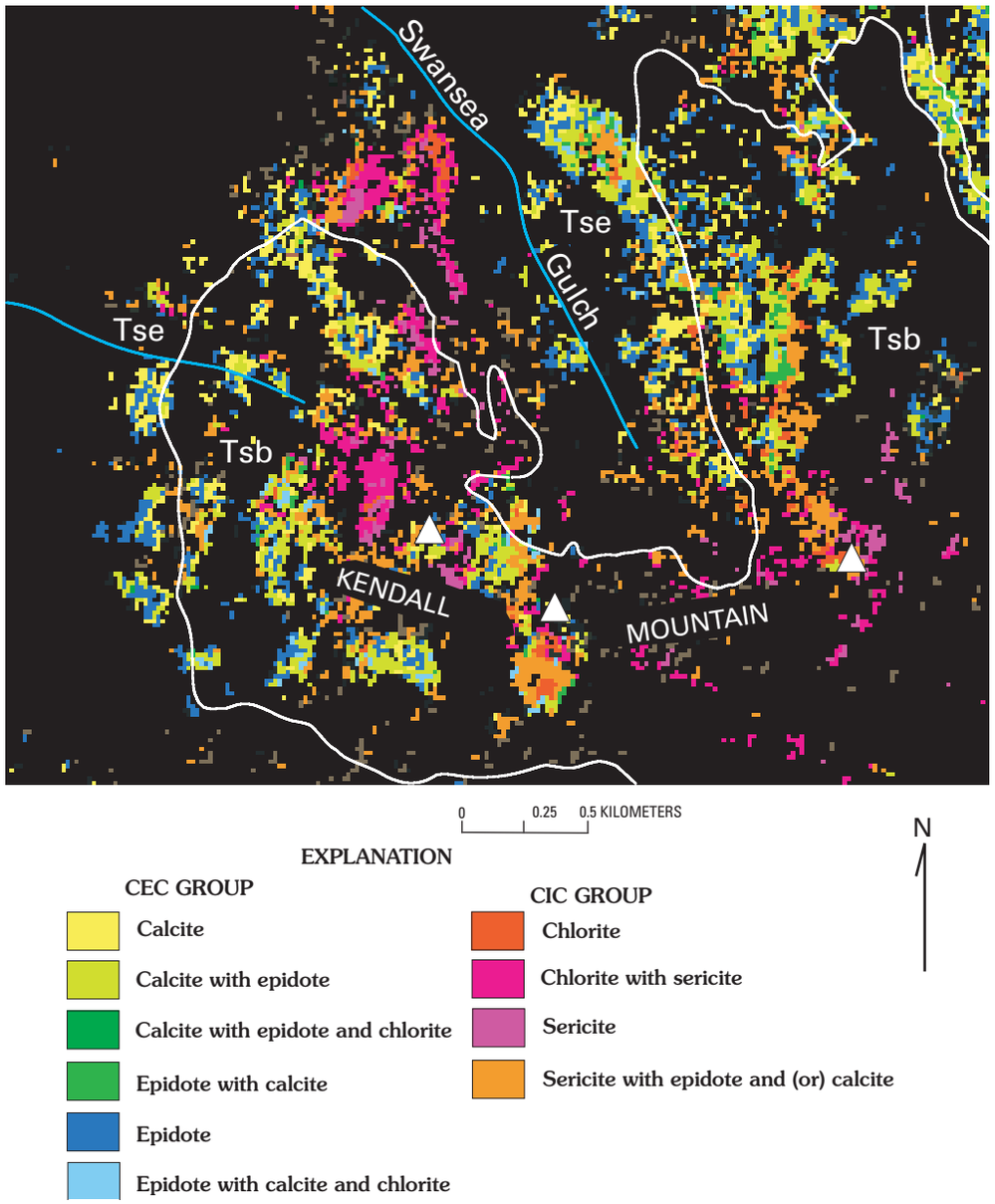

Figure 3—Continued. AVIRIS mapping images. *C*, Alteration assemblage minerals in Kendall Mountain area, south of Silverton. Both the Eureka and Picayune Megabreccia Members (Tse) and overlying Burns Member (Tsb) are altered to the CEC assemblage. White triangle, peak; white line, contact.

area data set. Mean[3] concentrations, as calculated for each of these areas, range from 777 to 946 ppm manganese, 10 to 36 ppm lead, 67 to 110 ppm zinc, and 33 to 50 ppm copper. Total iron abundances in the Mount Moly and Eureka Graben area samples also overlap statistically and have a mean of 3 weight percent. In contrast, total iron concentrations in the combined Red Mountains–OPAM area samples are markedly higher than in the other two areas, with a mean of 4.8 weight percent. The differences in total iron may represent both differences in original bulk rock composition and varying abundances of volumetrically minor pyrite. Although pyrite does not appear as an essential product of this alteration assemblage (Burbank and Luedke, 1969), it is widely disseminated, owing to the high density of veins and fracturing within the entire study area. In the following discussions on the chemistry of rocks from various hydrothermally altered and mineralized systems, these basin-wide "baseline" or unmineralized values will provide useful comparisons with data from mineralized and more intensely altered rocks.

[3]The term "mean" as used in this manuscript refers to geometric mean calculations.

Table 3. Summary of rock geochemical data from the Mount Moly, Red Mountains, OPAM, and Eureka Graben areas.

[*n*, number; QSP, quartz-sericite-pyrite; V-QSP, vein-related quartz-sericite-pyrite; gmean, geometric mean; < , less than; n.d., not determined]

	Al	Ca	Fe	K	Mg	Na	P	Ti	Mn	Ag	As	Ba	Cu	Mo	Pb	Sr	Zn
	percent								ppm								
Mount Moly area																	
Surface Outcrop Samples:																	
Hydrothermal-propylitic (*n*=9)[1]:																	
25th percentile	7.87	1.43	2.52	3.27	1.33	2.40	0.13	0.39	800	n.d.	n.d.	578	23	1	30	570	68
75th percentile	8.25	2.36	3.38	3.52	1.42	2.86	0.14	0.46	1,300	n.d.	n.d.	693	61	3	41	707	91
gmean	8.13	1.78	3.04	3.11	1.27	2.55	0.13	0.42	946	n.d.	n.d.	624	34	2	36	666	81
Weak sericite-pyrite (*n*=5)[2]:																	
25th percentile	7.76	0.21	2.10	3.15	0.58	2.28	0.07	0.31	175	n.d.	n.d.	720	37	9	17	290	46
75th percentile	8.03	0.40	2.20	4.00	1.08	2.54	0.11	0.38	650	n.d.	n.d.	770	72	16	50	520	63
gmean	7.98	0.29	2.48	3.14	0.82	2.38	0.09	0.36	313	n.d.	n.d.	819	59	12	58	413	45
all USGS																	
QSP (*n*=12)[3]:																	
25th percentile	8.42	0.08	0.43	3.43	0.26	0.32	0.09	0.44	34	n.d.	3	563	14	3	27	123	20
75th percentile	9.23	0.12	1.30	3.49	0.41	0.54	0.12	0.55	64	n.d.	10	890	31	16	95	310	36
gmean	8.71	0.09	0.70	3.47	0.32	0.32	0.11	0.50	54	n.d.	6	624	23	8	49	205	25
7 USGS, 5 Ringrose, 1982																	
Drill Core Metals Data—3 Meter Sample Splits[4]:																	
QSP-unoxidized (*n*=30)																	
25th percentile	n.d.	n.d.	n.d.	n.d.	n.d.	n.d.	n.d.	n.d.	n.d.	n.d.	n.d.	n.d.	260	14	20	n.d.	79
75th percentile	n.d.	n.d.	n.d.	n.d.	n.d.	n.d.	n.d.	n.d.	n.d.	n.d.	n.d.	n.d.	560	40	33	n.d.	130
gmean	n.d.	n.d.	n.d.	n.d.	n.d.	n.d.	n.d.	n.d.	n.d.	n.d.	n.d.	n.d.	374	22	28	n.d.	109
QSP oxidized (*n*=73)																	
25th percentile	n.d.	n.d.	n.d.	n.d.	n.d.	n.d.	n.d.	n.d.	n.d.	n.d.	n.d.	n.d.	8	5	12	n.d.	<5
75th percentile	n.d.	n.d.	n.d.	n.d.	n.d.	n.d.	n.d.	n.d.	n.d.	n.d.	n.d.	n.d.	30	23	25	n.d.	11
gmean	n.d.	n.d.	n.d.	n.d.	n.d.	n.d.	n.d.	n.d.	n.d.	n.d.	n.d.	n.d.	15	11	18	n.d.	8
Hydrothermal-propylitic (*n*=50):																	
25th percentile	n.d.	n.d.	n.d.	n.d.	n.d.	n.d.	n.d.	n.d.	n.d.	n.d.	n.d.	n.d.	130	12	20	n.d.	42
75th percentile	n.d.	n.d.	n.d.	n.d.	n.d.	n.d.	n.d.	n.d.	n.d.	n.d.	n.d.	n.d.	280	48	34	n.d.	58
gmean	n.d.	n.d.	n.d.	n.d.	n.d.	n.d.	n.d.	n.d.	n.d.	n.d.	n.d.	n.d.	194	24	28	n.d.	35

Table 3. Summary of rock geochemical data from the Mount Moly, Red Mountains, OPAM, and Eureka Graben areas.—Continued

	Al	Ca	Fe	K	Mg	Na	P	Ti	Mn	Ag	As	Ba	Cu	Mo	Pb	Sr	Zn
	percent								ppm								
Combined Red Mountains–OPAM areas[2]																	
Propylitic (*n*=15):																	
25th percentile	8.13	1.86	4.62	1.94	1.40	1.86	0.15	0.47	935	2	12	519	41	2	20	238	83
75th percentile	8.59	3.30	5.26	2.96	1.98	2.49	0.16	0.57	1,230	2	30	958	64	2	33	673	110
gmean	8.38	1.92	4.83	2.31	1.52	1.66	0.14	0.50	927	2	19	718	50	2	26	396	110
QSP (*n*=20):																	
25th percentile	7.16	0.04	0.29	2.38	0.23	0.02	0.03	0.43	23	2	10	290	3	2	29	58	10
75th percentile	8.33	0.12	2.30	3.33	0.40	0.09	0.11	0.61	59	2	29	1,063	16	5	113	188	37
gmean	7.42	0.07	0.87	2.82	0.21	0.05	0.06	0.46	35	2	18	530	8	3	62	106	20
Silicified or vein structure (*n*=16):																	
25th percentile	0.23	0.01	0.50	0.04	0.01	0.01	0.01	0.04	6	4	50	56	12	2	220	67	8
75th percentile	1.63	0.06	8.23	2.20	0.01	0.03	0.19	0.25	18	51	2,419	221	291	17	3,740	796	32
gmean	0.76	0.03	2.05	0.30	0.01	0.01	0.05	0.09	12	14	260	122	55	6	870	177	18
Acid-Sulfate Assemblage: Argillic (*n*=8)																	
25th percentile	6.68	0.14	0.38	0.04	0.01	0.01	0.14	0.43	4	2	10	457	6	2	70	372	6
75th percentile	8.40	0.19	1.90	1.01	0.09	0.03	0.21	0.51	17	2	37	904	28	3	571	787	19
gmean	7.90	0.14	0.86	0.18	0.02	0.02	0.16	0.46	9	2	25	607	11	3	237	309	9
Quartz-pyrophyllite (*n*=13):																	
25th percentile	4.40	0.09	0.09	0.04	0.01	0.01	0.12	0.19	4	2	10	375	3	2	99	332	5
75th percentile	6.50	0.16	0.54	0.90	0.02	0.06	0.18	0.51	14	2	20	1,020	27	2	396	1,100	13
gmean	4.17	0.10	0.26	0.18	0.01	0.04	0.11	0.34	8	3	20	470	7	2	255	512	8
Quartz-alunite (*n*=13):																	
25th percentile	6.80	0.05	0.21	2.00	0.01	0.24	0.13	0.17	4	2	10	99	3	2	123	567	4
75th percentile	9.00	0.15	1.20	3.20	0.01	0.47	0.22	0.29	12	2	14	247	20	2	1,130	976	15
gmean	7.53	0.09	0.54	2.45	0.01	0.25	0.13	0.23	9	2	13	162	8	2	358	550	8
Acid-sulfate-drill core (*n*=34):																	
25th percentile	6.10	0.11	4.40	1.45	0.01	0.04	0.08	0.11	4	2	10	133	36	2	48	434	5
75th percentile	7.55	0.14	5.95	2.45	0.06	0.52	0.12	0.25	30	2	16	288	128	3	674	838	30
gmean	6.68	0.12	4.77	1.51	0.02	0.16	0.10	0.17	11	2	14	195	79	3	141	535	13

Table 3. Summary of rock geochemical data from the Mount Moly, Red Mountains, OPAM, and Eureka Graben areas.—Continued

	Al	Ca	Fe	K	Mg	Na	P	Ti	Mn	Ag	As	Ba	Cu	Mo	Pb	Sr	Zn
	percent								ppm								
Eureka Graben area[5]																	
Propylitic (*n*=48):																	
25th percentile	n.d.	n.d.	2.8	n.d.	n.d.	n.d.	n.d.	n.d.	660	<0.5	n.d.	n.d.	26	n.d.	7	n.d.	59
75th percentile	n.d.	n.d.	4.0	n.d.	n.d.	n.d.	n.d.	n.d.	900	<0.5	n.d.	n.d.	54	n.d.	14	n.d.	74
95th percentile	n.d.	n.d.	4.7	n.d.	n.d.	n.d.	n.d.	n.d.	1,330	<0.5	n.d.	n.d.	73	n.d.	20	n.d.	96
gmean	n.d.	n.d.	3.2	n.d.	n.d.	n.d.	n.d.	n.d.	777	<0.5	n.d.	n.d.	33	n.d.	10	n.d.	67
QSP-vein (V-QSP) (*n*=36):																	
25th percentile	n.d.	n.d.	1	n.d.	n.d.	n.d.	n.d.	n.d.	160	<0.5	n.d.	n.d.	16	n.d.	4	n.d.	25
75th percentile	n.d.	n.d.	2	n.d.	n.d.	n.d.	n.d.	n.d.	1,430	1	n.d.	n.d.	48	n.d.	14	n.d.	71
95th percentile	n.d.	n.d.	3	n.d.	n.d.	n.d.	n.d.	n.d.	4,200	4	n.d.	n.d.	152	n.d.	155	n.d.	106
gmean	n.d.	n.d.	1.5	n.d.	n.d.	n.d.	n.d.	n.d.	497	0.7	n.d.	n.d.	28	n.d.	11	n.d.	33

[1]Two samples analyzed at USGS labs by ICP-MS and ICP-40 element-AES; seven samples analyzed by XRF; data from Ringrose (1982).

[2]USGS labs by ICP-40 element-AES.

[3]Seven samples analyzed at USGS labs by ICP-MS and ICP-40 element-AES; five samples analyzed by XRF; data from Ringrose (1982).

[4]Mo by colorimetric method and atomic absorption (AA), AMAX and Skyline Labs, Denver Colo.; Cu, Pb, Zn, by AA, AMAX lab; data from McCusker (1983).

[5]Atomic absorption (AA); data from Langston (1978).

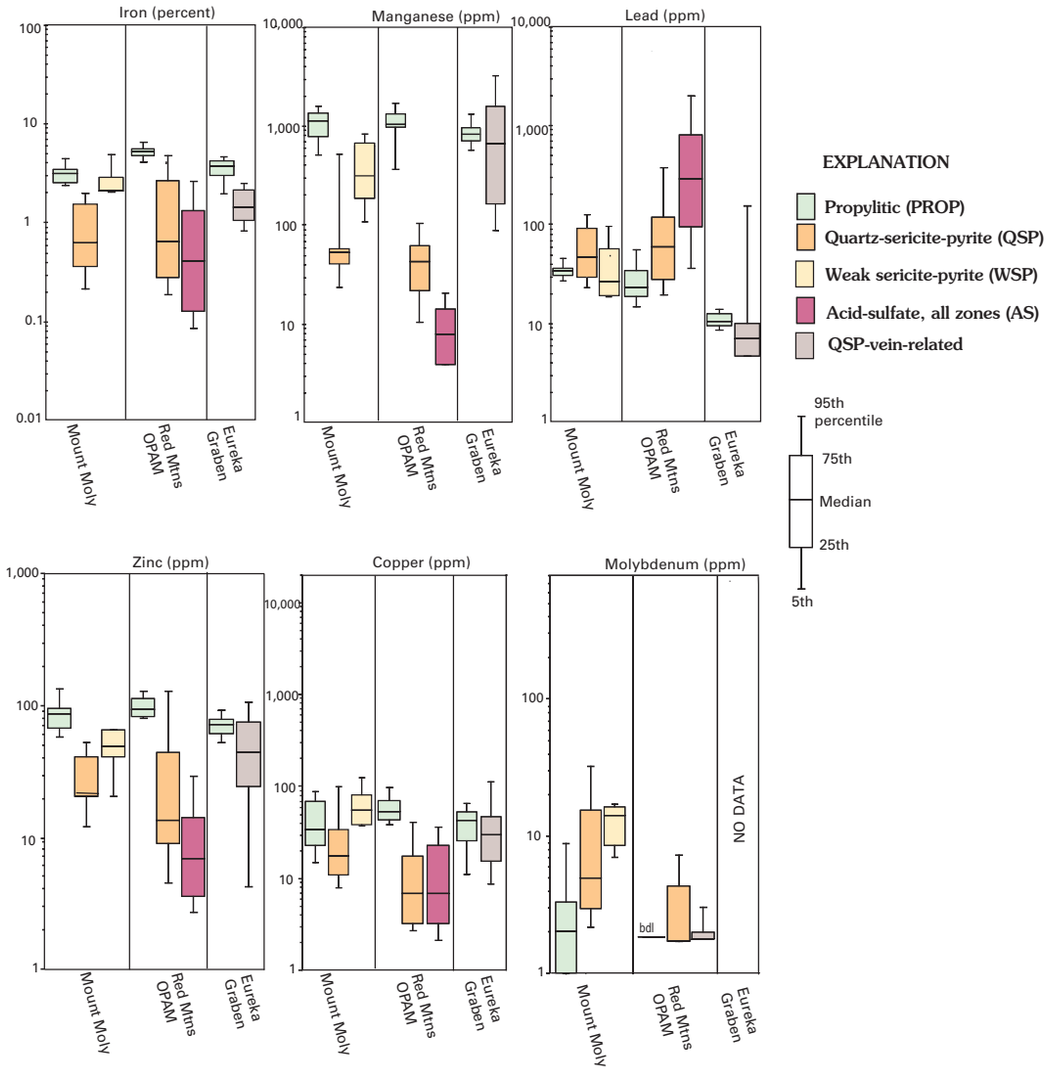

Figure 4. Box plots of outcrop rock chemistry data from alteration assemblages in the Mount Moly area, combined Red Mountains–OPAM area, and Eureka Graben area. See text for description of alteration assemblages. AS, combination of all AS zones from surface samples in table 3. No molybdenum data are available from the Eureka Graben area. All vertical scales are in parts per million (ppm) except iron (in percent); bdl, below detection limit.

Background Surface Water Chemistry

A discussion of the geochemistry of surface waters that interacted with all propylitically altered rocks in the study area is presented in Mast and others (this volume). Results of that study demonstrate that streams and springs draining areas of propylitically altered rock had moderate to high pH values (5.74–8.49), measurable alkalinity (1.4–68 mg/L), low dissolved metal concentrations (zinc=20–237 µg/L; copper=4–73 µg/L), and low concentrations of dissolved iron (30–310 µg/L) and aluminum (40–140 µg/L). Specifics on the relationship between propylitically altered rocks and related waters within each of the four major mineralized areas, however, will be discussed in their respective sections following. (Red Mountains and Ohio Peak–Anvil Mountain are discussed together.)

26–25 Ma Molybdenum–Copper Porphyry Mineralization and Alteration

Mount Moly Area Ore Deposits

More than 19 km^2 of intensely altered and pyritized rock reflects the presence of a subeconomic molybdenum–copper porphyry hydrothermal system in the Mount Moly area (fig. 1). Mineralization and hydrothermal alteration in this area are temporally and genetically related to a late (25 Ma) quartz monzonite phase of the 26 Ma Sultan Mountain stock (Ringrose and others, 1986; Bove and others, 2001). The main zone of molybdenum-copper enrichment is coincident with intense QSP-(quartz-sericite-pyrite) altered rock, high-density

quartz stockwork veining, and as much as 5 volume percent sulfides (McCusker, 1982). Disseminated sulfides in this zone consist mainly of pyrite, lesser chalcopyrite, and traces of molybdenite and bornite. The sulfides occur as tiny grains replacing feldspars and other phenocrysts and disseminated iron oxides in the groundmass.

Quartz-sulfide veins, most of which are within a central core of QSP-altered rock (fig. 5), form a stockwork of narrow (<1.3 cm), discontinuous veinlets. Veinlet density reaches a maximum (0.3–1.5/m^2) in a roughly 0.9 km^2 area centered around peak 3,792 m (fig. 5) (McCusker, 1982). The veinlets are typically filled with gray-blue translucent quartz along with scattered grains or discontinuous bands of pyrite with minor chalcopyrite, molybdenite, and bornite. Two sericite samples from wallrock adjacent to the stockwork yielded concordant K-Ar ages of about 25 Ma, close to the same age as biotite from nearby quartz monzonite intrusions (Ringrose, 1982; Bove and others, 2001). Drill hole data (McCusker, 1982) and our recent field studies indicate that the highest concentrations of copper and molybdenum and the most intense QSP alteration are distributed near the margins of the quartz monzonite intrusions. Detailed rock geochemical sampling delineates depletions of the trace elements zinc, manganese, and strontium within the innermost intensely altered zones and enrichments of these elements around the periphery of the hydrothermal system (Ringrose, 1982). Drill hole data (McCusker, 1982) indicate that oxidation and supergene leaching are present to depths as much as 100 m beneath the surface. Secondary minerals within this oxidized zone include hematite, goethite, ferrimolybdenite, and minor secondary copper sulfides including chalcocite, digeonite, and covellite. The secondary copper minerals are present mostly as thin films and as partial replacements after pyrite.

Relatively narrow (0.3–1 m), quartz base-metal veins are present on the periphery of the porphyry system, mostly on the northeast flank of peak 3,792 m. Mines include the Bonner—probably the largest producer in this area, Independence, Magnet, and Ruby Trust (Church, Mast, and others, this volume; fig. 5), whose veins are generally oriented north-south (Ringrose, 1982; McCusker, 1983). These veins contain silver and some gold in sulfide ores consisting principally of galena, sphalerite, and lesser pyrite, with minor fine-grained tetrahedrite-tennantite and chalcopyrite (Ringrose, 1982; McCusker, 1983). The primary gangue mineral is quartz, with lesser barite and carbonate minerals, and minor manganese-silicate minerals. Galena is mostly coarse grained and intergrown with irregular patches of subhedral sphalerite. Quartz is typically milky white, massive, and fine grained, although euhedral, vug-filling crystals are also present. Pyrite, tetrahedrite, and barite and carbonate gangue were generally precipitated after sphalerite and galena. Several of these polymetallic veins are molybdenite-bearing and cut quartz-molybdenite stockwork veins associated with the central QSP zone in the Mount Moly area (McCusker, 1982). The orientation, presence of molybdenite, and proximity of many of these polymetallic veins to the inner zone of QSP alteration suggest that some are contemporaneous with the low-grade molybdenum-copper porphyry system (26–25 Ma). In addition, $\delta^{18}O$ and δD values of sphalerite inclusions from peripheral base-metal veins resemble the magmatic water compositions of minerals within the central zone of QSP alteration and related quartz-molybdenite stockwork (Ringrose, 1982).

Hydrothermal Alteration in the Mount Moly Area

The detailed map of hydrothermal alteration assemblages in the Mount Moly area (fig. 5) was compiled from three principal sources: (1) field mapping by Ringrose (1982), (2) field mapping by the USGS for this study (1996–99), and (3) remotely sensed mapping by AVIRIS spectroscopy (Dalton and others, this volume). Pervasive QSP-alteration grades outward into weak sericite-pyrite and hydrothermal propylitic assemblages, and finally into the regional propylitic assemblage. For simplicity, the hydrothermal propylitic and weak sericite-pyrite assemblages have been combined into a generalized "weak sericite-pyrite" assemblage, as shown in figures 1 and 5.

The large area of QSP-altered rock (3.5 km^2) is centered roughly on the summit of peak 3,792 m and is coincident with steep, highly colorful hematite and jarosite-stained slopes. In this zone, intrusive and volcaniclastic rocks as well as flow rocks are intensely altered and are characterized by complete replacement of feldspars and groundmass by coarse-grained sericite, which is readily discerned with a hand lens. Secondary quartz is also commonly present as a blue-gray microcrystalline "flooding" throughout the groundmass and within dense networks of thin stockwork veinlets. Fine-grained pyrite (≤1–2 mm) is disseminated throughout rock and is present in fractures and veinlets; abundances typically range from 2 to 5 volume percent. Geochemical data show that both disseminated pyrite and fracture-filling pyrite have low trace-metal abundances (table 2) and are similar in composition to QSP-related pyrites analyzed from other parts of the study area. Fracture-controlled zones of QSP-altered rock are also common on the margins of the main QSP alteration assemblage, cutting broad zones of more weakly altered rock.

Weak sericite-pyrite altered rock (WSP, fig. 5) is characterized by incipient to partial replacement of plagioclase by sericite; biotite and pyroxene are altered to chlorite, sericite, and fine opaques. These rocks are generally less silicified than their QSP counterparts and contain fewer quartz-sulfide stockwork veinlets. Hydrothermal propylitic alteration zones (combined in WSP assemblage, fig. 5), which formed contemporaneously with the porphyry hydrothermal system, are composed of fresh to weakly altered feldspar, chlorite- and epidote-altered biotite and pyroxene, and abundant veins and fractures filled with pyrite, chlorite, magnetite, and quartz. Rocks affected by this alteration are present along the outer margins of the porphyry system. An earlier formed regional propylitic assemblage characterizes about 25 percent of the rock within the Mount Moly area. Although this assemblage

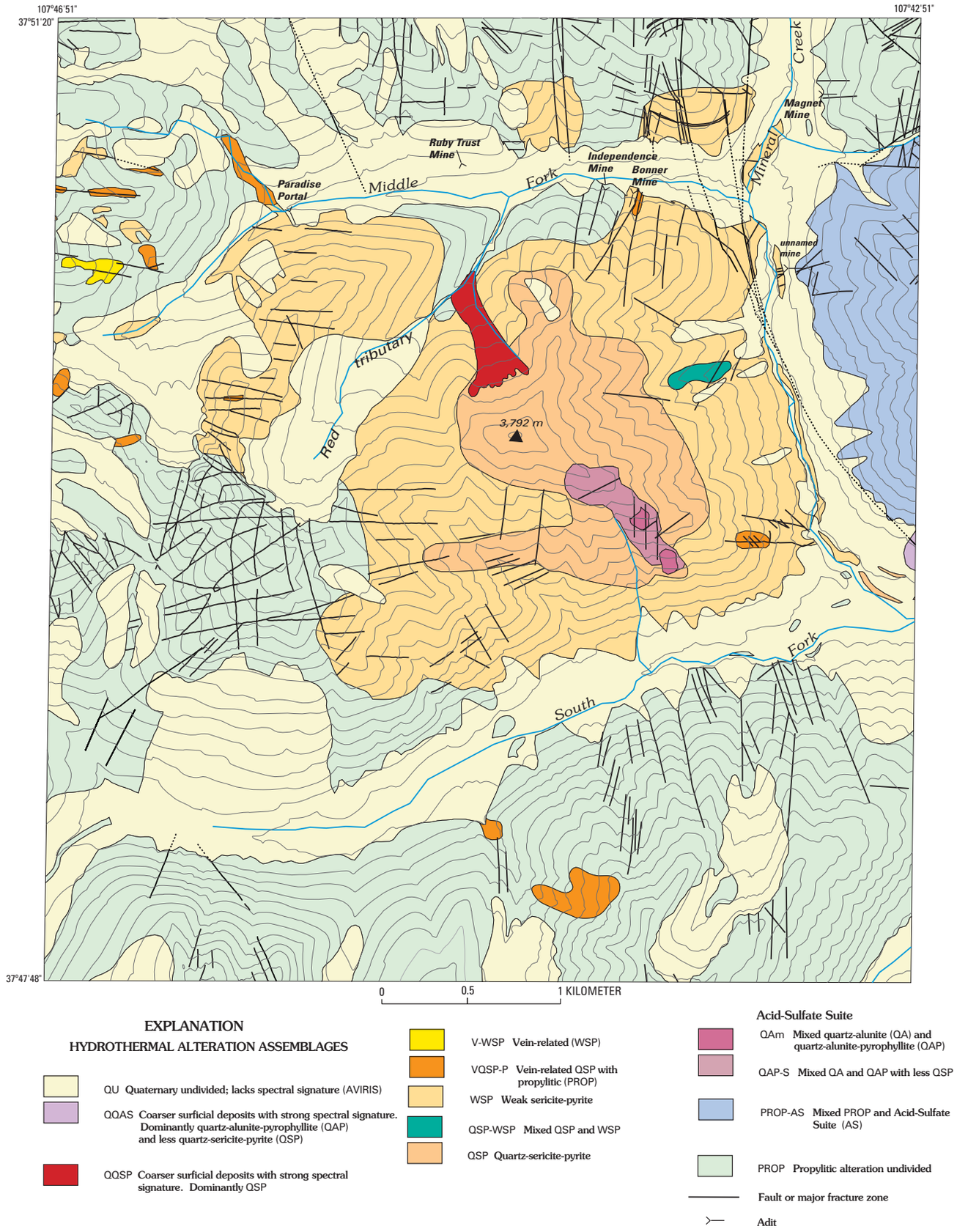

Figure 5. Alteration map of the Mount Moly area, centered around peak 3,792 m.

grossly resembles the Mount Moly area hydrothermal propylitic assemblage, it is distinguished largely by the absence of pyrite, quartz, and chlorite veinlets, and the scarcity of finely disseminated pyrite. The distribution of calcite within both regional and hydrothermal propylitically altered rocks is important because of calcite's inherent acid-neutralizing capacity (Mast and others, this volume).

Relations in drill core show that QSP alteration overprinted secondary biotite alteration at depth beneath peak 3,792 m (McCusker, 1982). Disseminated aggregates and flakes of secondary biotite and coarse-grained selvages surrounding quartz-molybdenite veins were encountered near the bottom of a 155-m drill hole collared approximately 305 m below the peak's summit. The secondary biotite assemblage is accompanied by vein and disseminated anhydrite and associated sericite. Gypsum, which is present within vein and fractures along with disseminated sulfides, was also reported locally within several exploratory drill holes (McCusker, 1982). Coarse-grained gypsum crystals are also present in mineralized fractures along the periphery of the Mount Moly altered area.

Alteration Zones Near the Southeast Margin of the Silverton Caldera

Although the most obvious area of weak sericite-pyrite alteration and mineralization is in the Mount Moly area, one of the five major areas discussed in this report, several large zones of weak sericite-pyrite to locally QSP-altered rock are roughly coincident with an elongate quartz monzonite intrusive body exposed along the projected southeastern ring-fracture zone of the Silverton caldera. These altered rocks discontinuously crop out in a 7,000 m long by 1,800 m wide zone on the east side of the upper Animas River, extending from Cunningham Creek to Eureka Gulch (fig. 1). Although these rocks contain elevated abundances of finely disseminated pyrite, AVIRIS mapping does not detect extensive zones of jarosite or goethite oxidation, which are generally coincident with more intensely altered and pyritic rock (Dalton and others, this volume). Limited grab sampling of altered rocks from this zone shows trace to minor amounts of gold and silver (Varnes, 1963). However, it is possible that these subdued metal anomalies are related to younger (< 18 Ma) northwest-striking veins that intersect this altered area. As shown in figure 1, areas of propylitically altered rock are intermittently interspersed throughout this zone.

Geochemistry of Altered Rocks

Geochemical data as grouped by alteration types in the Mount Moly area are summarized in table 3 and figure 4. Analyses of surface or outcrop samples (26 samples, table 3) show that magnesium, calcium, sodium, and manganese generally decrease with increasing alteration intensity from propylitic through weak sericite-pyrite to QSP-altered rocks. In contrast, potassium and aluminum abundances are most elevated in QSP-altered rocks but are not statistically different in the propylitic and WSP-altered groups. The relatively low iron content of QSP-altered samples, as shown in figure 4, results from the weathering of pyrite and loss of iron. Zinc and copper concentrations are generally higher in propylitic samples than in QSP and WSP samples, whereas lead and molybdenum are higher in QSP and WSP samples compared to propylitic samples.

Comparison of oxidized versus unoxidized QSP-altered rock from drill cores in the Mount Moly area (153 samples) (table 3 and fig. 6) depicts marked contrasts in zinc and copper

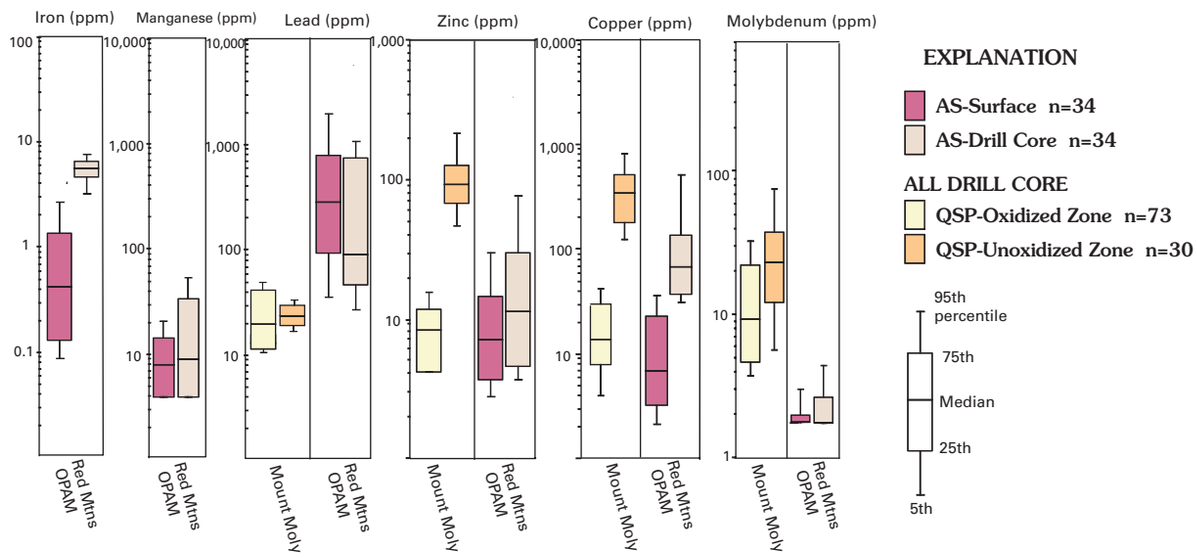

Figure 6. Box plots comparing surface and subsurface (drill core) rock chemistry data from acid-sulfate (AS) and quartz-sericite-pyrite (QSP) zones in the Red Mountains–OPAM and Mount Moly alteration areas. All vertical scales in parts per million (ppm); *n*, number of samples.

concentration, along with minor variations in molybdenum. Drill core logs indicate that zones of strong oxidation and pervasive bleaching are present to depths as much as 100 m below the ground surface. The mean copper concentration in unoxidized drill core intercepts of QSP-altered rock is 374 ppm, compared to 15 ppm in oxidized QSP-altered rocks. Similarly, mean zinc concentration changes from 109 ppm to 8 ppm in unoxidized versus oxidized QSP-altered core samples. Molybdenum concentrations, however, show only a slight decrease in the oxidized rocks (mean of 11 versus 24 ppm molybdenum). The higher copper concentration in unoxidized samples reflects the presence of secondary copper enrichment beneath the upper oxidized zone. That secondary enrichment has occurred is also supported by the partial replacement of pyrite by chalcocite, digeonite, and covellite within this deeper zone of enrichment (McCusker, 1983). In contrast, lead concentrations are not significantly different between the oxidized and unoxidized QSP core samples, reflecting the low solubility of lead-sulfide minerals (White and Brantley, 1995). The above-mentioned differences in metal concentrations as observed in oxidized and unoxidized rocks give a general portrayal of the relative mobility of some of these metals in low-pH surface water. Referred to as supergene oxidation, these processes postdate hydrothermal alteration and have been especially active from the time of Neogene uplift to the present (Steven and others, 1999; Yager and Bove, this volume).

Mine Dump Compositions

Analytical data summarizing the geochemistry of 15 mine dumps in the Mount Moly area are in table 4. Figure 7 compares these data to similar analyses from the four other mineralized areas discussed herein. Manganese abundance in mine dump samples from this area (262 ppm geometric mean; table 3) is relatively low compared to three of the mineralized areas shown in figure 7. This value is two times lower than the mean manganese concentration of surrounding propylitically altered rocks. These low manganese values reflect the paucity of manganese silicate and manganese carbonate gangue minerals in Mount Moly area vein deposits. Mean lead and zinc concentrations both exceed 1,500 ppm. Mean lead concentration is lower than that in any of the other four mineralized groups, whereas mean zinc is similar to the concentration of the other groups (fig. 7). Both lead and zinc abundances in the mine dump samples are >30 times that of all unmined rock samples collected in this area. Mean copper (192 ppm) and arsenic (171 ppm) are substantially lower in Mount Moly area dump samples relative to copper-arsenic-rich dumps such as those in the Red Mountains area (fig. 7). These low combined copper and arsenic values reflect the presence of relatively small quantities of tetrahedrite-tennantite within these ores (Ringrose, 1982; McCusker, 1983). Mount Moly area mine dump samples, however, have somewhat lower mean copper concentrations than do unoxidized rocks intercepted in exploratory drill holes (see subsurface metals data; table 3). Mean molybdenum concentration of mine dump samples is 36 ppm, with higher values exceeding 105 ppm. Along with dumps from the Eureka Graben area, Mount Moly area dumps contain the highest molybdenum concentrations of the five mineralized areas (fig. 7). These data support reports of molybdenite within the vein assemblage (McCusker, 1983) and suggest that some of these veins may be genetically linked to the 26–25 Ma Mount Moly Mo-Cu hydrothermal system.

Mine Water Chemistry

Water-quality data from eight mine-discharge samples in the Mount Moly area are shown in figure 8 and summarized in table 5. The chemistry of these samples is highly variable: pH ranges from 3.00 to 6.51 and concentrations from 1 to 22,000 µg/L aluminum, 530 to 5,900 µg/L manganese, 39 to 2,300 µg/L zinc, and 2 to 629 µg/L copper. As shown in figure 9, these mine samples, like those from the other four mineralized areas, have a roughly bimodal distribution of pH values. The chemistry of low-pH waters is particularly useful for this study, because metals, which can be used as geochemical signatures to discriminate between different types of mineral deposits, generally remain in solution. Where pH exceeds 4.5, reduced solubility results in the precipitation or loss of many metals. In addition, many of the higher pH waters may represent a substantial mixing of acidic waters with more alkaline waters from unaltered or nonmineralized sources.

Four mine discharge samples in the Mount Moly area have pH from 5.01 to 6.51, wide ranges in alkalinity (from 0 to 70 mg/L) and zinc concentration (39 to 620 µg/L), and very low concentrations of lead and copper (sum <13 µg/L). Manganese, which is more soluble at higher pH than most metals (Smith and Huyck, 1999), is widely variable, ranging from 530 to 5,900 µg/L. Three of these samples have high combined concentrations of calcium (>100 to 380 mg/L), strontium (>950 to 2,600 µg/L), and sulfate (>80 to 1,300 mg/L) compared to other samples from the study area (table 6). Aqueous $\delta^{34}S$ data, which have been used in this study to help constrain the sources of dissolved sulfate, range from +4.7 to +5.2 per mil in two of these high calcium-strontium-sulfate waters (Nordstrom and others, this volume, Chapter E8). These values are significantly heavier than those measured in sulfide vein minerals (–0.2 to +2.0 per mil) and disseminated pyrite (–3.1 to +2.5 per mil) from the surrounding alteration assemblages (table 7). These data indicate that waters may have interacted with isotopically heavier gypsum or anhydrite[4], which have $\delta^{34}S$ compositions larger than +14 per mil throughout the watershed. These data are supported by the presence of gypsum gangue material on several of these mine dumps. Two of the high calcium-strontium-sulfate waters (Paradise mine; mine # 168, Church, Mast, and others, this

[4]Upon oxidation or dissolution of minerals there is little or no fractionation of sulfur isotopes, so the resulting isotopic signature of surface waters should be representative of the geologic source. Once dissolved in surface water, the sulfur in sulfate can be fractionated by sulfate-reducing bacteria (Krouse and others, 1991), but only in instances of very low dissolved oxygen.

Table 4. Summary of mine dump geochemistry from five different mineralized areas.

[*n*, number of samples; n.d., not determined; gmean, geometric mean; ppm, parts per million]

	Al	Ca	Fe	K	Mg	Na	P	Ti	Ag	As	Ba	Cd	Cu	Mn	Mo	Ni	Pb	Sr	Zn
	percent								ppm										
Mt. Moly area (*n*=15)[1]:																			
25th percentile	n.d.	n.d.	n.d.	n.d.	n.d.	n.d.	n.d.	n.d.	53	158	n.d.	n.d.	98	140	17	n.d.	570	220	355
75th percentile	n.d.	n.d.	n.d.	n.d.	n.d.	n.d.	n.d.	n.d.	500	235	n.d.	n.d.	363	345	105	n.d.	3,500	320	7,750
gmean	n.d.	n.d.	n.d.	n.d.	n.d.	n.d.	n.d.	n.d.	149	171	n.d.	n.d.	192	262	36	n.d.	1,580	266	1,860
Red Mountains area (*n*=20)[2]:																			
25th percentile	4.7	0.05	3.4	0.53	0.02	0.06	0.10	0.01	5	120	290	2	140	7	4	6	600	355	260
75th percentile	7.6	0.10	10.3	2.55	0.45	0.15	0.17	0.45	59	9,200	470	20	26,000	175	6	18	14,300	993	5,330
gmean	5.7	0.07	6.1	0.96	0.11	0.09	0.12	0.06	24	943	368	6	1,930	39	5	9	1,870	602	935
Ohio Peak–Anvil Mountain area (*n*=6)[2]:																			
25th percentile	7.8	0.11	3.3	3.0	0.55	0.21	0.11	0.47	22	73	308	7	331	441	11	5	5,720	295	2,760
75th percentile	8.6	0.20	5.2	3.5	0.67	0.30	0.19	0.58	35	100	648	21	613	1,040	25	7	12,750	319	4,880
gmean	8.3	0.15	3.3	3.3	0.60	0.22	0.16	0.54	27	87	479	12	382	679	17	6	7,550	320	3,070
Eureka Graben area (*n*=18)[2]:																			
25th percentile	6.7	0.05	2.5	3.3	0.31	0.06	0.07	0.15	10	83	383	2	100	425	22	4	1,950	76	518
75th percentile	8.0	0.19	4.6	3.8	0.62	0.19	0.18	0.32	56	210	848	68	423	3,580	155	9	15,000	168	15,400
gmean	6.9	0.13	3.4	3.4	0.46	0.13	0.12	0.20	18	123	591	13	189	1,500	50	6	3,330	112	2,110
South Silverton area (*n*=8)[2]:																			
25th percentile	4.8	0.15	4.0	2.4	0.35	0.12	0.06	0.05	24	24	298	6	738	2,710	17	6	3,550	51	755
75th percentile	6.2	0.98	5.7	2.9	0.61	0.22	0.10	0.16	99	94	593	39	2,100	6,000	46	14	13,500	66	9,530
gmean	5.3	0.37	4.9	2.6	0.47	0.16	0.07	0.05	43	49	450	13	1,510	3,440	27	9	6,390	60	2,450

[1]Mo by colorimetric method and atomic absorption (AA), AMAX and Skyline Labs, Denver, Colo.; Cu, Pb, Zn, by AA, AMAX lab; remainder by XRF, Skyline and AMAX labs; data from McCusker (1983).

[2]Data from Fey and others (2000).

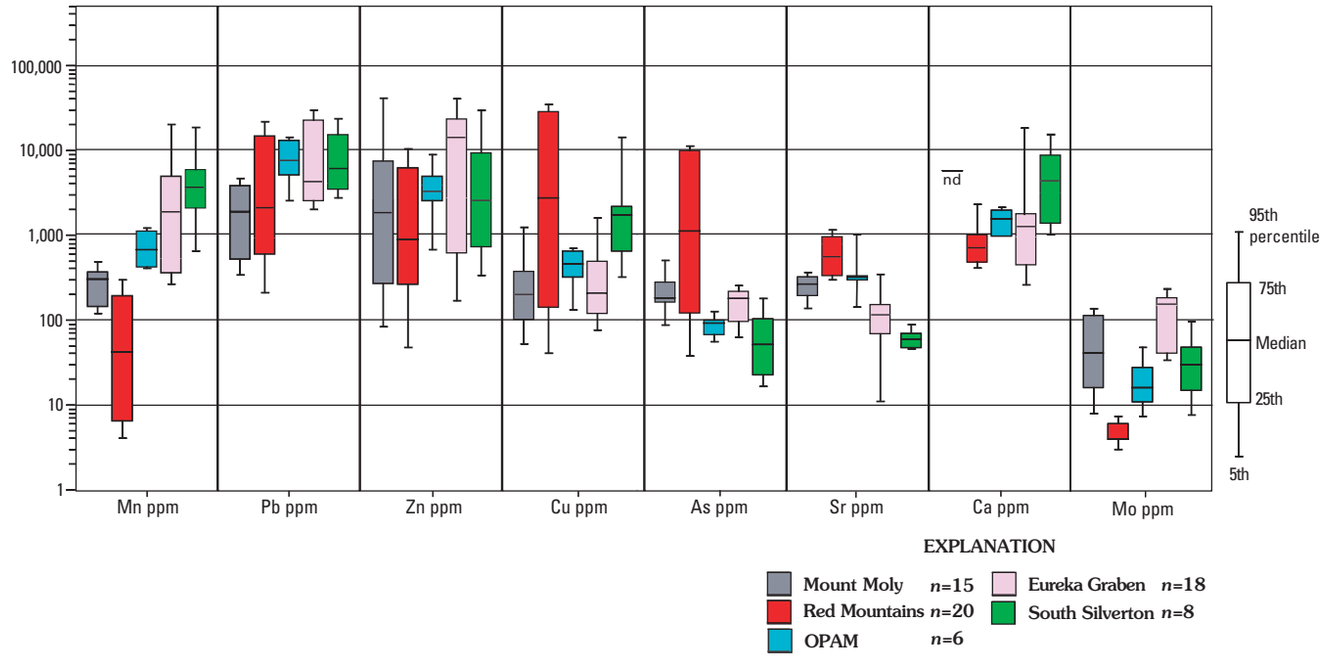

Figure 7. Box plots comparing mine dump data from the five mineralized areas. All vertical scales in parts per million (ppm); *n*, number of analyses; nd, not determined.

volume, Chapter E5; and nearby prospects; fig. 5) are characterized by anomalously high aluminum concentrations (8,600 µg/L and 22,000 µg/L) and are associated with thick aluminum hydroxide precipitates where they discharge over high-angle mine tailings (Peter Butler, Robert Owen, and William Simon, Unpublished report to Colorado Water Quality Control Commission, Animas River Stakeholders Group, 2001; Wright and others, this volume, Chapter E10). The precipitation of aluminum hydroxide at the pH range of the mine portal discharge—based on constraints on aluminum solubility with respect to pH—necessitates a mixing of acidic waters (pH <5.5) containing high dissolved aluminum with more alkaline waters (Nordstrom and Ball, 1986). The resulting rise in pH above 5.5 at or near the mine portals—the lower solubility range for aluminum—would then promote the precipitation of aluminum hydroxide from solution, as observed on the Paradise mine dumps (Nash and Fey, this volume, fig. 20). In addition to causing the precipitation of aluminum, the mixing of more alkaline waters with the acidic waters may have reduced the overall zinc concentrations of these waters, further obscuring the primary metal signatures of the vein deposits (Nordstrom and Ball, 1986).

As just discussed, a compilation of the low-pH mine water geochemistry from the Mount Moly area (pH <4.5) may help us distinguish the aqueous geochemical signatures of these mineral deposits and compare them to analogous data from the other mineralized areas. Geochemical data from four mine discharge samples with low pH in the Mount Moly area are summarized in table 5 and compared to similar analyses from the other mineralized areas in figure 10. Manganese concentration is moderately elevated compared to manganese in samples from the other four mineralized areas in the study area (fig. 10; table 5) and may reflect the presence of minor amounts of manganese-bearing gangue minerals in the associated veins. The mean concentrations of lead (21 µg/L), zinc (505 µg/L), copper (148 µg/L), and arsenic (<1 µg/L) are among the lowest of the acidic mine waters from the other mineralized areas (table 5). Mean sulfate and strontium concentrations are 254 mg/L and 208 µg/L, respectively. Aqueous $\delta^{34}S$ data from the Bonner and Independence mines (mine # 172 and # 171, respectively, Church, Mast, and others, this volume) (fig. 5) range from +5.6 to +6.4 per mil (Nordstrom and others, this volume). These values are heavier than those measured in sulfide vein minerals (–0.2 to +2.0 per mil) and disseminated pyrite (–3.1 to +2.5 per mil) from the surrounding alteration assemblages (table 7). As discussed previously, these waters may also have interacted with isotopically heavier gypsum, which is present along pyrite-bearing fractures on the periphery of the Mount Moly area.

Background Surface Water Chemistry

Geochemical data from all “background” streams and springs that interacted with “end-member” alteration assemblages (waters that dominantly drain a single alteration type) in the Mount Moly area are summarized in table 8. As shown in figure 11, the chemistry of water draining these different alteration assemblages varied, although variation within alteration assemblage was much less than variation across assemblages. Streams and springs draining QSP-altered rock were the most acidic (mean pH=3.22), having the highest mean concentrations of aluminum (18,400 µg/L), iron (22,200 µg/L),

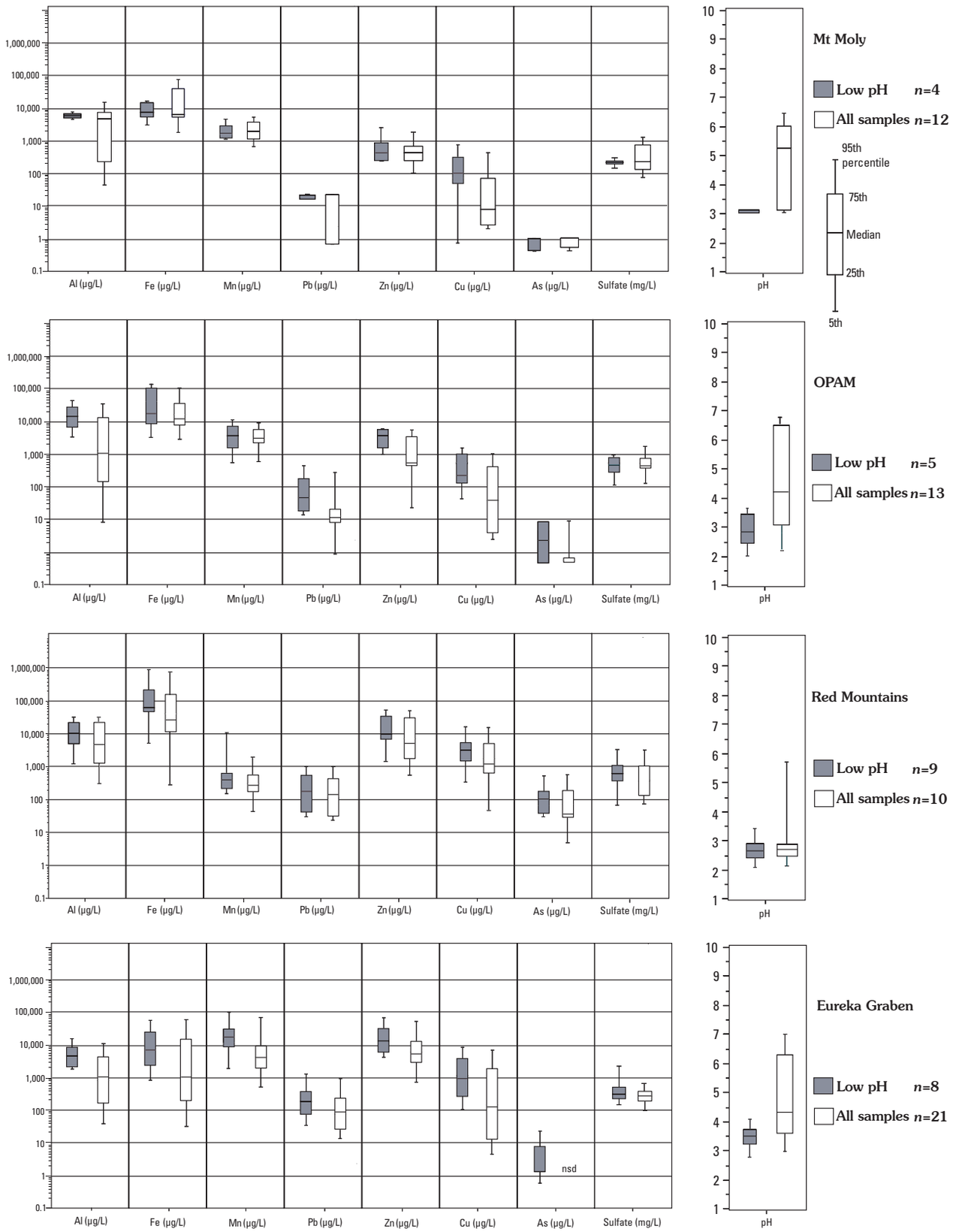

Figure 8. Box plots comparing chemistry of all mine water samples to only those with pH <4.5. Note: South Silverton discharge samples (11 of 12 samples > pH 4.5) shown only in figure 9; g/L, grams per liter; mg/L, milligrams per liter; µg/L, micrograms per liter; nsd, not sufficient data.

Table 5. Summary of mine water geochemistry from five different mineralized areas.

[SC, specific conductance; µS/cm, microsiemens per centimeter; µg/L, micrograms per liter; mg/L, milligrams per liter; gmean, geometric mean; *n*, number of samples; n.d., not determined]

	SC µS/cm	pH	Alkalinity mg/L as $CaCO_3$	SO_4	Ca	Mg	Na	K	Si	Al	As*	Ba	Be	Cd	Cr	Cu	Fe	Mn	Mo	Ni	Pb	Sr#	Zn
				mg/L						µg/L													
Mt Moly area:																							
pH <4.5 (*n*=4)[1]																							
25th percentile	560	3.12	n.d.	177	33.5	4.9	4.69	0.58	19.2	4,700	<1	3	<1	1.4	<15	53	4,770	1,140	<10	14	21	77	224
75th percentile	900	3.14	n.d.	363	95.3	8.8	6.73	0.84	22.4	6,970	1	13	1	13.4	15	629	6,940	2,870	15	14	21	404	2,280
gmean	693	3.13	n.d.	254	59.0	6.5	5.81	0.67	21.0	5,670	<1	8	<1	3.4	<15	148	5,790	1,600	<10	14	21	208	505
all samples (*n*=8)[1]																							
25th percentile	488	3.13	n.d.	153	34.1	4.8	4.48	0.50	16.1	288	<1	8	<1	0.9	<15	3	5,381	1,226	<10	11	1	125	245
75th percentile	1,165	5.87	18.5	572	172.1	14.8	7.00	0.81	24.0	7,379	1	14	1.5	2.3	<15	64	23,763	3,430	<10	14	21	1,388	599
gmean	680	4.60	n.d.	272	82.9	8.8	5.53	0.64	19.7	1,073	<1	10	1.1	1.7	<15	16	8,335	2,013	<10	<10	6	407	355
Red Mountains area:																							
pH <4.5 (*n*=9)[2]																							
25th percentile	935	2.40	n.d.	367	3.5	1.2	0.56	0.62	11.5	5,870	51.0	2	<1	43.5	<15	1,640	60,100	208	<10	16	42	39	9,770
75th percentile	1,840	2.79	n.d.	1,000	6.0	2.3	1.28	0.92	27.0	21,900	167.0	18	<1	170.2	<15	4,900	177,000	603	18	50	545	48	28,900
gmean	1,020	2.63	n.d.	514	5.5	2.3	0.85	0.87	16.6	7,870	103.2	7	<1	50.2	<15	2,340	63,300	401	14	28	177	37	10,600
all samples (*n*=10)[3]																							
25th percentile	614	2.40	n.d.	143	3.5	1.2	0.56	n.d.	8.5	1,849	30.0	2	<1	10.0	<15	638	11,252	205	<10	14	30	38	1,700
75th percentile	1,838	2.79	n.d.	1,000	7.2	3.3	1.43	n.d.	27.0	21,879	167.0	21	<1	170.2	<15	4,904	176,760	603	18	48	545	155	28,882
gmean	913	2.93	n.d.	446	7.2	2.3	0.90	n.d.	13.4	4,205	35.2	7	<1	33.7	<15	1,107	25,976	266	13	25	136	96	5,268
Ohio Peak–Anvil Mt area:																							
pH <4.5 (*n*=5)[1]																							
25th percentile	897	2.67	n.d.	416	25.2	10.3	1.23	n.d.	22.0	12,600	<1	6	<1	4.4	<15	204	10,200	2,960	n.d.	28	27	n.d.	2,170
75th percentile	1,620	3.62	n.d.	1,010	69.9	27.3	2.58	n.d.	35.0	29,500	11.3	19	4	35.3	<15	1,190	107,000	9,500	n.d.	70	233	n.d.	7,010
gmean	950	3.02	n.d.	498	43.4	15.4	1.86	n.d.	20.4	14,400	2.7	10	2	10.9	<15	314	23,900	3,750	n.d.	41	62	n.d.	3,640
all samples (*n*=8)[1]																							
25th percentile	1,055	3.21	n.d.	645	29.6	12.5	1.55	n.d.	17.5	250	<1	6.5	<1	1.35	<15	6	7,900	1,750	n.d.	14	11	280	729
75th percentile	1,783	6.70	47.5	1,025	239.5	20.9	7.63	n.d.	30.9	19,000	8.5	11	2	21.6	<15	632	53,378	8,325	n.d.	45	29	2,547	4,960
gmean	1,148	4.27	0.4	643	94.4	15.1	3.52	n.d.	19.6	1,129	2.0	9.4	1.2	4.94	<15	51	17,084	3,364	n.d.	25	16	706	751

Table 5. Summary of mine water geochemistry from five different mineralized areas.—Continued

	SC µS/cm	pH	Alkalinity mg/L as $CaCO_3$	SO_4	Ca	Mg	Na	K	Si	Al	As*	Ba	Be	Cd	Cr	Cu	Fe	Mn	Mo	Ni	Pb	Sr#	Zn
				mg/L						µg/L													
Eureka Graben area:																							
pH <4.5 (n=8)[4]																							
25th percentile	455	3.16	n.d.	164	24.0	3.5	0.37	0.63	8.6	1,480	<1	7	2	20.4	n.d.	218	1,910	5,700	<10	14	73	64	4,180
75th percentile	706	3.64	n.d.	363	59.1	6.2	1.61	0.94	12.9	5,250	7.1	12	4	106.0	n.d.	2,550	16,950	18,900	<10	22	278	254	19,200
gmean	541	3.37	n.d.	224	36.9	4.0	0.85	0.87	9.8	3,040	<1.2	8	2	42.1	n.d.	633	5,050	8,100	<10	18	170	124	9,570
all samples (n=13)[5]																							
25th percentile	378	3.36	0.0	147	26.3	2.8	0.5	0.6	4.2	116	<1	9.5	<1	7.8	n.d	10	121	1,223	<10	14	21	87	2,305
75th percentile	680	6.21	8.0	269	59.6	6.1	3.3	1.4	10.3	3,275	7.1	14	3	50.6	n.d.	1,409	11,519	7,339	<10	21	182	740	9,427
gmean	484	4.25	0.1	194	43.1	4.0	1.2	1.0	6.6	755	1.2	11	1	19.6	n.d.	120	842	3,307	<10	16	62	239	4,067
South Silverton area (n=12)[6]:																							
25th percentile	64	6.20		13	13.1	0.5	0.29	0.10	1.0	40	<1	6	<1	0.6	<15	5	3	6	n.d.	<10	1	n.d.	60
75th percentile	322	7.86		144	66.4	2.8	2.42	0.38	5.1	100	<1	15	<1	9.4	<15	98	130	503	n.d.	<10	114	n.d.	1,750
gmean	146	6.58		47	24.0	1.3	0.76	0.16	2.6	95	1.1	10	1	2.2	<15	27	26	63	n.d.	11	10	n.d.	313

[1]Mast and others, 2000; this volume.

[2]Seven samples from Mast and others, 2000; this volume; one from Colorado Department of Public Health and Education (CDPHE); Bove and Knepper, 2000; one sample from Division of Mines and Geology (DMG), Unpublished Cement Creek feasibility report, CDMG, 1998.

[3]Eight samples from Mast and others, 2000; this volume; one from Colorado Department of Public Health and Education (CDPHE); Bove and Knepper, 2000; one sample from Division of Mines and Geology (DMG), Unpublished Cement Creek feasibility report, CDMG, 1998.

[4]Four samples from Mast and others, 2000; four samples from Unpublished Cement Creek feasibility report, CDMG, 1998.

[5]Nine samples from Mast and others, 2000; four samples from Unpublished Cement Creek feasibility report, CDMG, 1998.

[6]All samples from Division of Mines and Geology (DMG), Unpublished Cement Creek feasibility report, CDMG, 1998.

*Arsenic data represents six analyses in both the Red Mountains and Eureka Graben areas.

#Red Mountains and Eureka Graben strontium data represent analysis of five and four samples, respectively.

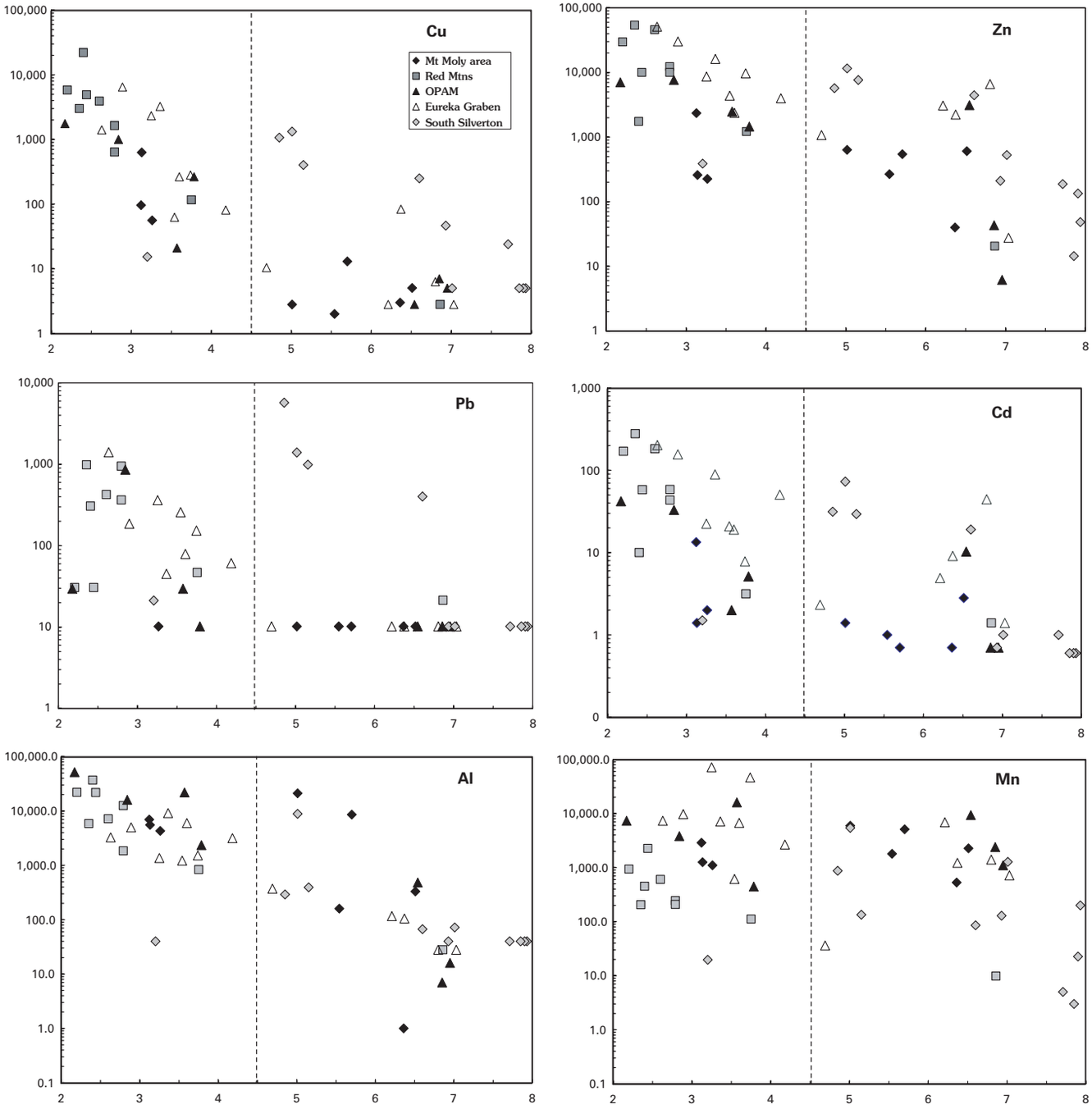

Figure 9. Graphs of metals versus pH for all mine waters from the five mineralized areas. All metal concentrations in micrograms per liter (*y* axes); pH, in standard units (*x* axes). Dashed vertical line is rough divide between low and high pH, as discussed in text.

potassium (1 mg/L), magnesium (10 mg/L), silicon (20 mg/L), zinc (247 µg/L), and copper (45 µg/L). The mean abundances of aluminum and iron were more than 2.5 times greater than in low-pH mine waters from this area, whereas ranges in zinc, copper, and sulfate were generally similar to those of low-pH mine waters. Although QSP-altered rocks have the lowest abundances in magnesium and manganese compared to other altered rocks in the Mount Moly area, mean concentrations of these elements in Mount Moly background QSP waters are among the highest of all water types. The relatively high magnesium and manganese concentrations in QSP waters is probably due to higher solubility of most base cations at these lower pH ranges and the availability of cations within islands of less-altered rock preserved within the larger QSP alteration zone. Mean sulfate concentration in these waters is very high (309 mg/L) compared to that of other background

Table 6. Ranges and geometric means of mine and background water geochemistry from five different mineralized areas.

[gmean, geometric mean; SC, specific conductance, in microsiemens per centimeter; nd, not determined; *n*, number of samples]

	SC µS/cm	pH	Alkalinity mg/L as $CaCO_3$	SO_4	Ca	Mg	Na	K	Si
				mg/L					
All mine waters (*n*=77)									
gmean	442	4.84	1.00	182	30.5	3.5	1.37	0.64	7.7
min	17	2.17	<1	3	2.0	0.2	0.07	0.64	1.0
max	3,140	8.17	122.00	5,000	400.0	42.0	10.00	0.64	38.0
All background waters (*n*=111)									
gmean	244	4.99	0.92	80	19.6	2.5	1.26	0.56	6.2
min	12	2.66	0.00	1	0.8	0.1	0.10	0.11	0.9
max	1,845	8.49	69.00	1,200	420.0	27.8	13.00	2.80	53.0

	Al	As	Ba	Be	Cd	Cr	Cu	Fe	Mn	Mo	Ni	Pb	Sr	Zn
	µg/L													
All mine waters (*n*=77)														
gmean	672	2.0	10	1	7.4	7	85	1,272	698	6	15	269	28	1,255
min	1	0.1	1	1	0.6	1	2	3	3	1	2	23	1	6
max	51,863	580.0	54	5	278.7	20	22,000	120,000	71,600	42	110	4,351	5,606	52,370
All background waters (*n*=111)														
gmean	518	nd	23	1	1.7	9	10	235	88	9	16	17	189	66
min	1	nd	1	1	0.3	1	1	1	1	1	1	1	6	20
max	54,020	nd	101	65	84.0	50	372	76,652	74,669	70	43	141	5,700	14,383

samples from the study area (table 6), whereas corresponding calcium (25 mg/L) and strontium (172 µg/L) are relatively low. $\delta^{34}S$ values from three QSP-related waters range from +1.7 to +3.9 per mil (Nordstrom and others, this volume, table 1), which is close to the range of all sulfides analyzed from the area (–3.1 to +2.5 per mil; table 7). These combined data suggest that much of the dissolved sulfate was derived from the oxidation of fine-grained pyrite in the QSP-altered rocks. These waters with sulfate that is likely related, for the most part, to the oxidation of pyrite contrast markedly with those that likely had more interaction with vein-filling gypsum or anhydrite within weakly sericitized rocks (WS-gyp; fig. 11). Waters likely influenced by the dissolution of isotopically heavy gypsum or anhydrite (WS-gyp) have measurable alkalinity, greater than two times the mean sulfate (702 mg/L), and more than nine times the calcium (251 mg/L mean) and strontium (2,370 µg/L) concentration of QSP waters. $\delta^{34}S$ values of three of the WS-gyp-related waters were substantially heavier ($\delta^{34}S$= +7.0 to +8.0 per mil) than the QSP waters, due to interaction with gypsum or anhydrite ($\delta^{34}S$= +14.6 to +18.0 per mil in the entire Animas River watershed study area; table 7; Casadevall and Ohmoto, 1977). WS-gyp waters have the highest manganese concentrations (1,490 µg/L mean) of all background streams and springs in the Mount Moly area. This may indicate dissolution of manganese silicate or manganese carbonate gangue minerals occurring with gypsum or anhydrite along fracture zones.

Streams and springs draining calcite-bearing propylitic-altered rock have the highest mean values of pH and alkalinity (6.74 and 16.4 mg/L, respectively) and the lowest mean dissolved metal concentrations (13 mg/L aluminum; 5 µg/L iron; 26 µg/L zinc; 3 µg/L copper) of all Mount Moly area water samples. Sulfate concentrations for these 10 propylitic samples (table 8) have a bimodal distribution (fig. 12); six samples from a low-sulfate group have concentrations ranging from 19 to 77 mg/L, whereas the remaining samples have values ranging from 210 to 263 mg/L. Sulfate shows a strong positive correlation with strontium and calcium, both of which also are bimodally distributed within this sample set (fig. 12). $\delta^{34}S$ data from three of these waters show fairly predictable associations, with the lightest (–2.8 and –0.8 per mil) and heaviest (+7.1 per mil) values correlated with the low and high sulfate-calcium-strontium groups, respectively. As discussed previously, the WS-gypsum-related waters show similar associations between anomalously high sulfate-calcium-strontium and heavy $\delta^{34}S$ values. Therefore, we suggest that sulfate in the propylitic waters is derived both by pyrite oxidation and gypsum or anhydrite dissolution.

Samples draining rocks of the weak sericite-pyrite assemblage (WSP) have a mean pH of 4.52 and fall compositionally between QSP and PROP samples, reflecting the transition between the two alteration assemblages (table 8; fig. 11). Alkalinity within most WSP samples is measurable and ranges up to 10 mg/L; calcite was still detected in many of these altered rocks. In contrast, the low pH of QSP

Table 7. Stable isotope data for vein and alteration minerals present within the study area.

[Samples not taken from five main mineralized areas are shown in italics (American tunnel, S. Silverton). Data in per mil values. x, vein sample; --, not meaningful or not determined]

Sample	Mineral	Vein	Mineralogical notes	$\delta^{18}O$	$\delta^{18}O_{Total}$	$\delta^{18}O_{SO4}$	$\delta^{18}O_{OH}$	$\delta^{34}S$ sulfide	$\delta^{34}S$ sulfate	δD
			Mount Moly area							
SDY3997	pyrite		Fine blebs of 1-2 mm dissem pyrite in QSP zone	--	--	--	--	2.5	--	--
SDY05A97	pyrite		Fine blebs of 1-2 mm dissem pyrite in QSP zone	--	--	--	--	0.7	--	--
SDPH01PY	pyrite		Medium-grained pyrite, fracture in hyd prop zone	--	--	--	--	0.9	--	--
SDY10B98	pyrite	x	Medium-grained pyrite in qtz vein in central QSP zone	--	--	--	--	–3.1	--	--
SDY0398	barite	x	Vein in QSP-altered rock	--	--	--	--	17.4	--	--
BONNERPY	pyrite	x	Late-stage pyrite in 3 mm vein	--	--	--	--	2.0	--	--
BONNERGA	galena	x	Coarse mid-stage vein galena	--	--	--	--	–0.2	--	--
BONNERSP	sphalerite	x	Coarse mid-stage vein sphalerite	--	--	--	--	0.3	--	--
PPSO4-1	gypsum	x	White, fine-granular, vein margin at Paradise Portal	--	--	4.7	--	--	14.6	--
			Red Mountains area							
IDB61B	pyrite		Finely disseminated pyrite, QSP zone Prospect Gulch	--	--	--	--	–1.5	--	--
IDB40	pyrite		Finely disseminated pyrite, QSP zone Prospect Gulch	--	--	--	--	–1.7	--	--
IDB98	pyrite		Finely disseminated pyrite, QSP zone Prospect Gulch	--	--	--	--	–4.7	--	--
IDB04 PY	pyrite		Finely disseminated pyrite, quartz-pyrophyllite-alunite zone Red Mtn #3	--	--	--	--	–5.0	--	--
HMT-804-602PY	pyrite		Finely disseminated pyrite, quartz-alunite zone 602' beneath upper Lark mine	--	--	--	--	–6.9	--	--
IDB1496	alunite		Fine-grained replacement alunite, Red Mtn #3	--	--	--	--	--	10.0	--
IDB0696	alunite		Fine-grained replacement alunite, Red Mtn #3	--	--	--	--	--	14.6	--
IDB1296	alunite		Fine-grained replacement alunite, Red Mtn #3	--	5.8	11.1	--	--	17.5	–63
IDB9997	alunite		Fine-grained replacement alunite, Prospect Gulch breccia	--	--	--	--	--	15.4	--
IDB10097	alunite		Coarse-grained vein alunite, Prospect Gulch	--	2.7	11.1	--	--	27.0	–94
LS998 PY	pyrite	x	Fine-grained vein pyrite, Lark mine stage 3b (see text)	--	--	--	--	–3.6	--	--
LS2B PY	pyrite	x	Fine-grained vein pyrite, Lark mine stage 3b (see text)	--	--	--	--	–3.9	--	--
GQWSTPY	pyrite	x	Fine-grained vein pyrite, Prospect Gulch, above Galena Queen, stage 3b (see text)	--	--	--	--	–2.8	--	--
LS998 SPH	sphalerite	x	Coarse vein sphalerite, Lark mine, stage 2a (see text)	--	--	--	--	–3.9	--	--
GQ498SPH	sphalerite	x	Coarse vein sphalerite, Galena Queen mine, stage 2a (see text)	--	--	--	--	–4.7	--	--
GQ398 GA	galena	x	Coarse vein galena, Galena Queen mine, stage 2a	--	--	--	--	–3.6	--	--

Table 7. Stable isotope data for vein and alteration minerals present within the study area.—Continued

Sample	Mineral	Vein	Mineralogical notes	$\delta^{18}O$	$\delta^{18}O_{Total}$	$\delta^{18}O_{SO4}$	$\delta^{18}O_{OH}$	$\delta^{34}S$ sulfide	$\delta^{34}S$ sulfate	δD
			Red Mountains area—Continued							
GQ498 PY	pyrite	x	Fine-grained vein pyrite, Galena Queen mine, stage 3b (see text)	--	--	--	--	–3.4	--	--
104SP	sphalerite	x	Coarse vein sphalerite, Henrietta mine, stage 2a?	--	--	--	--	–1.1	--	--
HENBAR-1	barite	x	Late-stage vein barite, Henrietta mine dump	--	--	--	--	31.5	--	--
IDB01	dickite		Replacement after plagioclase, waxy	4.6	--	--	--	--	--	–94
GQWEST	dickite		Waxy vein-related gangue	5.2	--	--	--	--	--	–90
NBELLE-1	kaolinite		Soft, white, along 0.5 cm veinlet, dump sample at National Belle; post-sulfides	–3.7	--	--	--	--	--	–123
IDB98	illite		$2m_1$/1m polytype, after breccia in upper Prospect Gulch, QSP zone	–0.3	--	--	--	--	--	--
PDB7B	illite		Poorly crystalline illite in weak sericite-pyrite zone (WSP) in upper Prospect Gulch	–3.5	--	--	--	--	--	--
			Ohio Peak–Anvil Mountain area							
SDB39	pyrite		Finely disseminated pyrite, QSP zone, mid Topeka Gulch	--	--	--	--	–2.3	--	--
SDB38	pyrite		Finely disseminated pyrite, QSP zone, mid Topeka Gulch	--	--	--	--	–5.4	--	--
TG-GNA	galena	x	Coarse-grained, mid stage-vein galena, lower Topeka Gulch	--	--	--	--	–0.8	--	--
TG-1	gypsum	x	Coarse, clear vein? gypsum; mine dump lower Topeka Gulch	--	--	3.6	--	--	17	--
TG-BAR	barite	x	Late-stage, vein barite, lower Topeka Gulch	--	--	--	--	--	28.9	--
SDB4196	alunite		Fine-grained replacement alunite, upper Topeka Gulch	--	--	--	--	--	24.0	--
			American tunnel							
B1-1918PY	gypsum	x	Fine-grained pyrite in vein with anhydrite, 1,918 ft below A.T.	--	--	--	--	–1.6	--	--
B1-1685	gypsum	x	Coarse, clear vein gypsum, 1,685 ft below A.T.	--	--	–1.9	--	--	16.7	--
B1-1918AN	anhydrite	x	Vein anhydrite, 1,918 ft below A.T.	--	--	–3.3	--	--	17.3	--
B1-1900	anhydrite	x	Vein anhydrite, 1,900 ft below A.T.	--	--	1.1	--	--	18.0	--
			Near South Silverton							
NSM-1	gypsum	x	Coarse, clear vein gypsum; adjacent to QSP margin	--	--	1.1	--	--	15.2	--

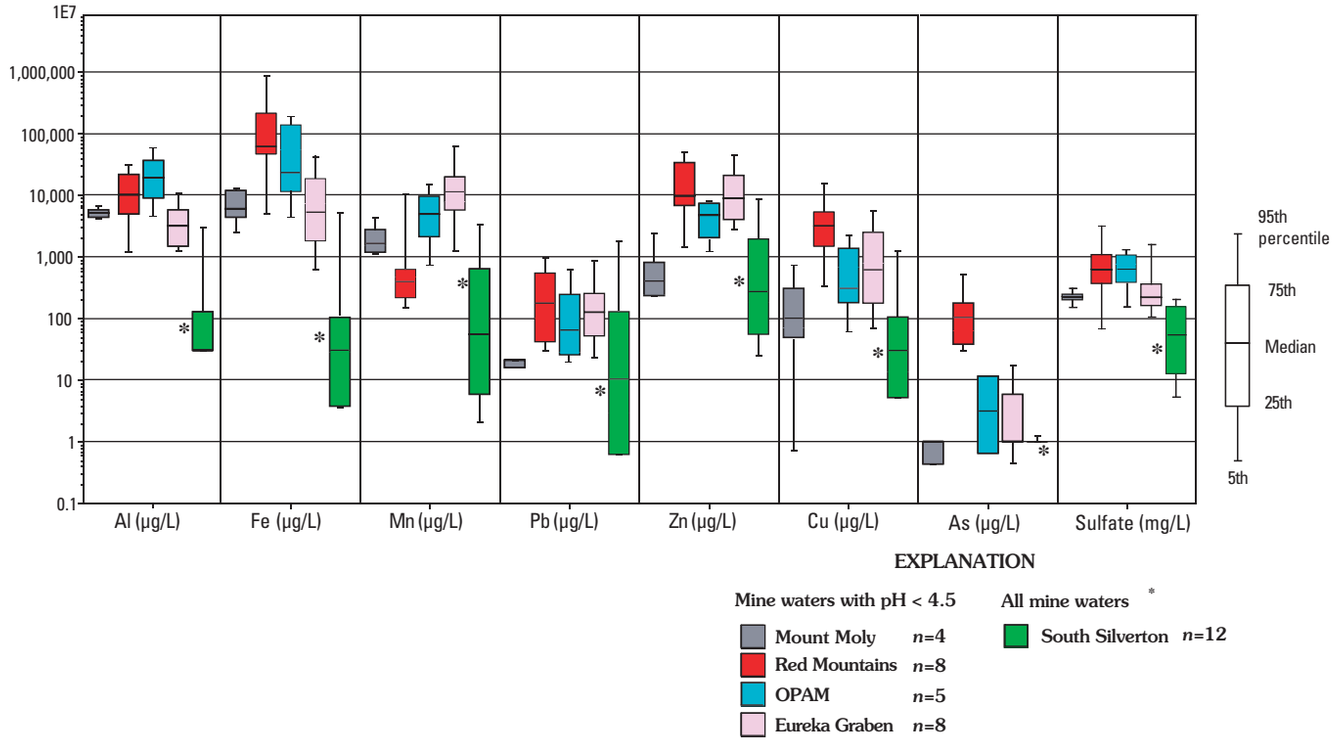

Figure 10. Box plots comparing low-pH mine water data from the five mineralized areas. Note that South Silverton data represent high-pH samples as only one sample had pH below 4.5. Vertical scales in micrograms per liter (µg/L) except for sulfate, in milligrams per liter (mg/L); *n*, number of analyses.

samples reflects the scarcity of calcite in the large volume of rock from which these waters drain. The paucity of calcite in QSP-altered rocks is attributed to the low pH of the ancient hydrothermal fluids that formed this mineral assemblage (Rose and Burt, 1979; Ringrose, 1982). Along with the changes in pH and alkalinity in these varied water types, note that dissolved magnesium increases from a mean of 2 to 3 mg/L in PROP and WSP waters, respectively, to 10 mg/L in QSP waters (table 8). These changes must be related to a marked increase in the rate of chlorite dissolution in these more acidic waters, as other magnesium-bearing minerals are absent in the associated altered rocks. These data confirm laboratory leach experiments (Jambor and others, 2000) documenting accelerated rates of chlorite dissolution in highly acidic solutions (pH <3.5). Although experimental data predict that chlorite dissolution in low-pH water has some acid-neutralizing potential (Lawrence and Wang, 1997; Jambor and others, 2000), the low pH of the QSP waters suggests that the degree of chlorite breakdown has done little to neutralize all the acid generated by pyrite oxidation.

As a group, all water samples collected in the Mount Moly area have higher concentrations of sodium compared to the other four mineralized areas, with upper concentrations ranging from 7 to 13 mg/L. Similar enrichments in sodium are only observed in two other areas within the entire study area—Chattanooga bend and Topeka Gulch (Yager and Bove, this volume, pl. 1). As discussed in Mast and others (this volume), waters in both areas were derived by interaction with rocks that were enriched in secondary albite, probably during the regional episode of propylitic alteration. Although not apparent in summary tables of end-member background waters (table 8), seven samples in the entire Mount Moly background data set have substantially elevated molybdenum concentrations (21–70 µg/L). In combination with elevated copper (25–372 µg/L), these data reflect the presence of molybdenite and secondary copper mineralization in this subeconomic porphyry system.

23 Ma Acid-Sulfate Alteration and Mineralization

The study area hosts two of the largest acid-sulfate hydrothermal systems in the western United States. The Red Mountains system (fig. 1) encompasses an area of roughly 22 km^2 and was host to economically important silver-copper-lead breccia-pipe and fault-hosted mineralization (Burbank and Luedke, 1969; Bove and others, 2000). The Ohio Peak–Anvil Mountain (OPAM) acid-sulfate system is very similar both in size (21 km^2) and character of alteration; however, unlike its northern counterpart, it is largely devoid of important mineral deposits. Both areas are located along the structurally complex northwest and southwest margins of the 27 Ma Silverton caldera.

Table 8. Summary of background waters from five different mineralized areas.[1]

[PROP, propylitic; PROP-V, propylitic with vein-related alteration; WSP, weak sericite-pyrite; WSP-gyp, WSP with gypsum in fractures; SC, µS/cm, specific conductance, in microsiemens per centimeter; n.d., not determined; nsd, not sufficient data for statistical summary; gmean, geometric mean]

		SC (µS/cm)	pH	Alkalinity mg/L as $CaCO_3$	SO_4	Ca	Mg	Na	K	Si	Al	Ba	Be	Cd	Cu	Fe	Mn	Mo	Pb	Sr	Zn
					mg/L						µg/L										
Mt Moly area:																					
PROP (*n*=10)	25th percentile	136	6.52	9.9	30	21.3	1.3	1.73	0.3	4.2	3	20	1	1.0	1	<3	<1	<10	<30	140	<3
	75th percentile	493	6.86	29.0	210	86.5	4.7	3.00	0.4	7.0	52	30	1	2.0	4	16	30	<10	<30	873	32
	gmean	237	6.74	16.4	75	39.6	2.3	1.98	0.3	4.7	13	24	1	1.5	3	5	6	<10	<30	292	26
WSP (*n*=10)	25th percentile	235	3.82	<0.5	92	24.5	2.6	3.68	0.4	11.8	480	19	1	2.0	4	312	260	<10	<30	178	20
	75th percentile	458	4.85	<0.5	178	55.9	4.6	5.08	0.7	18.9	2,300	25	1	2.0	4	814	490	18	<30	386	51
	gmean	301	4.52	<0.5	120	35.7	3.1	4.06	0.5	13.2	843	19	1	1.7	5	457	296	<10	<30	251	30
WSP-gyp (*n*=6)	25th percentile	1,173	4.72	1.1	600	207.5	6.6	6.08	0.6	12.8	414	9	1	1.0	8	402	642	<10	<30	1,570	20
	75th percentile	1,791	6.01	29.3	1,150	405.0	17.0	7.53	0.8	18.0	1,630	12	1	1.8	11	1,650	2,450	<10	<30	4,780	98
	gmean	1,413	5.06	2.9	788	286.2	9.8	7.13	0.7	15.3	343	10	1	1.5	13	826	1,180	<10	<30	2,660	40
QSP (*n*=10)	25th percentile	493	3.05	n.d.	185	16.1	4.9	5.01	0.9	16.2	8,710	16	1	2.0	21	15,300	822	<10	<30	70	253
	75th percentile	1,172	3.37	n.d.	658	81.1	26.1	6.12	1.1	24.6	49,900	36	1	2.0	131	54,900	1,379	<10	<30	640	351
	gmean	759	3.22	n.d.	333	27.7	9.8	3.73	1.0	20.2	18,400	22	1	2.1	45	22,200	775	<10	<30	181	247
Red Mountains area:																					
PROP (*n*=4)	25th percentile	48	5.80	8.2	7	6.2	1.0	0.32	0.2	1.1	<1	34	1	2.0	4	30	5	<10	<30	289	<3
	75th percentile	101	6.19	27.8	27	14.4	2.2	1.00	0.2	1.7	<1	62	1	2.0	5	39	25	23	<30	601	<3
	gmean	62	6.04	11.1	10	8.3	1.3	0.54	0.2	1.4	<1	46	1	2.0	4	37	9	16	<30	298	<3
PROP-V (*n*=4)	25th percentile	243	3.09	<0.5	108	12.9	2.0	0.34	n.d.	3.4	120	9	1	2.0	4	37	420	<10	<30	125	74
	75th percentile	671	5.18	4.5	197	35.1	8.3	1.08	n.d.	11.1	6,460	49	1	2.0	15	19,900	845	<10	<30	473	402
	gmean	251	4.12	0.6	52	12.3	2.8	0.50	n.d.	6.2	788	18	1	2.0	8	853	208	<10	<30	128	137
WSP (*n*=4)	25th percentile	93	3.98	<0.5	29	8.8	1.3	0.41	0.2	1.7	102	31	1	2.0	4	36	62	15	<30	152	<3
	75th percentile	130	5.41	7.6	52	15.8	2.2	0.78	0.4	2.6	662	37	1	2.0	6	174	233	22	<30	482	<3
	gmean	106	4.63	0.9	35	9.3	1.5	0.49	0.3	2.1	229	35	1	2.0	5	82	115	17	<30	144	<3

Table 8. Summary of background waters from five different mineralized areas.—Continued

		SC (µS/cm)	pH	Alkalinity mg/L as $CaCO_3$	SO_4	Ca	Mg	Na	K	Si	Al	Ba	Be	Cd	Cu	Fe	Mn	Mo	Pb	Sr	Zn
					mg/L						µg/L										
Red Mountains area:																					
QSP (*n*=5)	25th percentile	287	3.25	n.d.	118	6.3	4.1	0.22	0.5	6.1	1,760	27	1	2.0	12	461	469	12	<30	65	123
	75th percentile	654	3.72	n.d.	238	33.8	7.4	0.32	0.5	10.3	8,840	44	1	2.0	45	5,212	1,160	21	38	285	156
	gmean	348	3.33	n.d.	137	15.4	4.7	0.32	0.5	7.3	4,500	32	1	2.2	22	1,706	576	16	33	168	117
AS-all samples (*n*=13)	25th percentile	48	3.20	nsd	10	1.3	0.3	0.25	0.7	3.8	204	21	nsd	0.30	4	81	12	nsd	<30	nsd	20
	75th percentile	233	3.67	nsd	57	4.0	0.7	0.39	0.7	7.7	4,400	39	nsd	0.60	16	790	71	nsd	<30	nsd	45
	gmean	110	3.50	nsd	26	2.3	0.5	0.30	0.7	5.3	1,150	32	nsd	0.53	11	300	33	nsd	35	nsd	37
AS-subgroups																					
fresh sulfides (*n*=7)	25th percentile	206	3.03	n.d.	45	1.4	0.6	0.26	0.7	5.0	3,400	20	n.d.	0.3	14	565	46	n.d.	<30	n.d.	39
	75th percentile	286	3.40	n.d.	72	6.0	1.2	0.40	0.9	10.3	4,750	30	n.d.	0.5	45	1,100	145	n.d.	44	n.d.	106
	gmean	283	3.17	n.d.	61	3.0	0.9	0.32	0.8	6.9	4,080	24	n.d.	0.4	27	1,140	79	n.d.	41	n.d.	64
oxidized sulfides (*n*=6)	25th percentile	30	3.49	nsd	8	1.4	0.2	0.26	0.7	2.7	163	35	nsd	0.3	4	33	9	nsd	<30	nsd	<3
	75th percentile	57	4.40	nsd	10	2.0	0.3	0.30	0.7	5.6	323	75	nsd	2.0	4	83	17	nsd	<30	nsd	<3
	gmean	37	3.92	nsd	10	1.7	0.3	0.28	0.7	3.8	262	47	nsd	0.8	4	63	12	nsd	<30	nsd	<3
Ohio Peak–Anvil Mountain area:																					
PROP (*n*=2)	min	146	6.99	30.5	41	23.0	1.9	1.15	n.d.	2.4	<1	42	1	2.0	4	30	3	<10	<30	363	<3
	max	168	7.46	34.0	53	24.4	4.2	1.24	n.d.	3.7	63	93	1	2.3	4	37	13	<10	<30	405	<3
	gmean	157	7.22	32.2	47	23.7	2.8	1.19	n.d.	3.0	50	62	1	2.1	4	33	6	<10	<30	383	<3
QSP (*n*=9)	25th percentile	500	3.21	n.d	173	15.9	3.1	1.88	0.7	21.3	6,600	16	1	1.0	7	2,950	332	<10	<30	38	76
	75th percentile	673	3.56	n.d	370	55.0	7.6	6.00	2.5	47.0	16,000	29	2	2.0	41	13,000	1,300	16	<30	114	206
	gmean	396	3.52	n.d	132	21.0	3.9	2.96	1.3	24.1	5,150	16	1	1.4	20	4,370	539	13	<30	44	142
AS-oxidized sulfides (*n*=2)	min	17	3.88	n.d	4	1.5	0.3	0.97	0.3	8.1	74	39	1	2.0	4	33	3	<10	<30	13	<3
	max	70	5.53	2.6	21	4.2	0.7	1.12	0.4	10.1	599	78	1	3.1	4	211	46	<10	<30	34	29
	gmean	34	4.63	n.d.	9	2.5	0.5	1.04	0.3	9.1	211	55	1	2.5	4	83	12	<10	<30	21	24

Table 8. Summary of background waters from five different mineralized areas.—Continued

		SC (µS/cm)	pH	Alkalinity mg/L as $CaCO_3$	SO_4	Ca	Mg	Na	K	Si	Al	Ba	Be	Cd	Cu	Fe	Mn	Mo	Pb	Sr	Zn
					mg/L						µg/L										
Eureka Graben area:																					
PROP (*n*=3)	min	87	6.92	10.0	28	12.8	0.8	0.43	0.5	1.2	<1	12	1	2.0	4	30	3	<10	30	81	<3
	max	287	6.97	34.5	113	41.8	5.0	1.37	0.5	2.6	<1	34	1	2.0	4	30	4	14	30	349	237
	gmean	179	6.95	17.6	60	27.3	2.1	0.64	0.5	1.6	<1	19	1	2.0	4	30	3	11	30	145	46
PROP-V (*n*=13)	25th percentile	109	5.81	1.0	44	19.5	1.5	0.70	0.3	1.6	<1	18	1	2.0	4	30	9	<10	30	100	20
	75th percentile	254	7.16	21.2	103	37.9	3.1	1.14	0.5	3.1	112	25	1	2.0	5	30	922	<10	30	254	470
	gmean	184	6.24	5.1	69	27.8	2.4	0.82	0.4	2.3	142	22	1	3.0	9	31	53	<10	30	163	143
V-QSP (*n*=3)	min	609	3.26	n.d.	313	22.5	4.3	0.92	0.4	7.6	4,230	7	3	2.0	4	30	2,670	<10	30	60	640
	max	793	4.55	n.d.	430	76.6	11.5	2.98	2.2	10.6	39,700	15	65	84.0	309	5,690	74,700	<10	30	229	14,400
	gmean	711	3.88	n.d.	366	49.1	8.0	1.90	1.1	9.0	16,900	10	13	9.0	48	172	10,900	<10	30	113	3,530
South Silverton area:																					
PROP (*n*=4)	min	232	8.13	50.0	55	39.7	1.9	1.96	0.5	2.7	<1	20	1	2.0	4	30	3	<10	30	422	<3
	max	260	8.42	59.0	81	44.6	3.2	2.51	0.5	3.1	77	48	1	2.0	4	30	7	<10	30	585	<3
	gmean	225	8.15	52.7	61	37.6	2.4	2.02	0.5	2.8	52	21	1	2.0	4	30	5	13	30	358	21

[1]Values cited in the text for individual samples are available in the database CD-ROM; see Sole and others, this volume, Chapter G.

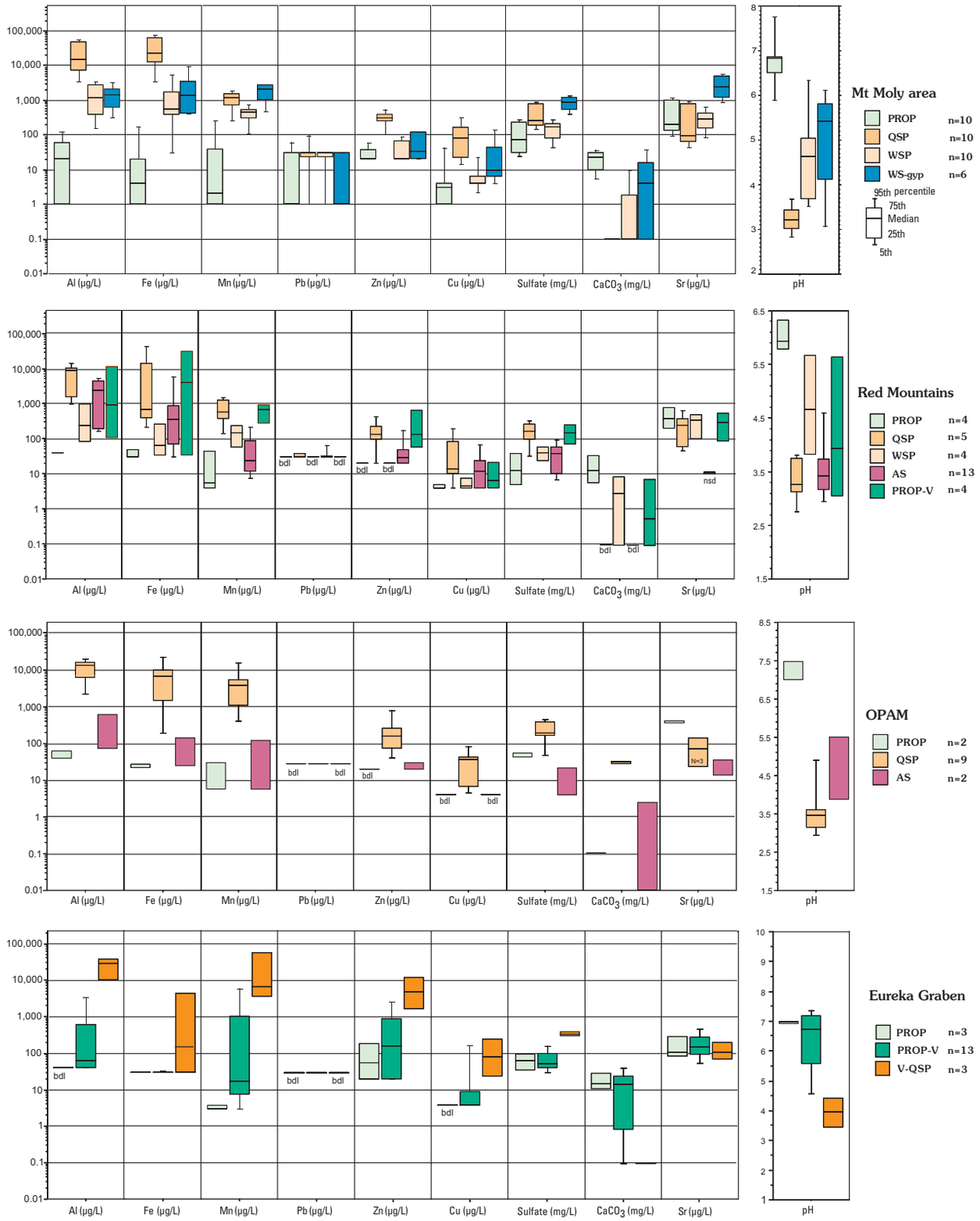

Figure 11. Box plots comparing geochemistry of background waters draining different alteration assemblages. South Silverton data are not presented because only PROP waters were sampled. See text for details on alteration assemblages; *n*, number of samples; Alk, alkalinity as $CaCO_3$; bdl, below detection limit. PROP, propylitic; PROP-V, vein-related propylitic; WSP, weak sericite-pyrite; WS-gyp (see text); QSP, quartz-sericite-pyrite; V-QSP, vein-related quartz-sericite-pyrite; AS, acid-sulfate.

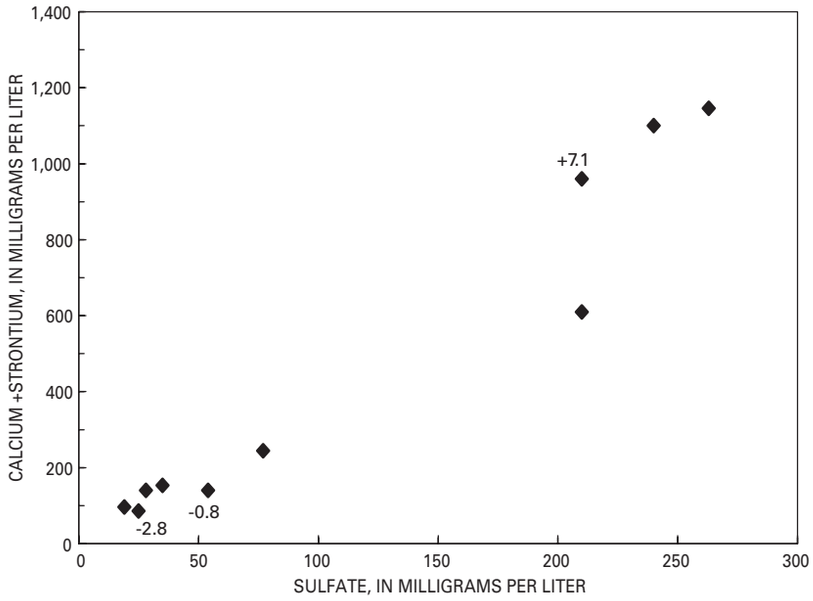

Figure 12. Dissolved sulfate versus calcium plus strontium in propylitic water in Mount Moly alteration area; shows corresponding values of $\delta^{34}S$ values for three of these samples. (See Nordstrom and others, this volume, table 1.) The calcium/strontium-rich waters that are also rich in sulfate probably have interacted with gypsum or anhydrite.

Red Mountains Area Ore Deposits

The majority of the economically important breccia-hosted deposits in the Red Mountains area lies within a belt trending N. 20°–30° E., roughly 6 km long and 2 km wide (fig. 13). This zone is bounded by Ironton Park on the north, the Carbon Lake mine area on the south, Red Mountain–Mineral Creeks on the west, and Red Mountains #2 and #3 on the east. It marks the intersection of the northeastern ring fracture zone of the Silverton caldera and a 6 km-wide zone of veins and faults trending N. 40°–45° W. (Yager and Bove, this volume, pl. 1). Here, many 23 Ma dacite porphyry stocks were intruded at high crustal levels (Bove and others, 2001). Other contemporaneous mines and prospects, with ores similar to that in the zone just described, are present at the heads of Prospect, Dry, Georgia, and Corkscrew Gulches (fig. 13) (Ransome, 1901; Bove and others, 2000).

Mines of the Red Mountains area were active between 1882 and 1900, whereas since 1900 there has been only minor mining activity (Hillebrand and Kelley, 1959). The deposits were noted for rich silver-lead-copper ores; individual deposits typically contained from 50 to a few hundred ounces silver and 15–40 percent lead and copper, and minor gold. Total production for these mines was between 10 and 20 million dollars, which was limited due to the small size and irregular shape of the orebodies, and the extremely corrosive nature of the mine waters (Hillebrand and Kelley, 1959). The area experienced a resurgence of exploration activity for gold in the late 1970s and early 1980s, as reflected by the myriad of drill roads near Red Mountain #3 and above Corkscrew Gulch (fig. 13).

In the vicinity of Red Mountain Pass (fig. 13), the breccia bodies are surficially expressed as prominent silicified knolls (45–150 m wide) that rise from 8 to 60 m above the valley bottoms (Ransome, 1901; Hillebrand and Kelley, 1959). The entire breccia masses are nearly vertical, irregularly cylindrical bodies (90–600 m long by 30–425 m wide) with crescent to ellipsoidal cross sections, surrounded by a zone of silicified and highly pyritic rock (Ransome, 1901). Some of the breccia bodies transition into relatively unbroken wallrock, whereas some of the smaller masses have abrupt boundaries. The better delineated breccia bodies are encircled by a zone of vertically sheeted jointing and appear to be localized at intersections of multiple fractures or faults.

East of Red Mountain Pass, in the headwaters of Prospect, Dry, and Corkscrew Gulches (fig. 13), hydrothermal breccias are also common; however, classic mineralized “breccia bodies,” such as those observed in the Red Mountain Pass area, are not as well exposed at the surface. Instead, mineralized hydrothermal breccias were generally localized along preexisting fissures and occur in irregular, anastomosing zones emanating outward from the fissure breccias (Bove and others, 2000). Several of the more classic-looking polymetallic vein deposits on the periphery of the Red Mountain acid-sulfate system (for example the Carbonate King in Corkscrew Gulch, the Henrietta mine, in south Prospect Gulch (mine # 84), and the Kansas City mine in Georgia Gulch (mine # 145; Church, Mast, and others, this volume, fig. 3) have associated breccias and acid-sulfate-related gangue minerals. The presence of these features indicates that the deposits are genetically linked to the mineralized breccias within the interior of the acid-sulfate system.

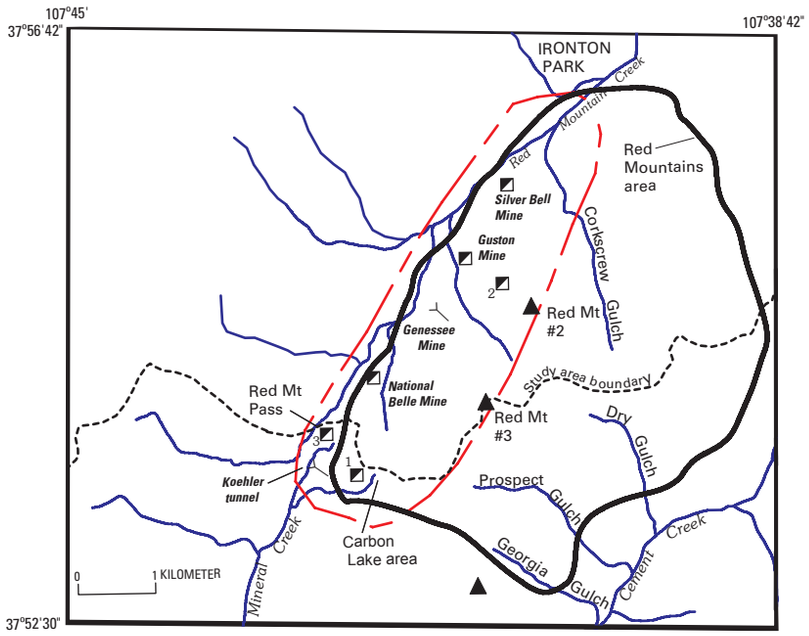

Figure 13. Zone of economically important breccia-hosted ore deposits (red line) in Red Mountains area. Congress and St. Paul mines (1); Grand Prize mine (2); Longfellow mine (3).

Although records are incomplete—because many of the mines were closed before geological studies could be made—Ransome (1901) reconstructed a vertical mineral zonation throughout the breccia deposits. The upper parts of the orebodies consist of silver-bearing galena, with sphalerite and pyrite. These ores grade downward into silver-rich copper ores of enargite, tetrahedrite, stromeryite, bornite, and chalcopyrite, which gradually diminish downward with increasing amounts of low-grade pyrite. The following general paragenetic sequence was ascertained by Nash (1975) from fragments of ore on mine dumps: (1) early acid-sulfate-related silicification with fine pyrite and high-temperature clays; (2) galena overlapped by sphalerite; (3) enargite and other copper minerals; and (4) barite, calcite, fluorite, bornite, and minor gold. Paragenetic studies of ore material from the Lark, Galena Queen, and Hercules mines in Prospect Gulch (D.J. Bove, unpub. data, 2002) confirm Nash's observations in the early ore-bearing stages, and also reveal complex interrelationships between repeated episodes of hydrothermal brecciation, ore mineralization, and acid-sulfate gangue deposition. Compositions of the major ore minerals from these Prospect Gulch mines (Wirt and others, 1999; D.J. Bove, unpub. data, 2002) are comparable to those in the Red Mountain Pass area, just to the west (see various analytical data in Ransome, 1901). The presence of abundant copper-arsenic-antimony-rich ores containing enargite and tetrahedrite-tennantite, as well as copper ores of chalcocite, bornite, and covellite, distinguish these and similar breccia ores from more typical polymetallic vein deposits within and outside the Red Mountains area.

In some mines such as the National Belle, Grand Prize (fig. 13), Enterprise, and Vanderbilt, oxidized ores were present in the upper 100 m of the deposit, either attached to the walls of caves, as broken detached masses within the caverns, or as bedded deposits with clayey mud and sand filling the caves (Schwarz, 1883). The ore-bearing caves, which were present throughout the upper silicified zones, can still be seen today along the cliff base and margins of the silicified outcroppings. Chambers are as much as 15 m in diameter and are interconnected by irregular rounded passages that branch out toward the surface and pinch and intersect at depth. Oxidized lead ores mined in these upper levels accounted for most of the early production. These ores consisted mostly of lead and iron carbonates and sulfates with galena cores, with various iron oxides and arsenates (Schwarz, 1883); the entire ore masses were encrusted by limonite and goethite. Botryoidal masses of sphalerite were also found within the caverns along with the highly oxidized galena. Intermingled with the cave ores were abundant fine "spongy" quartz, crystalline dickite/kaolinite, diaspore, pyrophyllite, and alunite.

Most of the Red Mountains breccia ores are unoxidized and generally formed beneath the shallow oxidized ore zone (Schwarz, 1883). These so-called "primary" ores (Ransome, 1901) generally begin where the cave ores cease. However, in many deposits, such as the Congress, St. Paul, Galena Queen, Yankee Girl, Guston, and Silver Bell (fig. 13), either the upper cavernous oxidized zone was eroded, or it never existed (Ransome, 1901). In these mines, unoxidized ores were commonly present near ground surface. Although the unoxidized

orebodies are typically massive and solid aggregates, ore specimens such as enargite, pyrite, and polybasite preserved from several mines are distinctly botryoidal or stalactitic in nature. Ores of this nature were reported to have grown within caverns and open spaces in the unoxidized ore zone (Ransome, 1901). The most common "primary" ores include enargite, galena, chalcopyrite, pyrite, chalcocite, bornite, tetrahedrite-tennantite, sulfobismuthites, and stromeryite (Schwarz, 1883). The upper unoxidized galena ores typically carried a few tens to 100 oz silver per ton and as much as 60 percent lead (Ransome, 1901). Deeper copper-bearing ores were almost always richer, with grades of 100 oz/ton to sometimes more than 1,500 oz silver/ton and 15–25 percent copper. Grades diminished in the lower pyrite-rich ores that contained less than 20 and 5 ounces silver and copper, respectively, per ton.

Ohio Peak–Anvil Mountain Mineralization and Ore Deposits

In contrast to the Red Mountains area, relatively few mines and prospects are associated with the OPAM acid-sulfate system (Church, Mast, and others, this volume, fig. 1). The best known of these is the Zuni mine (mine # 177, Church, Mast, and others, this volume) (fig. 14), although its importance was mostly associated with the occurrence of zunyite and guitermanite (mixture of obscure lead-bismuth minerals) (Ransome, 1901). Ore minerals in this deposit were zoned downward from anglesite into unoxidized guitermanite, changed gradually to a silver- and enargite-rich ore, and then into massive pyrite with low metal content. Similar to the Red Mountain deposits, some ore masses lined the walls of small caves and vugs in brecciated rock. Ransome (1901) reported several smaller prospects of the general type of the Zuni mine present on Anvil Mountain (Church, Mast, and others, this volume, fig. 2), but he also remarked on the limited size and grade of these deposits.

The May Day (mine # 181, Church, Mast, and others, this volume) and several unnamed mines in the Ohio and Topeka Gulch areas (fig. 14) mark the eastern margin of the OPAM acid-sulfate system. Ore minerals on associated waste piles from these mines include pyrite, galena, anglesite, and sphalerite, and ferberite (Fey and others, 2000). No copper-arsenic minerals were identified at these sites. The apparent scarcity in silver-bearing enargite ore minerals within this acid-sulfate system contrasts markedly with the Red Mountains area and explains the lack of mining and ore production therein. Considering the absence of the characteristic copper-arsenic ores, and without geochronologic data, it is difficult to constrain the age of mineralization from this area. However, the presence of acid-sulfate gangue material within some of the veins (S. Sutley, unpub. data, 2001), coupled with their close proximity to the main acid-sulfate system (fig. 14), suggests that some of the related ore deposits could have been contemporaneous with the acid-sulfate event. However, the occurrence of some late-stage tungsten-fluorite mineralization products within veins of this general area (Belser, 1956; Waegli, 1979), also suggests that some of this mineralization could be younger than 18 Ma. (See section, "Rhyolites and Associated Mineralization.")

Hydrothermal Alteration

Detailed field and laboratory studies in conjunction with AVIRIS remote spectroscopy (Dalton and others, this volume) are the basis for a compilation of maps showing the complex zonation of hydrothermal alteration assemblages and related structural features around the Red Mountains and OPAM acid-sulfate systems (figs. 14 and 15). More comprehensive details on the mineralogy and genesis of these hydrothermal systems are found in Bove and others (2001). The acid-sulfate mineral assemblage formed by replacement of the original volcanic host rocks by low-pH, sulfate-rich solutions (Rye and others, 1992; Bove and others, 2000). These solutions were localized along fault and hydrothermal breccia zones and permeated outward throughout intensely fractured wallrock (Bove and others, 2000; Dalton and others, 2000). Although these fluids must have originally flowed along steeply inclined conduits (Bove and others, 2000), they were also commonly localized along subhorizontal zones parallel to bedding and foliation within the lavas and volcaniclastics (fig. 16). These subhorizontal zones of high silicification could potentially act as partial baffles to ground water due to sharp permeability contrasts with overlying and more weakly altered rocks.

Surface mapping and careful paragenetic studies demonstrate that centers of acid-sulfate-altered rock are internally zoned and transition outward from quartz-alunite into pyrophyllite, dickite, and further into smectite, and (or) propylitically altered rock. However, as noted in some key localities, the acid-sulfate assemblage (quartz-alunite, pyrophyllite, dickite assemblages) grades directly outward into propylitically altered rock, without an intervening QSP zone. Similar observations were noted in studies of the Red Mountain Pass breccias by Burbank and Luedke (1969), who also noted the absence of a QSP assemblage within this laterally zoned sequence. Nonetheless, broad expanses of QSP-altered rock, such as that mapped on the southern margins of the Red Mountains area (fig. 15), are present between individual acid-sulfate zones. Although these mapped QSP zones extend from 3,250 m to as high as 3,780 m, the overall acid-sulfate zones generally dominate at higher elevations. As surmised from the lateral alteration sequences (no QSP zone present in horizontal sequence), it is likely that the QSP and acid-sulfate assemblages formed during alternating time intervals.

Relatively pervasive zones of QSP-altered rock are particularly well exposed along the deeply incised margins of the composite acid-sulfate zones in the Red Mountains (Prospect Gulch) and OPAM (Topeka and Ohio Gulches) areas (figs. 14 and 15). Detailed mapping and clay XRD studies show that

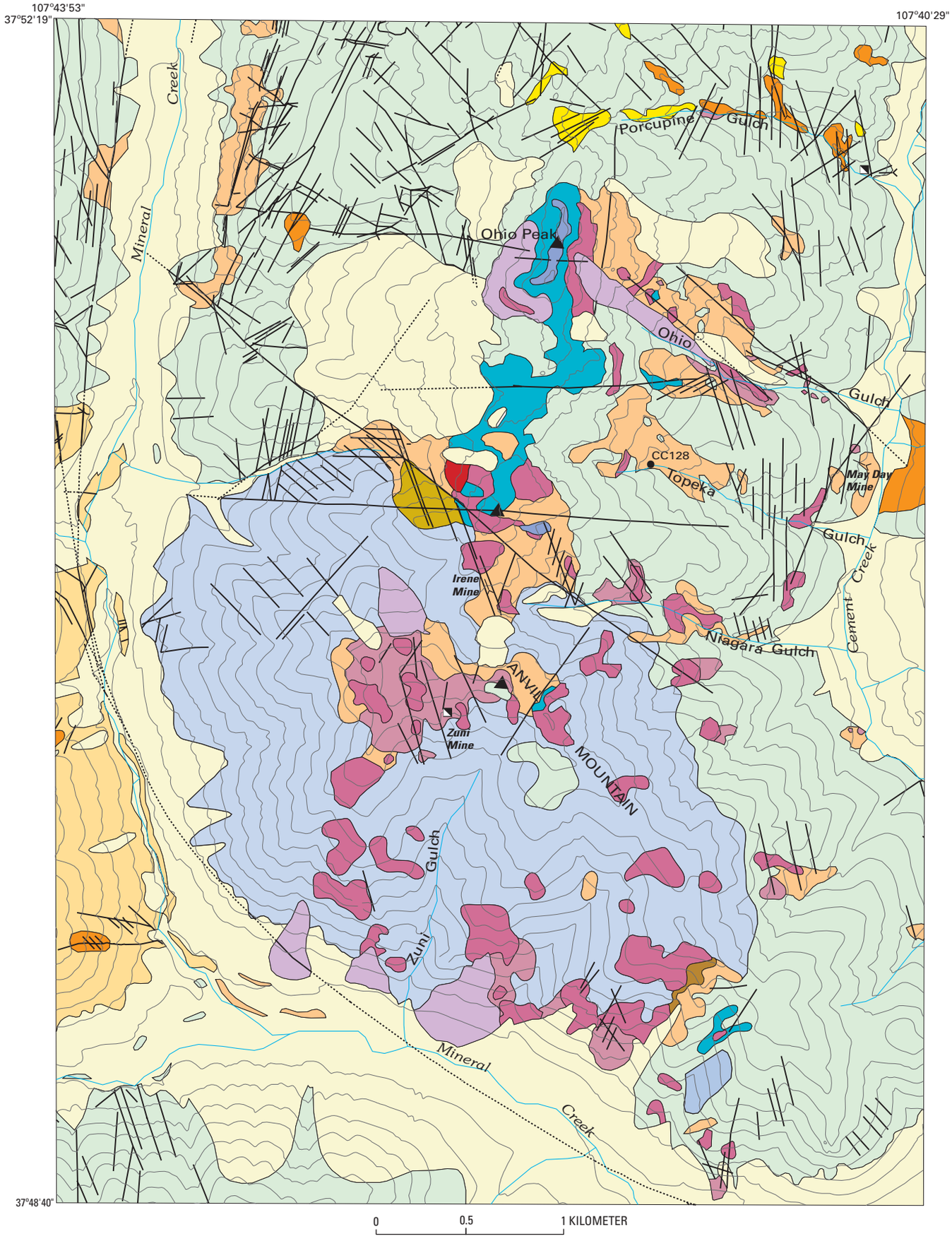
107°43'53"
37°52'19"
107°40'29"
37°48'40"
Mineral Creek
Porcupine Gulch
Ohio Peak
Ohio Gulch
CC128
Topeka Gulch
May Day Mine
Irene Mine
Cement Creek
Niagara Gulch
Anvil Mountain
Zuni Mine
Zuni Gulch
Mineral Creek
0
0.5
1 KILOMETER

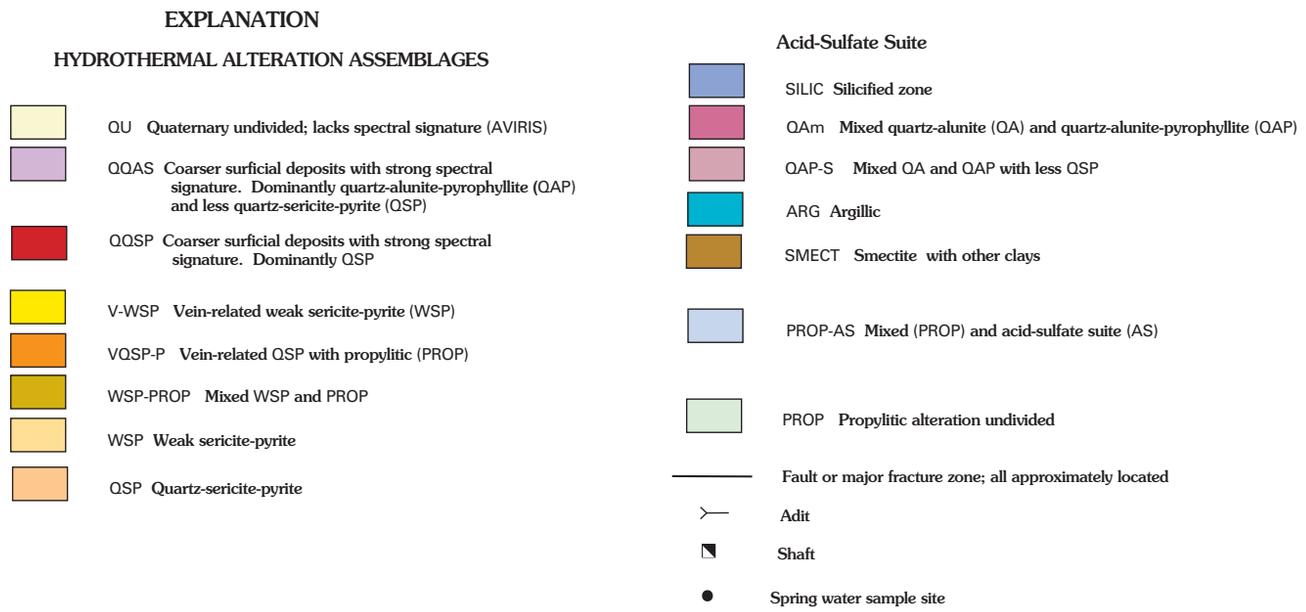

Figure 14 (above and facing page). Alteration map of Ohio Peak–Anvil Mountain (OPAM) area. Text gives detailed description of alteration types.

the QSP zone on the southwest margin of the Red Mountains acid-sulfate system (Prospect Gulch area; fig. 15) grades outward into a weak sericite-pyrite assemblage (Bove and others, 2000). In addition, mineralogical data (discussed later) indicate that a similar transition may be present on the eastern margins of the OPAM hydrothermal system. Propylitically altered rocks surround the Red Mountains and OPAM hydrothermal systems. Although most of this surrounding propylitic assemblage formed during a regional hydrothermal event (>26 Ma), some local propylitic alteration formed at ≈23 Ma, peripheral to mineralized and altered faults and fractures. Although this younger assemblage generally resembles the regional propylitic assemblage, it is distinguished largely by the presence of relatively coarse grained pyrite (1 mm cubes) disseminated and along fractures, and by quartz, chlorite, and magnetite within veinlets.

Mineralogical data from three exploratory drill holes in the vicinity of Red Mountain #3 (fig. 15) and adjacent Prospect Gulch (Bove and others, 2000) demonstrate that the acid-sulfate alteration zones have roots extending at least 300 m beneath the ground surface. Deeper exploratory drilling in the headwaters of Corkscrew Gulch (fig. 13) revealed that the pervasive zones of QSP-altered rock, at least in this area, are zoned upward and away from a deeper, potassic alteration assemblage (Gilzean, 1984). The potassic assemblage, as observed in these deep drill holes, is characterized by secondary potassium feldspar, biotite, fluorite, and andalusite. Abundant veins and veinlets of anhydrite with associated quartz, sericite, and pyrite are present within the deeper alteration assemblages, but are absent within the acid-sulfate zones (Gilzean, 1984).

Acid-Sulfate Alteration Assemblages

Silicification

Zones of silicification, which are spatially associated with the inner quartz-alunite-pyrophyllite zones, generally formed as replacements along mineralized pipelike to tabular hydrothermally brecciated masses and along brecciated faults and strong fracture zones (D.J. Bove, unpub. data, 2002). Examples of these silicified breccias include the previously discussed Red Mountain Pass mineralized breccia bodies, a large, moderately dipping breccia body near Red Mountain #3 (fig. 15) (Bove and others, 2001), and a similarly shallow-dipping mass centered near Ohio Peak (fig. 14). Disseminated pyrite (10–25 percent), enargite, and lesser covellite and galena are present throughout the entire silicified breccia at Red Mountain #3. However, sulfides are mostly oxidized in the uppermost 90 m of the entire mineralized zone. Silicified volcanic rocks and breccias range from light gray to highly bleached granular aggregates and dark jasperoidal masses composed of a microcrystalline mosaic of quartz (>75 percent), pyrite (5–25 percent), leucoxene (trace), and minor dickite, alunite, pyrophyllite, and diaspore (5–20 percent).

Quartz-Alunite Alteration

Similar to the silicic assemblage, quartz-alunite alteration was localized along hydrothermally brecciated fault and fissure zones (10–40 m across) as well as in areas of more massive hydrothermal brecciation (as much as 200–400 m wide). The quartz-alunite assemblage is defined by the presence of quartz, alunite, natroalunite, pyrophyllite, dickite,

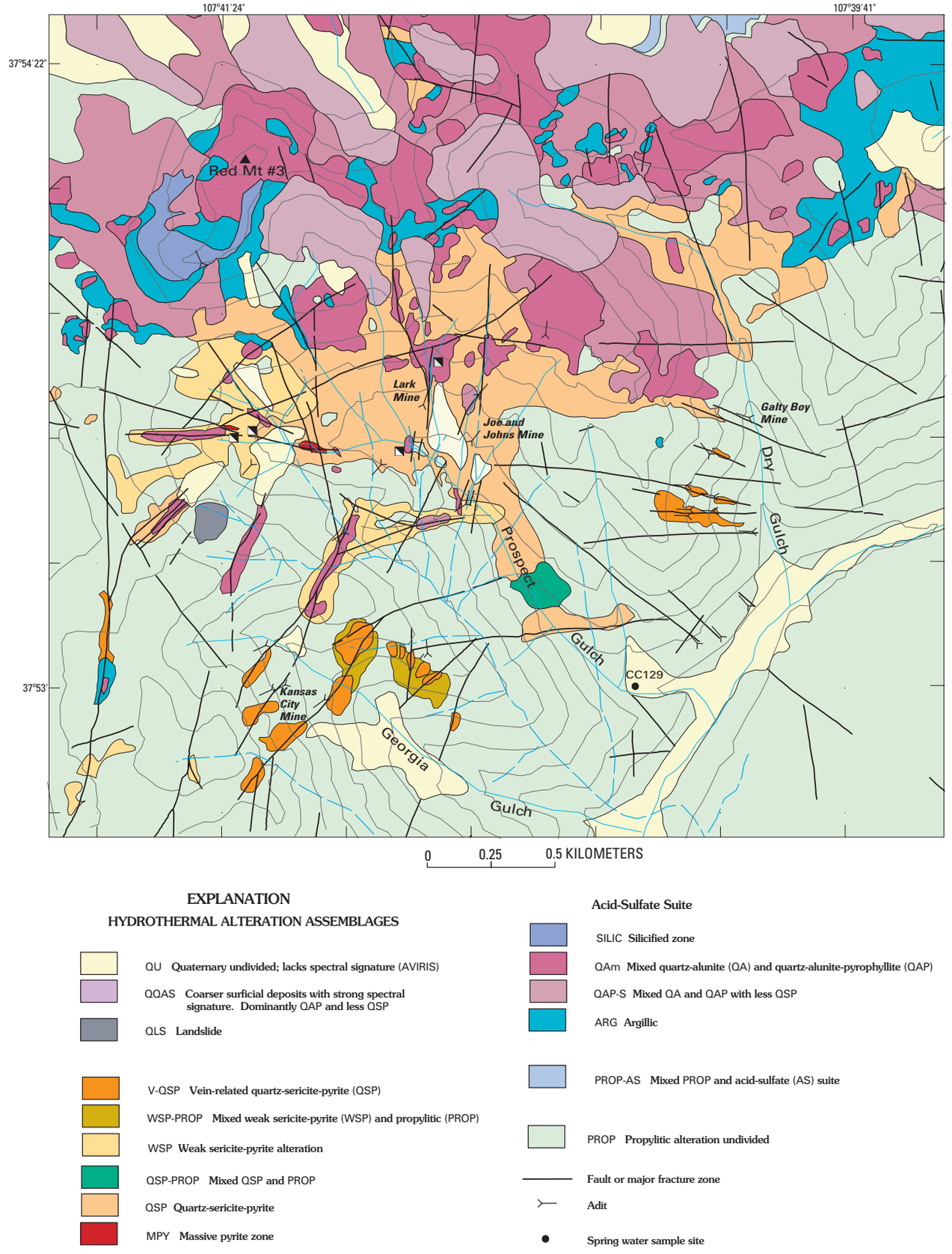

Figure 15. Alteration map of Red Mountains area.

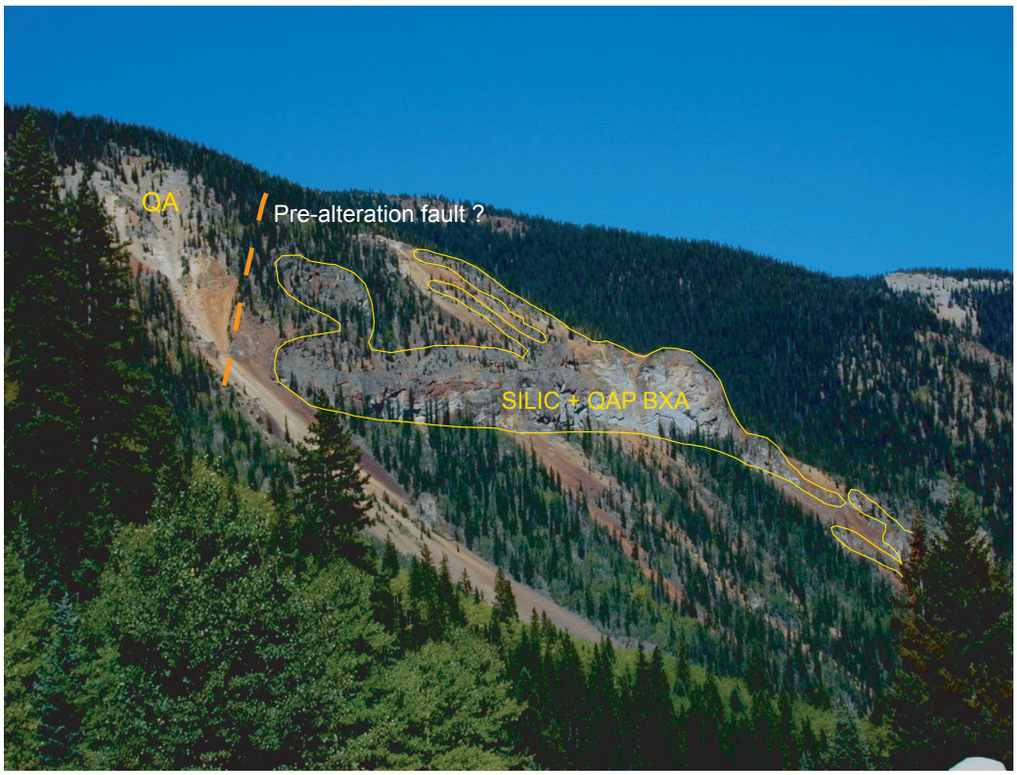

Figure 16. Highly silicified quartz-alunite-pyrophyllite breccia zone (SILIC+QAP BXA) along near-horizontal plane; base is subparallel to bedding of lavas. Near-vertical zones probably controlled by high-angle fractures. Area of photo is about 2 km across.

diaspore, and pyrite, with minor to trace amounts of zunyite, sulfur, and tridymite. These highly silicified rocks contain between 30 and 80 percent fine-grained quartz, with a mean of 50 percent. Pyrite, which is present as disseminations and present along tiny fracture networks, typically ranges from 20 to 30 weight percent within these altered rocks. Alunitized rocks are characterized by the breakdown of all primary rock constituents with the exception of zircon and resorbed quartz phenocrysts, where present. Biotite, hornblende, and primary opaque minerals are altered to leucoxene; hematite and jarosite formed as near-surface oxidation products of pyrite.

Compositional data as determined by AVIRIS remote spectroscopy (Dalton and others, this volume) indicate that alunite within the Red Mountains and OPAM areas ranges mostly from a nearly pure potassium end-member through intermediate potassium and sodium compositions. However, natroalunite has been identified in some localities by remote spectroscopic and XRD methods. An individual chemical analysis of alunite from the Red Mountain Pass area (Hurlburt, 1894) shows the presence of potassium and sodium in roughly equal proportions (table 2).

Quartz-Pyrophyllite and Argillic Assemblages

Quartz-pyrophyllite-altered rocks contain between 15 and 40 percent quartz, abundant pyrophyllite, and lesser alunite, sericite, diaspore, and finely disseminated pyrite. These rocks are difficult to distinguish from quartz-alunite-altered rocks in hand specimen and have many textural and morphologic similarities in thin section, as well. In contrast, rocks affected by argillic alteration are generally quite distinctive due to the presence of a soft waxy clay pseudomorphous after feldspar and along fractures. These bleached argillic zones, which form the broad outer margins around the quartz-alunite, quartz-pyrophyllite, and silicic zones, are characterized by the presence of dickite and quartz with varying amounts of pyrite. These rocks are poorly to only moderately indurated and contain between a trace and 40 percent fine-grained quartz. Zones of smectitic alteration are similar in appearance to the argillic zones but are characterized by the presence of smectite, chlorite, and variably altered feldspar grains.

Hydrothermal Sericitic Assemblages

Quartz-Sericite-Pyrite Assemblage

The quartz-sericite-pyrite (QSP) assemblage is characterized by the complete replacement of plagioclase, potassium feldspar phenocrysts, and groundmass by roughly 25–55 percent fine-grained pervasive quartz (40 percent average), abundant highly crystalline illite (sericite), and 10–20 percent finely disseminated and fracture-filling pyrite. Kaolinite may be present in varying abundances in some

localities. Abundant white, fine-grained kaolinite has also been observed in veinlets postdating ore mineralization near the National Belle mine, in the Red Mountain Pass area (fig. 13). Altered rocks of the QSP assemblage typically have a bleached appearance and are variably oxidized. Thin stockwork quartz veinlets are locally present.

Weak Sericite-Pyrite Assemblage

The weak sericite-pyrite assemblage, as mapped on the margins of the Red Mountains area (WSP; fig. 15), is characterized by the presence of weakly to unaltered plagioclase and metastable chlorite; these minerals are typically absent in the adjacent QSP assemblage. WSP rocks are less silicified than their QSP counterparts, containing between 15 and 25 percent and an average of 20 percent microcrystalline quartz. Illite (sericite) is also abundant along with more than 5–10 volume percent finely disseminated pyrite.

Origin, Age, and Relation to Intrusions

Geologic relations and isotopic dating indicate that acid-sulfate and QSP alteration, hydrothermal brecciation, and silver-copper-arsenic ore deposition in the Red Mountains area were intimately associated with episodic intrusion of dacite porphyry magma at about 23 Ma (Lipman and others, 1976; Gilzean, 1984; Bove and others, 2000; Bove and others, 2001). The contemporaneity of these events is verified by the following: (1) coeval K-Ar age determinations of about 23 Ma on both alunite and dacite porphyry intrusions in the Red Mountains area (Lipman and others, 1976; Gilzean, 1984; Bove and others, 2000; Bove and others, 2001), (2) geologic evidence for repeated episodes of alternating acid-sulfate alteration, silver-copper-arsenic ore deposition, and dacite intrusion (Lipman and others, 1976; Fisher and Leedy, 1973), and (3) paragenetic relations showing dikes of fresh dacite porphyry cutting QSP and QA-altered hydrothermal breccias that contain clasts of earlier intruded dacite porphyry. No outcrops of dacite porphyry have been identified in the OPAM acid-sulfate area. However, similarities in mineralogy, alunite isotopic composition (table 7), and geometry to that in the Red Mountains area suggest that both systems were contemporaneous and associated with similar intrusions.

The Red Mountains and OPAM acid-sulfate systems are highly analogous to magmatic hydrothermal acid-sulfate systems at Summitville, Colo., Lake City, Colo., and Julcani, Peru (Rye and others, 1992; Bove and others, 2002). All these localities have acid-sulfate alteration zones in near-surface epithermal deposits, which are characterized by deep vertical as well as horizontal zoning, the presence of coeval pyrite, phosphate analogs of alunite, and zunyite, and later gold, enargite, and other copper-arsenic-antimony-sulfide minerals (Rye and others, 1992). Our detailed geologic and stable isotope studies in the Red Mountains and OPAM areas (D.J. Bove, unpub. data, 2002) demonstrate that the alunite and pyrite formed from vapor plumes rich in H_2S and SO_4 due to the disproportionation of magmatic sulfur dioxide. Geologic and geochronologic constraints, as outlined in the beginning of this section, and stable isotope data suggest that these vapor plumes emanated from the high-level dacite porphyry intrusions and had very high H_2S:SO_4 ratios. Paragenetic studies (D.J. Bove, unpub. data, 2002) demonstrate that acid-sulfate alteration and ore mineralization occurred in alternating episodes. Detailed ore genesis studies of similar acid-sulfate systems at Summitville, Colo., and Julcani, Peru (Stoffregen, 1987; Rye and others, 1992) suggest that these alternations may be related to changes in magmatic fluid composition. These compositional changes could be explained by episodic pulses of dacite intrusion coupled with intermittent cycling of the magmatic vapor plumes.

The coexistence of both H_2S and SO_4 in the fluids that formed the Red Mountains and OPAM acid-sulfate systems explains the abundance of coexisting pyrite and alunite in the acid-sulfate mineral zones. The spatial association of pyrite and alunite at depth and at high levels in this hydrothermal system contrasts sharply with what appears in other large acid-sulfate systems in the Rocky Mountains (magmatic steam-heated systems such as Marysvale, Utah; Rye and others, 1992; Cunningham and others, 2005), where pyrite formed only in deeper zones beneath the alunite horizons. These inherent differences in deposit type have important implications with regard to pyrite exposure to surficial weathering and subsequent production of acidic runoff. On the one hand, magmatic-hydrothermal acid-sulfate systems, such as those observed in the study area, are generally associated with low-pH waters owing to more ubiquitous presence of pyrite, regardless of erosion depth (Bove and others, 1996; Bove and others, 2000). In contrast, surficial pyrite weathering and related acidic runoff appear only to be a factor in the magmatic steam-derived acid-sulfate systems, where the underlying pyritic zone is exposed from erosive processes (Cunningham and others, 2005). Thus, knowledge regarding the type or genesis of the particular acid-sulfate system can be used to predict the likelihood of impact from acidic drainage. This can be useful in preliminary assessments of acid-sulfate-altered areas where no water quality data are available, or in desert environments where surficial runoff is limited.

Geochemistry of Altered Rocks in the Red Mountains and Ohio Peak–Anvil Mountain Areas

The combined geochemical data for 69 surface samples from the Red Mountains and Ohio Peak–Anvil Mountain acid-sulfate areas are shown in table 3 and figure 4. These data were combined due to strong similarities in altered rock lithology, and because of poor sample representation of the OPAM acid-sulfate assemblage. Although the data represent most major alteration assemblages differentiated by geologic

mapping (figs. 14 and 15), samples from the weak sericite-pyrite assemblage were not presented because of low sample numbers. Major-element trends are similar to that of the Mount Moly area with substantially lower calcium, magnesium, and sodium in QSP and acid-sulfate (AS) versus propylitically altered rocks. Manganese content decreases from a mean of 927 ppm in propylitically altered rocks, to 35 ppm in QSP samples, to <12 ppm in AS-altered rocks. Lead abundance is highest in the AS assemblage (278 ppm mean) and decreases from a mean of 62 ppm in QSP-altered rocks to 26 ppm in propylitically altered rocks (table 3 and fig. 4). In contrast, mean zinc and copper abundances are highest in propylitically altered rocks (110 and 50 ppm, respectively) with substantially lower mean values in QSP and AS-altered outcrops. Molybdenum values in all altered rocks sampled are near analytical detection limits. Lower iron content within QSP and AS versus propylitically altered rocks is probably due to surficial oxidation of pervasive pyrite within the QSP and AS zones. Svanbergite [$(Sr, Ca)Al_3(SO)_4(PO)_4(OH)_6$] has been identified by XRD in acid-sulfate-altered rocks, which may account for the relatively high concentrations of strontium and phosphorus within this alteration suite (table 3). The formation of svanbergite is related to the release of H_3PO_4 and strontium into solution due to the breakdown of primary apatite and plagioclase by acid-sulfate-altering fluids (Stoffregen and Alpers, 1987; Bove and Hon, 1992).

Analyses of 34 drill core samples of unoxidized acid-sulfate-altered rock are summarized in table 3 and compared to outcrop data in figure 6. Iron abundance within unoxidized AS-altered drill core samples (4.77 percent mean) is statistically indistinguishable from that of surface samples of propylitically altered rock (4.83 percent mean) (table 3); however, rocks from corresponding AS-altered outcrops (0.86 percent mean) have notably lower iron content than AS drill core samples (fig. 6), probably due to pyrite dissolution. Lead abundances statistically overlap in oxidized surface and unweathered drill core samples (AS assemblage), reflecting the relative immobility of lead in oxidizing surface waters (Smith and Huyck, 1999). Similar to iron, differences in copper in surface (8 ppm mean) relative to unoxidized subsurface AS samples (79 ppm mean), are also likely due to sulfide oxidation in the near-surface environment (fig. 6). Copper values in unoxidized AS drill core samples (80 ppm mean) are analytically indistinguishable from those of samples of propylitically altered rock (50 ppm mean).

As shown in figure 6, copper and molybdenum abundances from the Red Mountains area in unoxidized drill core samples (AS-drill core) are notably lower than in unoxidized core samples from the Mount Moly area (QSP-unoxidized zone). However, studies by Gilzean (1984) documented subeconomic but substantial copper and molybdenum mineralization in deeper zones of potassic-altered rock in the Red Mountains area. No specifics regarding these data are included in the report by Gilzean (1984), however.

Mine Dump Compositions

Red Mountains Area

Analytical data summarizing the geochemistry of 20 mine dumps from the Red Mountains area are shown in table 4 and figure 7. The geochemical signature of these dumps is distinctive in comparison to data from the other four mineralized areas. Mean manganese concentration of 39 ppm is from 6 to 50 times lower than mean values from the other areas. Although mean abundances of lead (1,870 ppm) and zinc (935 ppm) are comparable to values in the other four areas, the mean concentrations of copper (1,930 ppm) and arsenic (943 ppm) are substantially higher. These concentration patterns reflect the characteristic presence of enargite and tetrahedrite-tennantite, which are commonly associated with ores from this area. In contrast, mean molybdenum concentration (5 ppm) is the lowest of the five groups.

Although manganese gangue minerals are largely absent in the Red Mountains ore deposits, pyroxmangite has been identified at the Kansas City mine in Georgia Gulch, which is hosted in propylitic-dominant terrain on the periphery of the acid-sulfate system (fig. 15). Veins of the Kansas City mine are along continuations of north- to northeast-trending faults that were exploited for acid-sulfate-style mineral deposits along the south side of Prospect Gulch (fig. 15). For this reason, mineralization at the Kansas City mine is thought to be contemporaneous with the 23 Ma acid-sulfate event. However, later episodes of ore mineralization may have also occurred along these structures. Mean manganese concentration within propylitic-altered rocks in the Red Mountains area is 927 ppm, whereas the large expanses of highly altered rock hosting most of the ore deposits are relatively manganese poor (<35 ppm mean). These data reflect that manganese solubility within hydrothermal fluids is strongly pH dependent (Casadevall and Ohmoto, 1977; Langston, 1978), and gangue ores may have only precipitated on the margins of the hydrothermal system where pH was higher. While mean calcium in these dumps (700 ppm mean) is the lowest among the five areas, mean strontium abundance (602 ppm) is the highest. These low calcium:strontium ratios can be attributed to the paucity of calcite, gypsum, and anhydrite within the entire Red Mountains acid-sulfate system, and the presence of discrete strontium-phosphate-sulfate mineral phases formed during acid-sulfate hydrothermal alteration (Stoffregen and Alpers, 1987; Bove and Hon, 1992).

Ohio Peak–Anvil Mountain Area

Analytical data from six mine dumps from the Ohio Peak–Anvil Mountain area are presented in table 4 and figure 7. Unfortunately, none of the dumps from the Zuni mine (fig. 14) and nearby prospects with enargite-bearing ores were sampled due to steep terrain and because of access restrictions. Data from the six mine dumps included in this study show mean abundances of 679 ppm manganese; 7,550 ppm lead;

3,070 ppm zinc; 382 ppm copper; 87 ppm arsenic; 17 ppm molybdenum; 27 ppm silver; and 320 ppm strontium. The range of manganese concentrations falls roughly in the middle of the five groups, but the range is significantly higher than in dumps from the Red Mountains acid-sulfate area. Higher manganese values in the OPAM area probably reflect that most of the mines are near the propylitic-dominated margins of this southern acid-sulfate system. Although late-stage manganese silicate and manganese carbonate gangue could be present in some of these vein deposits, they have not been observed in any significant quantity within associated dump material (D.J. Bove, unpub. data, 2002). However, huebnerite ($MnWO_4$), which is common in a number of the mines along Cement Creek (Belser, 1956), could contribute to the elevated manganese abundances. Ranges of lead and zinc abundance overlap with ranges from the other four mineralized areas (fig. 7), whereas copper and arsenic abundances, although substantially lower than those from dumps of the Red Mountains area, fall within the range of the other three groups. The low arsenic abundances within these dumps (87 ppm mean) contrast markedly with those of the Red Mountains area, where the mine dumps have a mean arsenic abundance of 943 ppm. In addition, mean copper abundance is nearly five times lower than in the Red Mountains mine waste material. These data reflect the overall scarcity of enargite and related ore minerals in mines of the OPAM area (Ransome, 1901), whereas these minerals are generally present in many of the Red Mountains ores. The lack of these minerals within the OPAM deposits is probably the explanation for the relatively small number of mines and prospects and the lack of ore production in this part of the Animas River study area.

Mine Water Chemistry

Red Mountains Area

Geochemical data from 10 mine discharge samples in the Red Mountains area are shown in figure 8 and summarized in table 5. Nine of these water samples had pH values <4.0 and were characterized by relatively high metal concentrations (cadmium+lead+zinc+copper=13,100 µg/L mean) compared to all mine discharge samples from the five mineralized areas. Only one sample had a high pH (6.86) and had low dissolved metal concentrations (cadmium+lead+zinc+copper=<21 µg/L). The composition of this high-pH mine sample can be explained by the dominance of propylitically altered rocks nearby, and the lack of sulfide minerals in the mine dump.

The compositions of the eight low-pH mine waters from the Red Mountains area are probably the most distinctive of all such waters in the study area (table 5; fig. 10). Along with Ohio Peak–Anvil Mountain mine discharge (discussed later), mean aluminum (14,400 µg/L), iron (63,300 µg/L), and sulfate (514 mg/L) concentrations are markedly higher than in low-pH waters from the other mineralized areas. In contrast, manganese and strontium concentrations are relatively low compared to other areas, perhaps due to the large volumes of acid-sulfate-altered rock. Highly elevated copper (2,340 µg/L mean), arsenic (103 µg/L mean), and zinc (10,600 µg/L mean) in association with elevated lead (177 µg/L mean), and cadmium (50 µg/L mean), are the most diagnostic signatures of the Red Mountains low-pH mine discharge (table 5; fig. 9). These metals probably reflect the characteristic occurrence of enargite and other copper-antimony-arsenic-bearing minerals within this mineralized system. Previous studies indicate that before recent reclamation, some mine waters just outside the study area (near Red Mountain Pass; fig. 13) (data not included in this study) had concentrations of arsenic ranging from 600 to 1,400 µg/L, and copper between 5,000 and 36,000 µg/L[5] (Bove and Knepper, 2000).

Low-pH mine waters representing acid-sulfate type mineralization on the periphery of the Red Mountains hydrothermal system differ geochemically from mine waters nearer the interior of the acid-sulfate system. Samples near the periphery of the acid-sulfate system have appreciably higher manganese, strontium, and base cation concentrations (Jim Herron, Bruce Stover, and Paul Krabacher, Unpublished Cement Creek reclamation feasibility report, Upper Animas River Basin, Colorado Division of Minerals and Geology, 1998; results not included in table 5) than mine samples collected nearer the interior of the hydrothermal system (table 5). This difference is likely the result of the availability of calcite, plagioclase, and chlorite within the surrounding propylitically altered wallrock.

$\delta^{34}S$ values for six low-pH mine waters from the Red Mountains region range from –4.4 to –0.2 per mil (Nordstrom and others, this volume, table 1). These data largely are within the compositional range of both ore and disseminated sulfides (–6.9 to –1.1 per mil) (table 7), indicating that sulfate in the mine waters was largely to entirely derived from the oxidation of these isotopically light sulfide minerals.

Ohio Peak–Anvil Mountain Area

Geochemical data from 13 mine waters in the OPAM area are shown in figure 8 and summarized in table 5. The geochemistry of these mine waters is highly variable with pH ranging from 2.17 to 6.95 and concentrations of 7 to 51,900 µg/L aluminum, 445 to 16,000 µg/L manganese, <20 to 7,400 µg/L zinc, 3 to 1,760 µg/L copper, and 1 to 12 µg/L arsenic. As previously discussed, these mine waters, like those from the other four mineralized areas, can be generally divided into two groups—low and high pH—based on variability of dissolved metal concentrations (fig. 9). Three of the mine waters are circumneutral (pH 6.54 to 6.95), have wide ranges in alkalinity (20 to 137 mg/L) and dissolved zinc (<20 to 3,050 µg/L), and have low dissolved lead (<21 µg/L) and copper (<5 µg/L) concentrations. Manganese concentrations range from 1,100 to 9,300 µg/L.

[5]Waters were sampled for the Colorado Department of Health and Public Education (CDHPE) between 1989 and 1990 (compiled in Bove and Knepper, 2000). Mine reclamation took place from 1996 to 1998.

Two of the three circumneutral-pH waters have high combined concentrations of calcium (>193 mg/L), strontium (>1,950 µg/L), and sulfate (>860 mg/L) compared to all mine waters in the five areas (table 6). Aqueous $\delta^{34}S$ values for two of these high calcium-strontium-sulfate waters are +8.0 and +10.5 per mil (Nordstrom and others, this volume). These values are significantly heavier than those measured in sulfides from veins or disseminated pyrite from the surrounding alteration assemblages (–5.4 to –0. 8 per mil; table 7). These data indicate that some sulfate in these waters was derived from isotopically heavier gypsum or anhydrite, which have $\delta^{34}S$ compositions larger than +14 per mil throughout the watershed. These data are supported by the presence of gypsum gangue material (+17 per mil; table 7) on both of these mine dumps. Both of these high calcium-strontium-sulfate waters are characterized by high iron concentrations (8,600 µg/L and 22,000 µg/L), whereas one sample has moderately elevated aluminum (484 µg/L). Similar to the Paradise mine water in the Mount Moly area, these data suggest mixing of acidic and higher pH water somewhere within the mine workings. As indicated in previous discussions, the mixing of more alkaline water with the acidic water may have reduced the overall zinc concentrations of these waters, further obscuring the primary metal signatures of the vein deposits (Nordstrom and Ball, 1986).

As shown in figure 10, low-pH mine water from the OPAM and Red Mountains areas has similarly elevated abundances of aluminum, iron, lead, and sulfate; zinc is moderately elevated in OPAM low-pH discharge relative to low-pH mine waters in the other mineralized areas (tables 5, 6), although mean concentration (3,640 µg/L) is about half that of the Red Mountains low-pH mine waters. Mean copper concentration in OPAM low-pH mine water (314 µg/L) is nearly double that of Mount Moly low-pH mine discharge, but nearly six times lower than that measured in Red Mountains discharge (2,340 µg/L). Likewise, arsenic concentrations within OPAM low-pH water (2.7 µg/L) are low compared to Red Mountains acidic mine drainage, which has a mean concentration of 103 µg/L. Low concentrations of arsenic in both low-pH mine discharge and dump material are consistent with geologic reports (Ransome, 1901) and studies of dump material (S. Sutley, unpub. data, 2000) indicating the absence of enargite in all but a few mines in this area. Mean manganese (3,750 µg/L) and magnesium (15 mg/L) concentrations in OPAM acidic mine discharge are also elevated relative to concentrations in low-pH mine waters from all but one of the other mineralized areas. The elevated manganese and magnesium concentrations could reflect that these associated mines are hosted within propylitically altered wallrock on the periphery of the acid-sulfate system. Similar compositions are observed in mine water on the periphery of the Red Mountains acid-sulfate system (Unpub. Cement Creek reclamation feasibility report, CDMG, 1998), as discussed in the previous section. However, these elevated manganese concentrations could also be related to the dissolution of huebnerite ($MnWO_4$), which is reported on dumps in this area (Belser, 1956). $\delta^{34}S$ values for three of the five low-pH OPAM mine waters range from –4.9 to –0.5 per mil (Nordstrom and others, this volume, table 1) and are within the range of ore and disseminated sulfides for the area (–5.4 to –0. 8 per mil; table 7); these data indicate little to no interaction with isotopically heavier sulfate from gypsum or anhydrite.

Background Surface Water Chemistry

Red Mountains Area

The chemistry of background springs and streams in the Red Mountains area shows a wide range of compositions that are related to the intensity of hydrothermal alteration (table 8; fig. 11). Waters interacting with QSP-altered rocks have the lowest pH values and the highest mean sulfate, aluminum, iron, silicon, and metal concentrations of all water samples collected in this area. Although both the QSP and acid-sulfate water (AS) have similarly low pH values, mean calcium, magnesium, and manganese concentrations are at least four times higher in the QSP waters. One possible explanation is the partial replacement of wallrock during QSP alteration, which effectively stranded “islands” of unaltered to weakly altered rock that did not undergo significant leaching of these elements during the hydrothermal process. In contrast, the acid-sulfate alteration zones are more homogeneous and rarely contain intervals with unaltered feldspar, chlorite, or calcite. This relative homogeneity is probably the result of more efficient dispersion of the ancient vapor-dominant hydrothermal fluid throughout these highly fractured and brecciated rocks. Although mean calcium concentration varies widely within the five water types (15.4 mg/L and 2.3 mg/L in QSP and AS waters, respectively) (table 8), sodium abundance is quite low, ranging from 0.3 to 0.5 mg/L (geometric mean). These data contrast markedly with the more sodium-rich samples in the Mount Moly area (as much as 13 mg/L), and may indicate a scarcity of secondary albite in the Red Mountains area.

As shown in table 8, AS waters were separated into two subgroups based on water geochemistry and inferences from field data. The first subgroup (fresh sulfides) is characterized by a mean iron concentration of 1,140 µg/L and is thought to represent waters draining AS-altered areas containing fresh pyrite. Waters of this group have been observed in areas of unoxidized pyritic rock exposed in deeply incised drainages. In high areas unaffected by steep downcutting, these unoxidized zones are generally present at depths >60 m beneath the ground surface. In contrast, the second subgroup of AS waters (oxidized sulfides) has a mean of 63 µg/L dissolved iron. These waters have been observed to drain high-elevation areas dominated by surficial deposits, which are largely depleted in unoxidized pyrite due to weathering. Samples from water draining rocks with fresh sulfides have lower pH and significantly higher concentrations of aluminum, iron, manganese, zinc, copper, and sulfate than the oxidized waters (table 8). Differences in iron and metals in these waters mirror similar differences in the rocks in which they interact (fig. 6; for example, AS-drill core versus AS-surface).

Whereas mean sulfate concentration within Red Mountains background waters can be moderately high (for example, 137 mg/L in QSP waters), strontium is generally low (168 µg/L) compared to waters that have interacted with gypsum or anhydrite (Nordstrom and others, this volume, table 1). These data correspond with the light $\delta^{34}S$ values that are typical of all the Red Mountains water, ranging from –4.9 to –0.6 per mil. These values are well within the range of various sulfide minerals from this area (–6.9 to –1.1 per mil; table 7), which indicates that gypsum, anhydrite, and alunite were not significant sources of the dissolved aqueous sulfate. These data are important because they indicate that background water had little to no interaction with isotopically heavy $CaSO_4$ phases that are only present deep beneath the acid-sulfate roots of this hydrothermal system. Furthermore, these data suggest that dissolution of alunite ($\delta^{34}S$ from +10 to +27 per mil; table 7) was limited within the pH range of these background waters (table 8).

Streams and springs interacting with propylitically altered rock have the highest mean values of pH and alkalinity (6.04 and 11.1 mg/L, respectively) and the lowest mean dissolved metal concentrations (aluminum=<1 µg/L; iron=37 µg/L; zinc=<3 µg/L; copper=4 µg/L) of all water samples collected in the Red Mountains area. Mean sulfate concentration for the propylitic waters is 10 mg/L, whereas calcium and strontium means were 8.3 mg/L and 298 µg/L, respectively. Similar to the Mount Moly area, water draining the weak sericite-pyrite assemblage (WSP) falls compositionally between QSP and PROP water, reflecting the transition between the two alteration assemblages (table 8; fig. 11). Background waters influenced by vein or fault structures (PROP-V) have highly variable compositions: pH ranges from 3.0 to 6.5, mean sulfate ranges from 1 to 351 µg/L, and mean zinc ranges from 20 to 1,070 µg/L. The origin of each of the PROP-V waters is circumstantially unique and is discussed in detail by Bove and others (2000).

Ohio Peak–Anvil Mountain Area

As shown in table 8 and figure 11, background water in the Ohio Peak–Anvil Mountain area also varies according to the alteration assemblage that it drains. Water interacting with the QSP assemblage in the OPAM area (mean pH=3.5, sulfate=132 µg/L, and zinc=142 µg/L) is compositionally very similar to QSP water in the Red Mountains area, with the exception of mean sodium and silicon, which are higher in concentration in the background OPAM waters (3.0 and 24.1 mg/L, respectively). Instead, these sodium and silicon concentrations are very similar to Mount Moly area QSP-related waters, suggesting that reactions involving secondary albite were also important in the vicinity of Ohio Peak–Anvil Mountain. $\delta^{34}S$ values from six QSP-related water samples range from –6.7 to –1.5 per mil (Nordstrom and others, this volume, table 1), which are within the range of three sulfide mineral samples analyzed from this area (–5.4 to –0.8 per mil; table 7). These data indicate that much of the sulfate was derived from the interaction with disseminated pyrite within the QSP-altered rocks. Like the AS (oxidized sulfides) waters of the Red Mountains area (table 8), these samples have intermediate pH values (3.88 and 5.50) and relatively low sulfate (4 and 21 µg/L) and low metal (<3 and 29 µg/L Zn) concentrations compared with other background waters (table 8). The two propylitic waters in the OPAM area are similar to those in the Red Mountains area with high pH (6.99 and 7.46), measurable alkalinity (31 and 34 mg/L), relatively low calcium (23 and 24 mg/L) and strontium (363 and 405 µg/L), and very low metal concentrations (table 8).

18–10 Ma Polymetallic Vein Systems—Northeast-Trending Veins

Eureka Graben Area

A significant portion of mineral production within the western San Juan Mountains was from vein deposits localized along collapse and resurgent structures associated with the San Juan, Uncompahgre, and Silverton calderas (Burbank and Luedke, 1969; Lipman and others, 1976). Related structures include faults and subsidiary fractures of the northeast-trending Eureka graben system. These graben structures host many of the most economically important vein deposits in the Animas River watershed (Jones, this volume, Chapter C). Veins of the Eureka graben area are defined by a broad zone from Wood Mountain southwest to the Bonita fault and are bounded by Tuttle Mountain to the north and the Toltec fault on the south (fig. 17). Nearly all the important gold mines within the Silverton caldera lie within a relatively narrow belt, roughly within the center of the Eureka graben area (fig. 17). Near the center of this narrow gold zone are the large producing mines in the Eureka district that included the Sunnyside, Gold Prince, and Silver Queen mines in Eureka and the head of Placer Gulch, and the Sound Democrat and Scotia and Vanderbilt mines near Treasure Mountain. The Gold King and the Golden Fleece mines border this zone on the east and west, respectively (fig. 17). Mines in the Mineral Point, California Gulch, and upper Cement Creek areas also developed veins of the Eureka graben system. Although similar in overall mineralogy and gross paragenesis, these veins are more typical of polymetallic vein deposits in the Silverton area as they are conspicuously deficient in gold-rich ore (Ransome, 1901; Burbank and Luedke, 1969; Casadevall and Ohmoto, 1977; Langston, 1978; Standen and Kyle, 1985; Koch, 1990; Bartos, 1993).

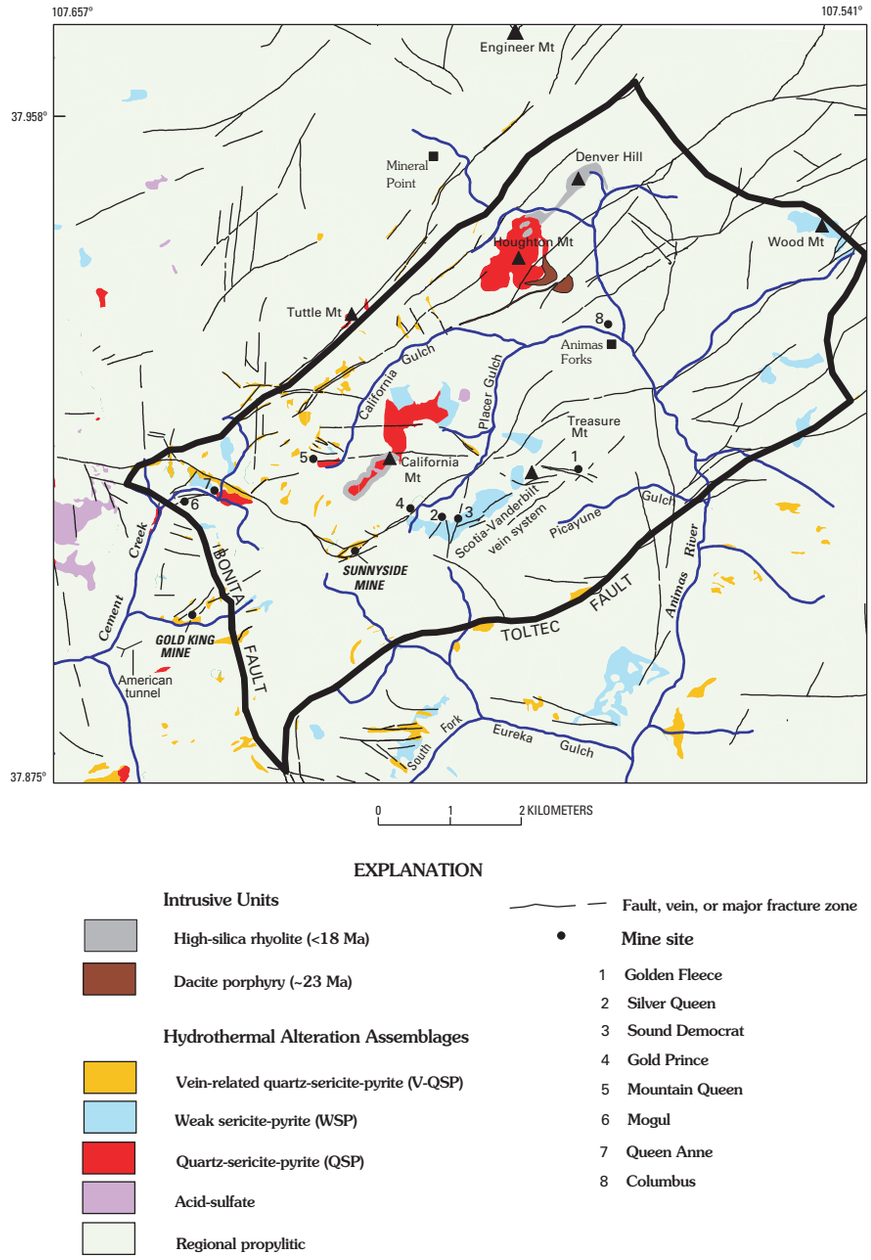

Figure 17. Generalized geologic and alteration map of Eureka Graben area.

A relatively small data set of K-Ar, fission-track, and Rb/Sr dates broadly constrains the age of these polymetallic veins to about 18–10 Ma (Lipman and others, 1976; Bove and others, 2001). Previous workers have demonstrated that this polymetallic vein mineralization was coeval and perhaps some was genetically related to the emplacement of numerous small intrusions of high-silica rhyolite and granite (Lipman and others, 1976; Bartos, 1993). Data presented in this study (see section, "Rhyolites and Associated Mineralization") further refine these observations and indicate that at least one important stage of this mineralization is related to these intrusions.

Eureka Gulch, Treasure Mountain, and Placer Gulch Gold-Rich Veins

The Sunnyside mine (fig. 17) was a major gold producer (Casadevall and Ohmoto, 1977), and until closure in 1991, produced more than 800,000 ounces of gold and 14 million ounces of silver (Bartos, 1993; Jones, this volume). Typical ore grades were 0.16 oz gold/t, 1.57 oz silver/t, 2 percent lead, 0.2 percent copper, and 3 percent zinc (Casadevall and Ohmoto, 1977). In the later years of mining, the 3,050 m American tunnel (fig. 17) provided the primary access to workings that extended

2,100 m laterally and 610 m vertically (Casadevall and Ohmoto, 1977). Two types of veins were distinguished based on outcrop character. Veins of the first type form bold, manganese-stained outcrops at the surface and yielded most early production in the area. Other veins have little to no surface expression and were worked in the subsurface (Casadevall and Ohmoto, 1977). Vein mineralization of the Sunnyside mine was generally complex (fig. 18), and as many as six major stages have been recognized (Casadevall and Ohmoto, 1977; Langston, 1978). Early to intermediate stages include quartz-pyrite and massive sulfide ores, whereas ores of gold-telluride-quartz, manganese, and quartz-fluorite-carbonate-sulfate formed later. Ores of the massive sulfide stage (stage 3; fig. 18) consist largely of massive anhedral aggregates of intergrown sphalerite and galena, with lesser pyrite, chalcopyrite, and tetrahedrite (Casadevall and Ohmoto, 1977). The majority of gold deposition followed the massive sulfide stage and preceded the manganese ore stage. Deposition of manganese ores, which occur in thick (3 m average) tabular bodies subparallel to veins, followed gold-quartz mineralization. These late-stage ores are characterized by light-pink masses of fine-grained pyroxmangite ($MnSiO_3$), lesser rhodochrosite, and quartz. Manganese ores within the Sunnyside mine average 20 volume percent of the entire vein material (Casadevall and Ohmoto, 1977). Similar veins throughout the Eureka Gulch, Treasure Mountain, and Placer Gulch areas (fig. 17) are also highly endowed in this late-stage ore, with weighted averages of 6 percent manganese taken across 3 m vein widths (calculated from data in Belser, 1956).

Vein and fracture-filling anhydrite and gypsum with quartz, sericite, pyrite, and other sulfides are also associated with the manganese ore stage. These veins have been observed at the American tunnel level (3,260 m elevation) and as much as 600 m deeper in exploration drill holes. The latest stage of mineralization is marked by vug and veinlets filled with quartz, fluorite, calcite, huebnerite, and minor sulfides (Casadevall and Ohmoto, 1977; Langston, 1978).

The Scotia-Vanderbilt vein system on the southeast side of Treasure Mountain (fig. 17) is along a continuation of the strong N. 40° E. vein set present at the Sunnyside mine. The Scotia-Vanderbilt veins are exposed along strike for nearly 2 km and have widths up to 30 m (Standen and Kyle, 1985). The vein system consists of three major sets of mineralized

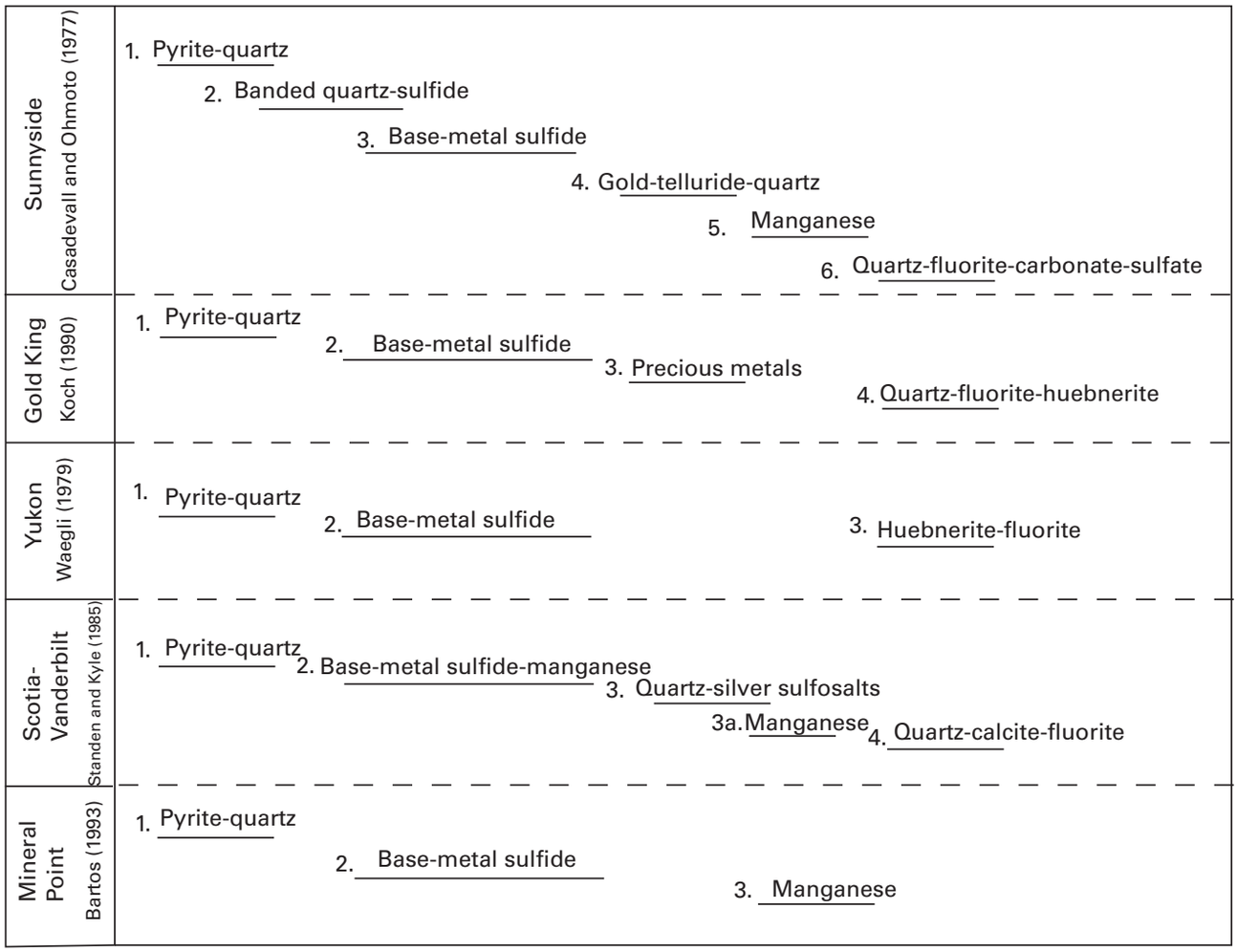

Figure 18. Paragenetic stages of vein mineralization from Eureka Graben area and adjacent areas. Note occurrence of late vein stages with fluorite and huebnerite, which are commonly associated with geochemical enrichments in molybdenum.

fractures. The first averages a trend of about N. 50° E. and includes the Scotia and Vanderbilt veins. A second set of shorter veins is nearly perpendicular to the first set, and trends about N. 55° W. A third system of nearly transverse veins, represented by the notably gold-rich Golden Fleece vein (fig. 17), averages about N. 75°–80° E., and appears to postdate the other two sets (Standen and Kyle, 1985). As typical of other areas, the volume of ore minerals is generally greatest near the intersections of these prominent structures (Casadevall and Ohmoto, 1977; Burbank and Luedke, 1969). The veins are composed mainly of quartz, pyroxmangite, and calcite with sulfides of pyrite, sphalerite, galena, and chalcopyrite in decreasing order of abundance. Ore also may contain free-gold, sulfobismuthites of lead and silver, and small amounts of tetrahedrite, molybdenite, native silver, and native copper (Ransome, 1901). The Scotia-Vanderbilt vein system can be generally subdivided into four main episodes (Standen and Kyle, 1985), which are roughly similar in character to those described within the Sunnyside deposit (Casadevall and Ohmoto, 1977) (fig. 18). Electron microprobe studies from vein minerals show some substitution of arsenic, gold, and silver within chalcopyrite, as much as 0.2 percent silver in galena, and 0.2 percent silver and 1.6 percent arsenic in pyrite (Standen and Kyle, 1985).

Other mines in the gold belt (discussed in the preceding section), such as the Sound Democrat, Silver Queen, Sunnyside Extension, and San Juan Queen (fig. 17) have ore mineralogies and stages that closely resemble that of the Sunnyside and Scotia-Vanderbilt mines (Ransome, 1901). Most are prominent veins with bold outcrops that are generally stained black due to the oxidation of pyroxmangite. In the subsurface, these veins are characterized by alternating bands of ore and barren pyroxmangite. Orebodies range from a few centimeters to 10 m in thickness. The ore minerals include roughly subequal proportions of sphalerite and galena, which together generally exceed abundances of other ore minerals. Free-gold along with quartz was reported in all of the just-mentioned mines, and silver occurred commonly within lead sulfobismuthites (Ransome, 1901). Gangue minerals included quartz, pyroxmangite, and locally fluorite and calcite. The pyroxmangite stage is always poor in ore minerals, but small amounts may occur with the richest ore.

Some of the gold-rich mines, including the Golden Fleece, Lead Carbonate, and Gold King (fig. 17), are reported to be lacking in the intermediate base-metal stages (Ransome, 1901; Langston, 1978; Koch, 1990). Instead, these mines are noted for the occurrence of free-gold commonly associated with pyrite-quartz in small quartz veinlets, and vuggy quartz and carbonate gangue (Langston, 1978; Koch, 1990). The Golden Fleece mine contained a small, tight vein that produced rich free-gold ore (Ransome, 1901). The vein, which trends N. 75° E., ranges in thickness from about 1 to 20 cm and is accompanied by clay gouge. Ore is free dendritic gold in a gangue of quartz and rare rhodochrosite. Quartz occurring with the gold ore is very dark owing to abundant inclusions of pyrite, galena, sphalerite, and possibly other ore minerals. Massive sulfides and pyroxmangite were absent. The Gold King–Davis vein system consists of two subparallel veins that merge downward into a root zone of one major, northeast-trending vein (Koch, 1990). These veins formed along subsidiary faults and fractures of the Eureka graben that also host one of the important veins of the Sunnyside mine. The Gold King–Davis veins can be traced for more than 1 km along strike and have maximum widths of 5 m. Mineralization at the Gold King mine formed deposits in four discrete stages: (1) massive pyrite and milky quartz, (2) base-metal sulfides of chalcopyrite, galena, and sphalerite, (3) the precious-metal suite of sulfosalts, free-gold, and gold and silver tellurides, and (4) quartz, fluorite, huebnerite with minor manganese silicates (fig. 18) (Koch, 1990). Total production from the mine included 603,738 metric tons of ore averaging 0.6 oz gold/t, 2.9 oz silver/t, 0.7 percent lead, and 0.5 percent copper (Koch, 1990).

Base-Metal Veins with Late-Stage Manganese Silicates

Mineral Point

Mineral Point, located about 5 km north of the Sunnyside mine (fig. 17), covers about 10 km^2. More than 100 veins are exposed in this area, although only about 20 of these had some production. Incomplete mill figures suggest small amounts of hand-sorted silver-gold ore were mined, mostly prior to 1900, with assays as high as 0.9 oz gold/t, and 56 oz silver/t (Bartos, 1993). About 20,000 tons of ore was produced from 1901 to 1941 with general grades of 0.01 oz gold/t, 1.9 oz silver/t, 0.1 percent copper, 2.3 percent lead, and 0.8 percent zinc (Kelley, 1946). Post-World War II production was minimal.

Mineral Point veins are also mostly along northeast-trending Eureka graben structures, but some are along east-west and northwesterly orientations. Veins cut dacite intrusions at Houghton Mountain (fig. 17), suggesting their age to be <23 Ma. However, similarities in mineralization style suggest they are within the same general age span as many of the gold-rich veins. (See previous section.) Vein widths range from 0.3 to 3 m, averaging 1 m, and are typically simple in texture and mineralogy (Bartos, 1993). However, some veins are complex, exhibiting multiple opening and filling of fissures. Three general stages of mineralization (fig. 18) have been identified in Mineral Point veins: (1) quartz-pyrite, (2) banded quartz-sulfide, and (3) manganese-carbonate (Bartos, 1993). In contrast to many of the veins to the west, these veins lack an intermediate to late precious-metal stage (fig. 18), and stage 3 manganese is generally only present within large, continuous, northeast-trending veins. Some of these veins contain a late-stage mineral assemblage containing huebnerite (Belser, 1956) and are enriched in molybdenum.

California Gulch

The California Gulch mining area includes the main glacial valley and adjacent ridges of California Gulch above Animas Forks (fig. 17). The most significant mining and prospecting occurred along the north wall of the valley, spanning

the Mountain Queen mine (mine # 41) at the top of the basin to the Columbus mine at Animas Forks (fig. 17). Ore production from the principal mines—Mountain Queen, Little Ida (mine # 15), Burrows (mine # 16), Vermillion (mine # 17), Frisco tunnel (mine # 19), and Columbus (mine # 23)—totaled about 19,000 tons from 1880 to 1950 (Burbank and Luedke, 1969), averaging <0.01 oz gold/t, 0.2 oz silver/t, 0.1 percent copper, 9 percent lead, and 5 percent zinc. After 1950, ventures in this area were largely exploratory. Most veins filled prominent northeast-trending Eureka graben structures (such as the Vermillion, Columbus, Dakota veins; pl. 4 in Burbank and Luedke, 1969), although some in the upper basin are along strong east-west fissure zones (for example, the Mountain Queen, Custer, Indian Chief, Belcher; pl. 4 in Burbank and Luedke, 1969), and a few near Animas Forks filled northwesterly structures. The largest orebodies formed along the intersections of northeast-and northwest-trending veins (Burbank and Luedke, 1969). Veins are quartz-rich, ranging from 0.3 to 60 m across, and many can be traced along strike for several kilometers. The ore mineralogy and paragenetic stages are generally very similar to those of veins in the Mineral Point area, although late-stage manganese silicate gangue may be more abundant (fig. 19). The abundance of manganese silicate gangue is reflected in the presence of manganese-cemented conglomerates (of probable Holocene age) within the upper reaches of California Gulch (Verplanck and others, this volume, Chapter E15; Church, Fey, and Unruh, this volume, Chapter E12). As indicated by production figures and geologic reports (Ransome, 1901; Kelly, 1946; Burbank and Luedke, 1969), these veins were mostly rich in lead and zinc sulfides, marginal in copper, and largely devoid of intermediate to late-stage gold mineralization. However, late vein-related fluorite and huebnerite (Ransome, 1901; Belser, 1956) and associated molybdenum, fluorine, and tungsten anomalies, as observed in various sample media (D.J. Bove and others, unpub. data, 2002), are present in upper California Gulch, north of California Mountain.

Zoning of Manganese Silicate Gangue Material

Manganese silicates are abundant in veins of the north Eureka Graben area, and a definite central zone is present away from which they tend to diminish (fig. 19). This center is localized roughly along the Sunnyside-Mastodon vein trend. Calculations from assay analyses indicate that 10–14 m widths of these 20–60 m wide veins are composed entirely of normative pyroxmangite (Young, 1966; Langston, 1978). From this central area, the manganese content diminishes greatly to the west towards the Ross Basin area (Young, 1966). This westward decrease in manganese continues toward the Red Mountains area. Manganese silicates are also generally rare within veins west of the Bonita fault and decrease north of Ross Basin toward the Poughkeepsie Gulch area. Pyroxmangite also is rare within precious-metal veins to southwest of the central zone of manganese enrichment (Langston, 1978), and decreases in abundance similarly to the northeast towards Mineral Point and Engineer Pass.

Vein-Related Hydrothermal Alteration

X-ray diffraction and petrologic studies indicate that vein-related alteration in the Eureka Graben area consists of a proximal quartz-sericite-pyrite-zunyite assemblage and a distal sericite-kaolinite facies with increasing chlorite and calcite at the transition with the propylitized wallrock (Standen and Kyle, 1985). Nearest the vein, wallrock is typically altered to an envelope of fine-grained quartz, which grades into the completely recrystallized assemblage of quartz-sericite-zunyite-pyrite (Casadevall and Ohmoto, 1977). Towards the distal sericite-kaolinite facies, tiny euhedral grains of primary apatite appear, and relicts of feldspars and mafics can be recognized. Widths of the alteration envelope vary with vein width, although fault gouge locally seals the wallrock from the associated vein alteration. The proximal alteration zone typically ranges from half to one times the vein width; however, width of the distal alteration zone varies considerably, but generally is one to two times the vein width (Standen and Kyle, 1985). In some localities, intersections of multiple veins are marked by coalesced alteration zones as much as 0.3 km wide in area.

Rhyolites and Associated Mineralization

A series of small, high-silica rhyolite intrusions and dikes crop out along a 5 km long zone trending roughly N. 30° E. from California Mountain to Denver Hill (fig. 17). This zone of rhyolites extends another 5 km northeast of the study area and includes dikes in the Engineer Pass area and an extrusive dome complex at Dolly Varden Mountain (Hon and others, 1986). The rhyolites within the study area are generally aphanitic and finely flow banded. They are locally vesicular and contain rare fine-grained quartz phenocrysts. Geochemical data indicate that these rocks are enriched in large ion lithophile (LIL) elements (Lipman and others, 1982; P.J. Bartos, unpub. data, 2001) and have many compositional similarities (SiO_2>75 percent; K_2O>4.5 percent; Rb>300 ppm) to rhyolites associated with well-known molybdenite deposits (Ludington, 1981; White and others, 1981; Hildreth, 1979). However, key elements such as niobium (20–50 ppm), tungsten (3–9 ppm), and fluorine (0.1 percent), although highly elevated, fall at the lower limits of or below the diagnostic levels of deposit-associated rhyolites. Rhyolitic intrusions at Houghton and California Mountains are associated with 0.75–1 km^2 zones of pervasive QSP-altered rock containing a dense network of hairline quartz veinlets (fig. 17). Pyrite within these zones is typically altered to iron oxides and jarosite, and kaolinite probably formed due to related supergene processes (Bartos, 1993). The rhyolite near Denver Hill (fig. 17) is generally very weakly altered; however, it is locally silicified and pyritized, especially near its brecciated margins. Rare molybdenite mineralized material has been reported in breccia zones in the rhyolites near Denver Hill (Lipman and others, 1982), and molybdenum concentrations in all the altered rhyolites typically range from 20 to 50 ppm, along with 2–5 ppm copper, and 20–50 ppm lead (D.J. Bove, unpub. data, 2002). Molybdenum is also anomalously concentrated

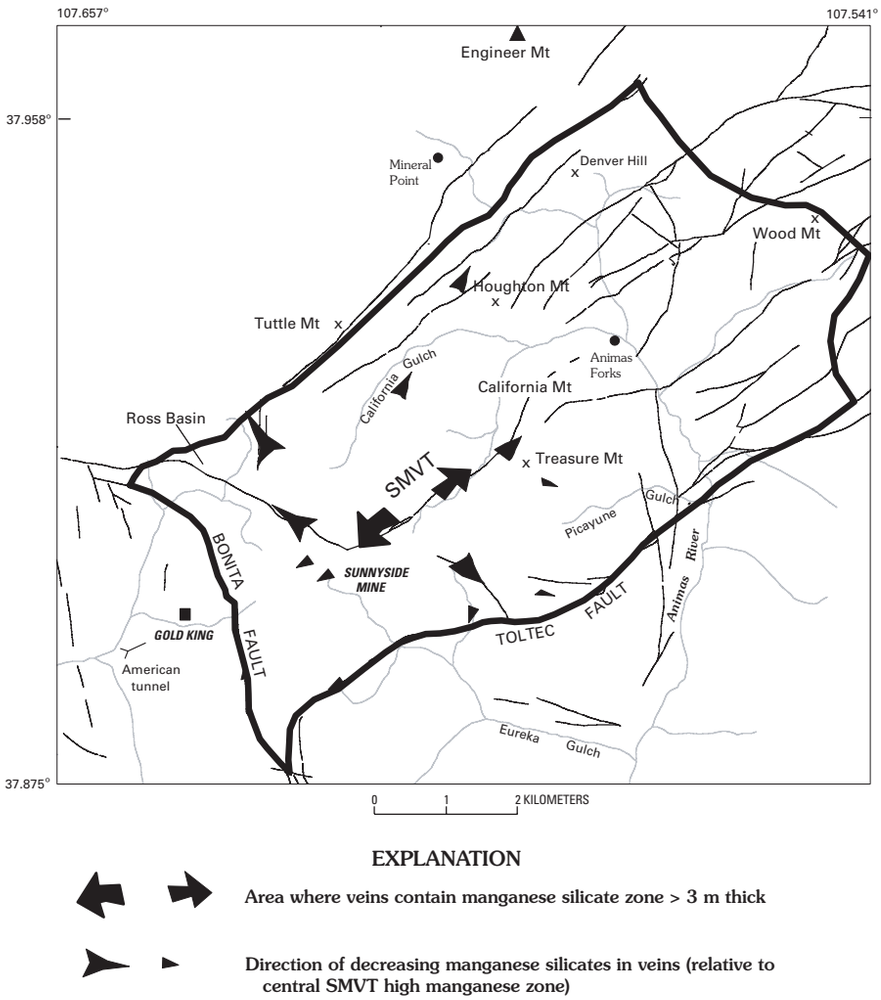

Figure 19. Eureka Graben area showing manganese silicate zoning trends. Center of zone is along Sunnyside-Mastodon vein trend (SMVT). Data compiled from Langston (1978), Young (1966), and this study.

in mine dumps surrounding the Denver Hill, Houghton Mountain, and California Mountain rhyolites, ranging as high as 100–200 ppm. In addition, vein-related fluorite and huebnerite, which are paragenetically later than most gold and base-metal mineralization in the area (fig. 18), have also been reported in mines near all three of these intrusions (Ransome, 1901; Belser, 1956). Fluorite, huebnerite, and elevated molybdenum are also characteristic of a late-stage vein assemblage observed at the Sunnyside and adjacent mines and in a roughly 3 km wide zone extending from Kendall Mountain along Cement Creek to just north of Gladstone (Belser, 1956).

A prominent elliptical aeromagnetic high (about 1,500 m across) was delineated near the Gladstone area along the N. 30° E. trend of the previously mentioned rhyolites (Smith and others, this volume, Chapter E4). Although no rhyolite intrusions have been exposed in this area, the nearby American tunnel (fig. 17) exposes numerous veins containing late-stage fluorite and some huebnerite (Thomas Casadevall, oral commun., 2000). In addition to the aeromagnetic data, evidence of a buried intrusion in this area is suggested by mineralogic data from two deep (610 m) exploratory holes drilled from the main level of the American tunnel. Rocks near the bottom of these holes were cut by intensely sericitized veins and associated breccias characterized by an assemblage of anhydrite, pyrite, and fine-grained andradite. Fluid inclusions within a quartz-sericite-andradite veinlet from this deep core interval contained a daughter mineral tentatively identified as halite (Casadevall and Ohmoto, 1977). The occurrence of halite within these inclusions indicates a minimum salinity of 26.5 equivalent weight percent NaCl—in marked contrast to salinities <3.6 equivalent weight percent from all other fluid inclusions measured from the Sunnyside vein system (Casadevall and Ohmoto, 1977). The presence of such high salinities in conjunction with sericitic-altered breccias and veins, hydrothermal anhydrite and garnet, and the aeromagnetic anomaly suggests the possibility of a genetic relationship to an underlying intrusion. Similar mineralogic assemblages and high-salinity fluids are documented within greisen zones related to rhyolite-granite intrusions and molybdenum porphyry systems (White and others, 1981).

The association between high-silica rhyolites and late-stage fluorite, huebnerite, and molybdenum in polymetallic veins in the study area bears some similarities to Climax-type porphyry molybdenum systems. Detailed studies of Climax-type deposits have documented the genetic relationship between LIL-enriched, high-silica rhyolite-granite intrusions and late veins radial to these intrusions, which contain quartz, base metals and precious metals, and later fluorite, huebnerite, and molybdenite (Bookstrom, 1989). Probably one of the best local examples of such relationships is in the Cuba Gulch area, about 4 km east of Eureka, and just outside the study area. At this locality, a 17.1 Ma high-silica rhyolite dike is associated with anomalous concentrations of tin, tungsten, niobium, and molybdenum in adjacent rock and stream-sediment samples (Bove and others, 2001). Field studies indicate that this dike is associated with mineralized tourmaline-bearing pebble dikes, fluorite, and sparse molybdenite (Hon, 1987a).

Geochemistry of Altered Rock and Vein-Adjacent Zones

Geochemical data from regional propylitic and QSP vein-related rock (V-QSP) from the Eureka Graben area (Langston, 1978) are summarized in table 3 and figure 4. Comparisons of these data indicate that iron is statistically higher in propylitized rocks, whereas values of lead, manganese, and silver (not shown) in the upper concentration ranges are considerably higher in V-QSP-altered rocks. However, zinc and copper are analytically indistinguishable between these two groups of altered rocks. The marked decrease in iron in the V-QSP-altered rocks probably reflects near-surface pyrite weathering and mobilization of iron. The decrease in iron and the sporadically high concentrations of silver, lead, and copper in some samples suggest that the V-QSP zones, prior to oxidation, may have been enriched in these metals. This is substantiated by petrographic studies (see section on vein-related alteration in <18 Ma polymetallic vein systems), which indicate an abundance of fine-grained base-metal sulfides in alteration envelopes adjacent to polymetallic veins. A wide range in manganese concentrations (<160 ppm to >4,200 ppm) is noted for samples from the V-QSP zones. The presence of manganese silicate gangue material (some samples taken above productive ore zones; Langston, 1978) interspersed throughout the V-QSP zone probably accounts for the high range of manganese concentrations. Chlorite, epidote, and thin manganese surface coatings in the altered wallrock likely contribute to the lower manganese abundances. It is notable that manganese, lead, zinc, and copper are statistically indistinguishable in propylitic rocks from the Eureka Graben, Mount Moly, and Red Mountains–OPAM areas. Pyrite from regional propylitically altered samples of the Eureka Graben area, like their disseminated counterparts in the Red Mountains and Mount Moly areas (table 2), are similarly devoid of metals and arsenic (Standen and Kyle, 1985).

Mine Dump Compositions

Mean manganese abundance (1,500 ppm) in dumps from the Eureka Graben area ranks second highest among the five mineralized areas (table 4; fig. 7). However, many of the mine dumps from the zone of highest manganese abundance, as delineated in figure 19, could not be sampled due to access restrictions on private land. Ranges of lead and zinc (mean of 3,330 ppm and 2,110 ppm, respectively) generally overlap with those from dumps in the other four mineralized areas (fig. 7), whereas the range of copper (189 ppm mean) is much lower than in samples from the Red Mountains and South Silverton areas. Arsenic concentrations, which overlap statistically with those of the Mount Moly area samples, are substantially higher than those in OPAM and South Silverton samples, but are much lower in comparison to the Red Mountains data. Like the Mount Moly area, ores are known to contain tetrahedrite-tennantite and some chalcopyrite rather than enargite. Molybdenum concentration is statistically higher than in all other mineralized areas with a mean of 50 ppm. Six of eight Eureka Graben-area dumps with the highest molybdenum concentrations (110–300 ppm) are clustered in the Houghton Mountain and Denver Hill areas (fig. 17). The other two dumps with anomalously elevated molybdenum are on the southeastern periphery of Houghton Mountain. The remaining 10 dumps from other parts of the Eureka Graben area have molybdenum abundances <47 ppm. These data reflect the association between young high-silica rhyolite intrusions such as at Houghton Mountain and Denver Hill, and a late-stage assemblage within related veins containing fluorite, huebnerite, and elevated molybdenum.

Mine Water Chemistry

Geochemical data from 13 mine waters in the Eureka graben area are shown in figure 8 and summarized in table 5. The geochemistry of these waters is highly variable: pH ranges from 2.63 to 7.03, and dissolved concentrations range from 28 to 9,170 µg/L aluminum, 36 to 71,600 µg/L manganese, 27 to 49,800 µg/L zinc, 3 to 6,450 µg/L copper, and <19 µg/L arsenic. As shown in figure 9, these mine waters, like those from the other four mineralized areas, can be generally divided into low- and high-pH groups.

Five of the thirteen mine waters have near-neutral pH (6.21 to 7.01), whereas one sample was borderline acidic (pH 4.69). These samples had a wide range in alkalinity (<0.1 to 122 mg/L), and they contained dissolved zinc ranging from 27 to 6,540 µg/L, <21 µg/L lead, and 3 to 84 µg/L copper. Manganese concentrations were widely variable, ranging from 36 to 6,860 µg/L, whereas both aluminum (3 to 373 µg/L) and iron (<21 to 226 µg/L) concentrations were relatively low. Calcium (59 to 113 mg/L), strontium (683 to 780 µg/L), and sulfate (300 to 540 mg/L) were moderately elevated in three of these waters (table 5). However, these concentrations are markedly lower than the subset of high-calcium-strontium-sulfate waters in the Mount Moly and OPAM areas, which had more than double the concentration of each of these elements.

The overall geochemical signature of eight low-pH mine waters from the Eureka Graben area is distinctive in comparison to low-pH discharge from mines in the other mineralized areas (fig. 10). Although aluminum, iron, and sulfate concentrations plot roughly in the middle of low-pH mine water data from the other areas, mean manganese concentration (8,100 µg/L) is 2 to 34 times higher than that of low-pH mine waters from the other mineralized areas. Manganese concentrations of 71,600 µg/L have been reported in discharge from the Silver Queen mine (Jim Herron, Bruce Stover, Paul Krabacher, and Dave Bucknam, Unpublished Mineral Creek feasibility investigations report, Upper Animas River Basin, Colorado Division of Minerals and Geology, 1997), and concentrations as high as 92,400 µg/L (see database, Sole and others, this volume) have been measured in discharge from the American tunnel—the main haulage tunnel to the Sunnyside and other important Eureka graben veins (fig. 17). These manganese-rich waters reflect the abundance of manganese minerals within many of the Eureka graben vein structures. In addition to manganese, these mine waters have high concentrations of copper and zinc (mean of 633 and 9,570 µg/L, respectively), and intermediate levels of copper (633 µg/L mean) and lead (170 µg/L mean) compared to low-pH mine waters from the other mineralized areas. Although base-metal concentrations are elevated, mean arsenic abundance was low (<1 µg/L mean), reflecting the absence of enargite or other arsenic-bearing minerals within this mineralized area.

Although no stable isotope data are available for either low or higher pH mine discharge within the Eureka Graben area, a $\delta^{34}S$ value of +7.9 was measured for mine water issuing from the American tunnel portal. This value is intermediate between vein and disseminated sulfides (–6.3 to +2.7 per mil) and gypsum and anhydrite phases (+15.3 to +19.0 per mil) associated with the Sunnyside mine workings (table 4 in Casadevall and Ohmoto, 1977; table 7, this study). These data suggest that sulfate within waters draining the extensive Sunnyside mine workings was derived by dissolution of both light sulfide and heavy sulfate minerals. The presence of late-stage gypsum and anhydrite within many of the Eureka graben veins suggests that other mine waters within this mineralized area could have similar intermediate $\delta^{34}S$ compositions.

Background Surface Water Chemistry

Background water within the Eureka Graben area contrasts sharply with background samples from the previously described mineralized areas due to the relatively small volume of intensely altered rock—nearly 75 volume percent of area is propylitically altered—and the strong interplay with mineralized vein structures (table 6; fig. 17). Field studies indicate that three QSP-related waters sampled in the Houghton Mountain, California Mountain, and South Eureka Gulch areas (fig. 1) (table 3 in Mast, Evans, and others, 2001) derived metals from interaction with unmined vein structures along their flow path (V-QSP waters). The composition of these waters shows the distinct influence of both the surrounding QSP-altered rocks (pH=3.26 to 4.55) and vein structures with which they interact (Mn=2,670–74,700 µg/L; Cu=4–309 µg/L; Zn=640–14,400 µg/L). In contrast, propylitic waters influenced by veins and other mapped structures (PROP-V) have a mean pH of 6.52 and a mean zinc concentration of 143 µg/L (table 8). Several of these samples contained anomalously high concentrations of manganese (1,210 to 19,800 µg/L), copper (23 to 189 µg/L), and zinc (154 to 4,240 µg/L), values similar to metal abundances in the V-QSP waters. The maximum manganese (74,700 µg/L) and zinc (14,400 µg/L) concentrations from V-QSP and PROP-V waters are more than 17 times greater than the highest abundance of these elements in any of the non-vein-related waters from the Mount Moly, Red Mountains, or OPAM areas. These data suggest that these distinctly metal rich waters (V-QSP or PROP-V) must have interacted with some mineralized vein material. Specifics regarding flow paths for these types of water/mineralized rock interactions, however, have yet to be resolved. Although metal concentrations are quite high in some of these waters (V-QSP or PROP-V), contributed metal loads would be minimal as discharge is at most 0.2 ft^3/s.

Relative to the volume of propylitically altered rock in this area, associated water samples are very poorly represented (n=3). Compared to other background samples discussed in this study (table 6), these samples have relatively high pH (6.9) and low to moderate alkalinity (10 to 35 mg/L), strontium (81 to 349 µg/L), and sulfate concentrations (28 to 113 mg/L) (table 8). One of these three samples has anomalously elevated zinc concentration (237 µg/L), whereas zinc abundances in the other samples are near analytical detection limits. It is probable that the sample with elevated zinc interacted with some mineralized vein material, although no mineralized structures were noted nearby. $\delta^{34}S$ values from three water samples from the Eureka Graben area range from –2.4 to 0 per mil (Nordstrom and others, this volume, table 1). These values are generally within the range of sulfides in the study area (table 7). These data augment aqueous geochemical data (table 8) showing a mean strontium concentration of 151 µg/L for the entire Eureka Graben area data set. As pointed out in a previous discussion, such low strontium concentrations are indicative of at most, very limited interaction with gypsum or anhydrite.

Aqueous Geochemical Signatures of High-Silica Rhyolite Intrusions and Late-Stage Vein Assemblages (F, W, Mo)

Studies regarding the geochemistry of high-silica rhyolites and the late fluorine-tungsten-molybdenum-bearing assemblage (see section, "Rhyolites and Associated Mineralization") were conducted to investigate potential dispersion of the diagnostic LIL-elements into local surface waters. Preliminary study results show that waters anomalously enriched in fluoride (>2 mg/L), potassium (>1.5 mg/L), beryllium (>5 µg/L), and to a lesser extent molybdenum, correlate strongly with exposures of high-silica rhyolite

intrusions and related late-stage vein assemblages containing fluorite, huebnerite, and elevated molybdenum (D.J. Bove and others, unpub. data, 2002). This association is particularly well illustrated in the California Gulch area, where inflows with high fluoride concentrations (2.8 to 22 mg/L) (Kimball and others, this volume, Chapter E9) closely bracket the extent of a small, QSP-altered rhyolite intrusion near California Mountain (fig. 20). Local occurrences of fluorite and huebnerite have also been documented in this vicinity (Ransome, 1901; Belser, 1959), and related mine discharge also contains characteristically elevated concentrations of fluoride, beryllium, and potassium (Peter Butler, Robert Owens, and William Simon, Unpublished report to Colorado Water Quality Control Commission, Animas River Stakeholders Group, 2001).

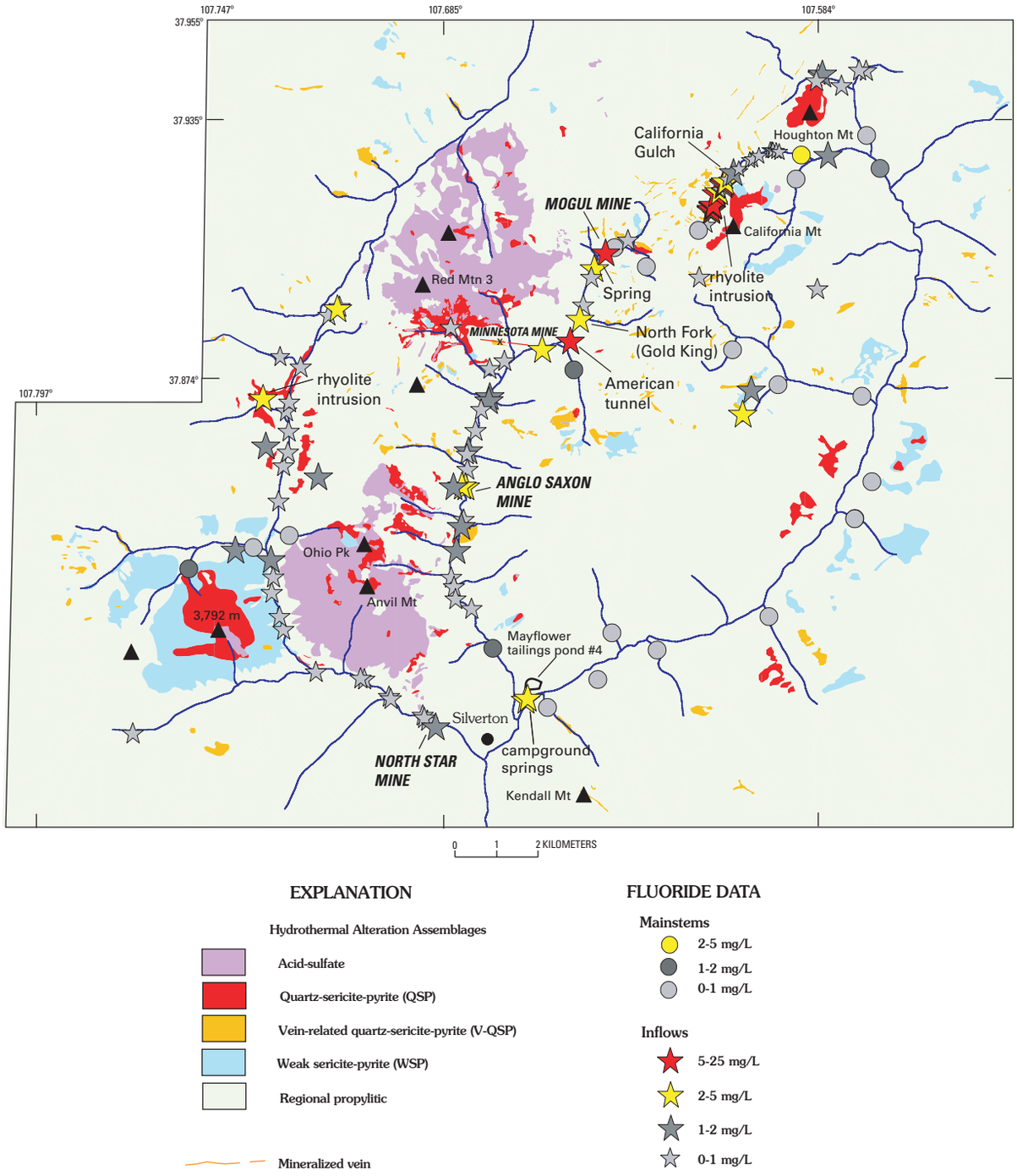

Figure 20. Fluoride data from mainstem streams and miscellaneous inflows superimposed on generalized alteration map of study area. Fluoride data from Kimball and others (this volume, Chapter E9), D.J. Bove and K. Walton-Day (unpub. data, 2002), Unpub. report to Colorado Water Quality Control Commission, ARSG, 2001.

Ten springs, seeps, mines, or smaller tributaries sampled outside of the California Gulch area also contain fluoride concentrations in excess of 2 mg/L (fig. 20). Potassium (>1 mg/L) and beryllium (>3 µg/L) also show corresponding enrichments in most of these waters (Unpublished report to Colorado Water Quality Control Commission, ARSG, 2001). Seven of these localities (American tunnel, Gold King via North Fork Cement Creek, Anglo Saxon mine (mine # 183) and nearby spring, small mine in the South Fork of Eureka Gulch, the Longfellow mine/Koehler tunnel (# 77 and # 75), and a spring along the Minnesota vein extension) (fig. 20) correlate with mines or springs influenced by vein systems containing late-stage fluorite and huebnerite. However, the elevated fluoride concentrations in the remaining three waters are more difficult to explain. One of these waters, which was collected from the Mogul mine in 1999, had the highest fluoride concentrations in the entire study (21.8 mg/L) (all sample data based on post-1996 sampling) (Walton-Day and others, this volume, Chapter E24; Sole and others, this volume; D.J. Bove and others, unpub. data, 2002). The high fluoride concentration of the Mogul mine discharge contrasts sharply with the low fluoride concentrations at the nearby Queen Anne (mine # 34) and Grand Mogul mines (mine # 35) (<1 mg/L fluoride), which exploited similarly mineralized and parallel vein structures. Furthermore, fluorite has not been reported as a vein constituent at the Mogul mine nor has it been observed on the associated waste dumps (Ransome, 1901; Burbank and Luedke, 1969; T. Hennis, private mine owner, oral commun., 2001). However, dramatic increases in fluoride concentration in upper Cement Creek (above the North Fork, fig. 20) between 1996 and 1999 (0.6 to 2.4 mg/L), suggest that fluoride concentrations at the Mogul mine may have been much lower prior to 1996 (Briant Kimball, written commun., 2001). The extrapolated increase in fluoride concentration at the Mogul mine over this 3-year time interval was accompanied by large increases in discharge as well as manganese, sulfate, and metal loads (Walton-Day and others, this volume). Studies by Walton-Day and others (this volume) suggest that these changes may be related to the 1996 plugging of the American tunnel (fig. 20), which caused the rise of its mine pool and resulted in the influx of this water into the Mogul mine workings. The extrapolated four-fold increase in fluoride concentration in the Mogul mine discharge between 1996 and 1999 is consistent with the scenario postulated by Walton-Day and others (this volume), as it reflects the uniquely high fluoride concentration of the American tunnel mine water (3 to 18 mg/L fluoride; 9 to 85 µg/L beryllium; 1 to 1.3 mg/L potassium; 30 to 90 mg/L manganese; database in Sole and others, this volume).

Two metal-rich seeps (2,430 and 8,310 µg/L zinc; 50 and 80 mg/L manganese) near the south Silverton campground (fig. 20) also have high fluoride (3.9 and 4.6 mg/L), potassium (3.9 to 5.2 mg/L), and elevated beryllium (1.3 and 2 µg/L) concentrations. The 45,000 m^2 Mayflower tailings pond #4 (site # 510, Church, Mast, and others, this volume), located less than 400 m upgradient, represents a potential source for these high-fluoride and metal-rich seeps. Historical records indicate that this tailings pond, which was erected in 1976, is composed entirely of Sunnyside mine waste (William Jones, oral commun., 2002). Considering the characteristically high fluoride, beryllium, potassium, and manganese concentrations of waters interacting with Sunnyside vein material (such as the American tunnel mine discharge), tailings pond #4 is likely to be the primary metal source for these seeps. Although the nearby Aspen mine (fig. 20) contains some fluorite gangue material (Ransome, 1901), the associated mine waters contain <1 mg/L fluoride, no detectable beryllium or potassium, and <15 µg/L manganese (Unpublished report to Colorado Water Quality Control Commission, ARSG, 2001). Thus it is apparent that fluoride in combination with beryllium, potassium, and perhaps molybdenum can be utilized as natural occurring pathfinder elements for correlating water chemistry to key geologic features and mineralized source areas in the Animas River watershed.

<18 Ma Polymetallic Vein System—Northwest- and Northerly-Trending Veins

South Silverton Area

The South Silverton area (figs. 1 and 21) includes the alpine ridges and the deep glacial cirques and valleys southeast of Silverton. Ore deposits are principally within simple fissure-filling veins that average 1–5 m wide, but are as much as 10 m wide (Ransome, 1901; Varnes, 1963). With exception of the gold-rich Shenandoah-Dives mine, ores were predominantly low grade and base metal rich, with low gold:silver ratios (Bartos, 1993; Ransome, 1901; Varnes, 1963). Areas of hydrothermally altered rock are largely confined to narrow zones surrounding the veins and some broad but still localized areas related to 26 Ma quartz monzonite intrusions. More than 90 volume percent of South Silverton area is characterized by regional propylitically altered rock. These regionally altered rocks are mostly of the CEC subgroup—as described in detail in the section on regional propylitic alteration—and contain abundant epidote, chlorite, and calcite.

Veins were localized along two principal fracture systems: the first group, or the "western shear system" (fig. 21; west of Cunningham Creek), includes mineralized northwest-trending fractures, a complementary or conjugate set of weakly to unmineralized northeast-trending shear fractures, and a very productive set of northerly-trending tensional fractures. The second major group of fractures, or the "eastern shear system," is characterized by a group of mineralized northwest-trending veins in the eastern part of the South Silverton area (fig. 21; east of Cunningham Creek).

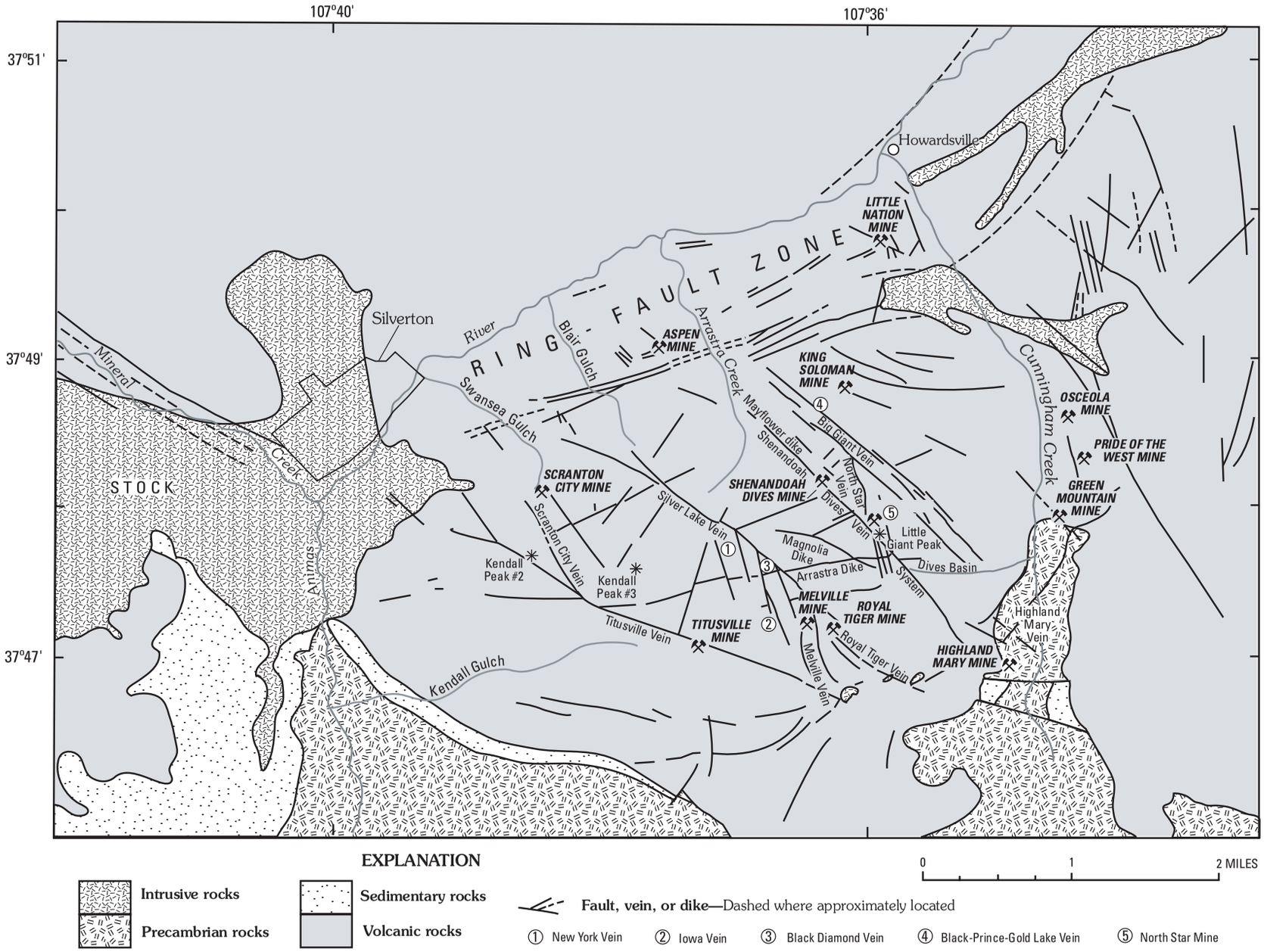

Figure 21. South Silverton mineralized area. Western shear zone is west of Cunningham Creek; eastern shear zone comprises Cunningham Creek and area to the east. Modified from Varnes (1963).

Western Shear System

The northwest-trending shear fractures of the western shear system host some of the most prominent veins or dike-filled veins in the South Silverton district, including the Shenandoah-Dives, Titusville, Silver Lake–Royal Tiger, Aspen, Big Giant, and the Magnolia dike (fig. 21). This fracture system appears to be the southern continuation of a similarly mineralized, northwest fracture zone that is prominent west of the Red Mountains area (Yager and Bove, this volume, pl. 1). Earlier studies postulated that the northwest fracture zone west of the Red Mountains was related to emplacement of the Stoney Mountain stock (Lipman and others, 1976). However, another possibility, as suggested by regional fracture patterns, is that these northwest fracture systems are part of an overall regional structural trend. The associated fractures in the South Silverton area have undergone considerable right-lateral and normal vertical displacement and generally dip to the northeast at moderate angles. Early reports state that ore minerals within these veins consisted chiefly of galena accompanied by sphalerite, chalcopyrite, pyrite, and minor tetrahedrite (Ransome, 1901). Gangue minerals were mostly quartz with calcite, barite, and local fluorite and gypsum. Silver values were said to be significantly low and considered relatively unimportant compared to that of lead (Ransome, 1901). The occurrence of free-gold with late quartz and (or) sphalerite and chalcopyrite was observed at that time only in the Royal Tiger and North Star veins, respectively.

Later production records, however, indicate that the South Silverton area was one of the principal gold producers in the western San Juan Mountains. The bulk of this later production was from the Shenandoah-Dives mine, which recovered roughly 4.5 million tons of ore with high gold:silver ratios rivaling that of Sunnyside mine in the Eureka Graben area (Bartos, 1993). The N. 40°–50° W.-trending Shenandoah-Dives vein system—one of the major faults of the western shear system—can be traced from Arrastra Creek southeastward over the high ridges and cirque basins for a distance of about 3,700 m to its terminus marked by the Highland Mary mine (fig. 21). Partly along this interval the vein follows along the andesitic Mayflower dike. The veins of the Aspen mine (fig. 21) may mark the northwest extension of the Shenandoah-Dives vein system (Varnes, 1963); however, talus cover in lower Arrastra Creek obscures this possible connection. Individual holdings along this vein complex, including the Mayflower mine in Arrastra Creek, the North Star mine on Little Giant Peak, and the Dives mine in Dives Basin (Varnes, 1963, pl. 2), were consolidated into the Shenandoah-Dives Mining Co. after 1926 (Varnes, 1963). Descriptions from these individual mines by Ransome (1901) suggest that ores were zoned from galena to silver-bearing tetrahedrite and gold-rich chalcopyrite with depth. Anglesite was abundant in the highest levels of the Shenandoah-Dives mine and represents oxidation at very high vein levels (Varnes, 1963).

The North Star mine and Empire group on Sultan Mountain are along northwest-trending veins that are likely part of the northwest-trending shear set. The mineralogy of these veins is similar and comprises galena, sphalerite, tetrahedrite, chalcopyrite, and pyrite with a gangue of quartz and some barite (Ransome, 1901). Late fluorite and huebnerite have also been reported in the North Star and Empire lodes.

The north-trending tensional fractures were the last of the "western" shear group to form, and they probably resulted as a consequence of continued shearing along the northwest-trending group (Burbank, 1933). As a group, these fractures strike N. 10°–30° W. and trend diagonally across the long narrow blocks bounded by the northwest-oriented shear fractures; dips are much steeper than those of the northwest veins, averaging about 80°. As the veins that filled the north-trending fractures approach the northwestern lodes, they tend to deflect and show a significant decrease in ore metals. Generally, the northerly veins were some of the most productive of the district, and include the Melville, New York, Iowa, Royal, and Black Diamond (fig. 21). The associated orebodies were reported to be more regular and of higher grade than many of the northwest-trending veins. Like the northwest veins, galena was also the dominant ore mineral; however, chalcopyrite and pyrite were typically more abundant in the northerly-trending veins and gold values were generally higher, running several ounces/ton (Ransome, 1901; Varnes, 1963).

Eastern Shear System

The veins of the "eastern shear system" (Varnes, 1963) are mostly located within or east of the Cunningham Creek area (fig. 21). These veins have filled northwest-trending shear fractures and a set of "radial" fractures that trend normal to the margins of the Silverton and San Juan calderas. The radial fractures are thought to have formed during resurgence of the San Juan caldera (28.0 Ma) prior to collapse of the Silverton caldera (27.5 Ma) (Hardwick, 1984); the associated fractures in this group show no lateral displacement. Also included in the eastern shear system are a number of weakly mineralized, arcuate granite porphyry dikes and related northerly-trending fractures and veins.

The Green Mountain and Little Nation mines (fig. 21) are characteristic of the northwest-trending veins of the eastern shear system. The Green Mountain vein, which in part is hosted in Precambrian schist, trends N. 40°–45° W. with dips near vertical. Total production (to 1948) has been estimated at 35,000 tons averaging 0.03 oz gold/t, 3 oz silver/t, 0.2 percent copper, 4 percent lead, and 3 percent zinc (Hardwick, 1984). The ore minerals consisted of abundant sphalerite and galena, with some chalcopyrite and pyrite, in a quartz gangue (Ransome, 1901). The Little Nation mine, located about 1,000 m southwest of Howardsville (fig. 21), is one of the few mines situated near the ring-fault zone of the Silverton caldera. The workings followed several discontinuous veins that trend about N. 50° W. and were characterized by lead-silver ores.

The Pride of the West, Osceola (fig. 21), and Little Fanny mines worked a system of parallel vein structures along one of the "radial" fracture systems. The associated veins are

located outside the structural margin of the Silverton caldera, and just inside of the earlier formed San Juan caldera (Yager and Bove, this volume, pl. 1). The ore deposits formed near the intersection of the radial fracture system with the buried structural margin of the San Juan caldera. Production of more than $10 million worth of base and precious metals has been recorded from these mines (Hardwick, 1984). Weighted average grades from this production were 0.08 oz gold/t, 5.3 oz silver/t, 0.3 percent copper, 6.8 percent lead, and 2.1 percent zinc (as calculated from table 1 in Hardwick, 1984). The main metallic minerals in order of approximate abundance are galena, sphalerite, pyrite, chalcopyrite, and minor magnetite and hematite. Native gold was reported locally at the Pride of the West and Osceola mines, and native silver and tetrahedrite were observed at the Pride of the West and Little Fanny mines (Hardwick, 1984). The gangue mineral assemblage consists primarily of quartz with lesser pyroxmangite, calcite, and barite. Calcite is also present as late-stage vein-fillings that crosscut main stage ore and gangue minerals and as cavity-fillings (Hardwick, 1984). While all three mines contain typical fissure-filling vein deposits, the Pride of the West and Osceola mines contain both vein and carbonate replacement deposits. The replacement deposits are present exclusively where large megabreccia blocks of Paleozoic-age carbonate rocks (collapse from the topographic margin of the San Juan caldera) are intersected by metal-bearing veins. The replacement ore assemblage is very similar in bulk composition to the vein ores and varies from a massive variety to "zebra" textures that consist of metallic bands alternating with quartz gangue (Hardwick, 1984).

Vein-Related Hydrothermal Alteration

Only narrow zones of alteration surround the veins in the South Silverton area, with alteration envelopes characteristically three to five times the vein width (Ransome, 1901; Hardwick, 1984). A detailed alteration study was conducted by Ransome (1901) in Silver Lake Basin. His study showed that rocks greater than 15 m away from the vein were only altered to the regional propylitic assemblage and were not affected by the vein hydrothermal solutions. At 15 m from the vein, the rock in hand sample appears similar to the propylitically altered samples, but under the microscope, feldspars have been changed to an aggregate of calcite and sericite, while augite and biotite have been altered to chlorite, calcite, and some leucoxene. The groundmass of these rocks is altered to a mixture of quartz, chlorite, sericite, and minor leucoxene. At about 0.6 m away from the vein, minor disseminations of galena are noted megascopically, and the rock is mostly converted to a mixture of quartz, sericite, and pyrite (Ransome, 1901). As observed in thin section, pyroxene and plagioclase in these rocks are altered to varying percentages of quartz, sericite, calcite, and chlorite, whereas biotites are mostly altered to sericite, with some chlorite, calcite, and leucoxene (Ransome, 1901). The groundmass is completely altered to a fine mixture of dominantly quartz and sericite, with lesser chlorite. At or near the vein, the rock becomes lighter in color, contains fine pyrite and minor galena, and is cut by numerous thin quartz veinlets. As observed petrographically, both phenocrysts and groundmass have been completely altered to quartz and sericite; calcite and chlorite are completely absent (Ransome, 1901).

Studies in the Cunningham Creek area document similar alteration envelopes around the veins that consist of quartz, sericite, pyrite, and (or) kaolinite (Hardwick, 1984). Within this halo, sericite has selectively altered feldspar phenocrysts along grain boundaries and microfractures and replaced the fine-grained groundmass of the volcanic wallrocks. The intensity of alteration increases inward toward the vein, and the wallrock adjacent the vein is almost completely silicified.

Geochemistry of Altered Rocks

Rock sample data from the South Silverton area is generally scant. Because these data are few and mostly represent fresh to propylitically altered rocks, they were not included in this study.

Mine Dump Compositions

Analytical data summarizing the geochemistry of eight mine dumps in the South Silverton area are presented in table 4. A comparison of these data to similar analyses from the four other mineralized areas divided in this report is shown in figure 7. Manganese abundance in the South Silverton samples is relatively high compared to the other four mineralized areas (fig. 7), with a mean of 3,440 ppm. As shown in figure 7, the range of these data overlaps with samples from the Eureka Graben area, which is noted for veins with high proportions of manganese-silicate gangue material. However, the South Silverton data are strongly influenced by two dump samples from mines along the Titusville vein (fig. 21) on the south side of the district, which contains 12,000 and 21,000 ppm manganese. Material from these two dumps is heavily manganese stained due to the presence of rhodochrosite, which is especially abundant within this particular vein system (Ransome, 1901; Varnes, 1963). Other than the Titusville structure, only a few veins in the South Silverton area contain notable quantities of manganese silicate or manganese carbonate gangue material (Ransome, 1901; Hardwick, 1984). These veins, which are mostly located in the Cunningham Creek area (eastern shear system, fig. 21), are reported to contain pyroxmangite and manganese-rich calcite gangue. Several of the veins of the western shear system (fig. 21) also contain late-stage, sparry calcite that carries as much as 11,000 ppm manganese. Mean lead and zinc abundances within the South Silverton samples are 6,390 and 2,450 ppm, respectively. As shown in figure 7, the range of lead abundance generally overlaps with that of samples from the Red Mountains, OPAM, and Eureka Graben areas but is notably higher than in the Mount Moly area mine samples. Galena is one of the dominant base metals in many of the South Silverton veins.

The range and mean abundance of zinc are generally similar to those of the other four areas, with exception of the Red Mountain area dumps, which contain less than half the mean zinc abundance of the South Silverton area dumps. Copper, with a mean of 1,510 ppm, is similar in abundance to the Red Mountains dumps (1,930 ppm), and is substantially higher than in the other three mineralized areas (fig. 7). However, mean arsenic abundance (49 ppm), which is the lowest of the four areas, is nearly 20 times less than in the Red Mountains dumps (940 ppm). These data reflect the relative abundance of chalcopyrite in many of these veins along with some tetrahedrite-tennantite, as well (Ransome, 1901; Varnes, 1963; Hardwick, 1984). However, the South Silverton ores, unlike those of the Red Mountains area, lack enargite and other similar ore minerals.

The South Silverton mine dumps have the highest calcium:strontium ratios of the five mineralized areas (mean of 70). Similarly high ratios (mean of 130) are commonly observed either in mine dumps with notable quantities of calcite gangue or with vein material derived from mines hosted in Paleozoic limestones (Fey and others, 2000). In contrast, dumps that contain gypsum gangue minerals have substantially lower calcium:strontium ratios (mean of 4). These data suggest that calcite is the principal calcium-bearing gangue mineral on these dumps. This hypothesis is supported by preliminary geochemical studies on calcite, gypsum, and anhydrite from the study area (table 2) that show similarly contrasting ratios for these carbonate and sulfate minerals. Field studies (Ransome, 1901; Varnes, 1963; Hardwick, 1984; Fey and others, 2000) and AVIRIS mapping (Dalton and others, this volume) have also documented that gangue and wallrock-related calcite is relatively abundant within the South Silverton area.

Mine Water Chemistry

Mine discharge in the South Silverton area (table 5; fig. 9) was characteristically high in pH (range of 3.2 to 8.30; 6.75 mean), with measurements below 4.5 recorded at only 1 of the 12 sample sites. Eight of the twelve mine waters had measurable alkalinity, ranging from 5 to 73 mg/L. Most waters had relatively low aluminum (95 µg/L mean), iron (26 µg/L mean), and sulfate (47 mg/L mean) concentrations (table 5), which probably reflects the low solubility of these elements at these higher pH values. Manganese concentration, which ranges from 3 to 5,420 µg/L, is also typically low, as evidenced by a mean of 63 µg/L. However, these data do not include drainage from mines along the Titusville vein, one of the few structures in the area with manganese-rich gangue material (Nash and Fey, this volume, Chapter E6). The South Silverton mine waters have distinctively elevated base-metal concentrations when compared to higher pH waters from the other four mineralized areas (fig. 9). Zinc concentrations are highly variable, ranging from 12 to 11,300 µg/L; their mean is 313 µg/L. Although dissolved lead (<5 µg/L) and copper concentrations (<45 µg/L) were low in 9 of the 12 mine water samples, they were highly elevated in discharge samples from the Royal Tiger and Iowa mines (fig. 21), located in upper Arrastra Basin (lead 393 to 5,610 µg/L; copper 251 to 1,390 µg/L). Note that both these mines were dominated by silver-lead ores, and together accounted for 20–25 percent of the total lead production in the South Silverton mining area (Varnes, 1963). The high elevation of these mines suggests that they exploited oxidized ores such as anglesite in their upper levels (Ransome, 1901; Varnes, 1963). Lead and copper-bearing sulfates and salts, which were probably more prevalent in the oxidized portion of these veins, have higher kinetic rates of dissolution than their lead and copper sulfide counterparts (White and Brantley, 1995). However, other geochemical parameters, such as pH, dissolved sulfate and iron concentrations (Smith, 1999; Nordstrom and Alpers, 1999), and anion complexing, could also control the concentration of lead and copper dissolved within these mine waters. (See following section, “Discussion and Summary.”)

The lack of low-pH mine waters in the South Silverton area readily distinguishes this area from the other four areas subdivided in this report. As just discussed, the higher pH probably limits the dissolved concentration of aluminum, iron, sulfate, and metals in the majority of these mine waters. The low amount of acidity in these waters is probably due to neutralization by calcite, which is abundant in wallrock and vein-related gangue material. Greater than 90 volume percent of the rocks within this mineralized area have been affected by calcite-rich propylitic alteration, whereas pervasive zones of pyritic-bearing rock are relatively minor. Paleozoic limestones, which crop out on the southern margins of the South Silverton area (fig. 21; Yager and Bove, this volume, pl. 1), are a likely source for some of the carbonate that has been redistributed into propylitically altered rocks and many of the veins. Despite the high metal concentrations of some of these mine waters, the mainstem streams draining the South Silverton area are relatively low in dissolved metal concentrations in their lower reaches (pH 7.51 to 8.1; zinc 10 to 300 µg/L) (Unpublished Report to the Colorado Water Quality Control Commission, ARSG, 2001).

Background Surface Water Chemistry

End-member background waters from the South Silverton area are limited to five samples from the propylitic alteration group (table 8; fig. 11). Fortunately, however, these waters represent an alteration assemblage that covers the vast majority of this mineralized area (≈92 percent). The five propylitic-related waters have mean pH and alkalinities of 8.15 and 52.7 mg/L, respectively. These measurements are substantially higher than from propylitic samples in the other four mineralized areas, which may be related to near-proximity to pre-Tertiary limestones and an abundance of propylitic-related calcite. Other than these parameters, the South Silverton propylitic waters are generally similar to low-strontium (non-gypsum or anhydrite-related) propylitic waters from the other four mineralized areas.

Discussion and Summary

The Animas River watershed study area and vicinity were divided into five different areas (fig. 1) based on age and type of mineralization, associated styles of hydrothermal alteration, and structural setting. The major mineralized areas include (1) Mount Moly area, site of a 26 Ma Mo-Cu porphyry system (19.5 km^2); (2) Red Mountains, 23 Ma acid-sulfate system (22.4 km^2); (3) Ohio Peak–Anvil Mountain, 23 Ma acid-sulfate area (20.6 km^2); (4) Eureka Graben area, <18 Ma polymetallic vein mineralization (44.4 km^2); and (5) South Silverton, <18 Ma polymetallic veins (72.3 km^2). Combined geologic and aqueous geochemical studies within these five areas have led to a better understanding of the major sources of anthropogenic and natural acidity and metals in the watershed. Detailed mapping has shown how the degree of bedrock alteration controls the variability of water compositions within each of these source areas. Aqueous geochemical signatures can be quite distinctive in some of these areas and can generally be explained by the varying geologic and mineralogic characteristics. Some of these more diagnostic geochemical signatures have been useful in identification of the origin of unidentified metal-bearing discharge distal to these sources.

Mount Moly Mineralization and Hydrothermal Alteration

The Mount Moly area is characterized by subeconomic molybdenum-copper mineralization related to late-phase, quartz monzonite intrusions of the Sultan Mountain stock. Zones of oxidation extend to depths of about 100 m below the ground surface, beneath which secondary copper was enriched. Relatively narrow, silver-bearing base-metal veins are present mostly on the periphery of the hydrothermal system. Hydrothermal alteration assemblages change outward from a central QSP zone into a weak sericite-pyrite (WSP) zone, and finally into regional propylitic-altered rock. As we have shown, waters draining the inner QSP alteration zones are strongly acidic due to the weathering of finely disseminated pyrite, and they have high dissolved sulfate, aluminum, and iron concentrations. Because disseminated pyrite in the Mount Moly area is deficient in trace metals, most of the dissolved metals in these waters (copper 45 µg/L mean; zinc 247 µg/L mean; table 8) must have been derived from other sulfide minerals in surface and subsurface altered zones (mean of 374 ppm copper, 28 ppm lead, and 109 ppm zinc in unoxidized drill core; table 3), and from associated base-metal veins (mean of 192 ppm copper, 1,580 ppm lead, and 1,860 ppm zinc in mine dumps; table 4). Although mean copper abundance is 374 ppm in rocks of the deeper zone of secondary enrichment (>100 m below the ground surface), values are greatly diminished in the overlying QSP oxidized rocks (15 ppm mean). Thus, the low dissolved copper concentrations in most QSP waters (45 µg/L mean) can be explained by either (1) shallow weathering and minimal interaction with the deeper copper-enriched zone, or (2) mixed contributions from the upper copper-deficient and the lower copper-enriched zones. The Mount Moly mineralized area is the only one of the five where background waters with elevated copper concentrations (>11 to 200 µg/L) are devoid of dissolved zinc (<10 µg/L). In addition, a subset of these waters has molybdenum concentrations exceeding 25 µg/L. This small population of background waters with high copper:zinc ratios may be the best representation of weathering within the deeper zone of secondary enriched copper. The lack of zinc in these copper-bearing waters is consistent with the relatively high copper:zinc ratios in rocks in the mineralized core of this porphyry system. Thus, the moderately elevated mean zinc concentration (247 µg/L) as calculated for the overall QSP water data set (table 8) may primarily represent zinc derived from polymetallic veins, which are concentrated toward the perimeter of the porphyry system. This is consistent with rock geochemical dispersion patterns (zinc, manganese, and strontium enrichment on the periphery of the hydrothermal system; Ringrose, 1982) and increases of zinc and manganese concentrations in background waters towards the perimeter of the hydrothermal system (Mast and others, this volume).

The mean concentrations of the metals lead (21 µg/L), zinc (505 µg/L), and copper (148 µg/L) in Mount Moly area low-pH mine waters (table 5) are among the lowest abundances in low-pH mine discharge from the five mineralized areas (fig. 10). Arsenic (<1 µg/L) is also very low in these waters, whereas manganese is only moderately elevated (1,600 µg/L). Compared even to these acidic mine waters (pH <4.5), QSP background waters (table 8) contain more than 2.5 times more aluminum and iron, whereas concentration ranges in zinc, copper, and sulfate are generally similar. Mean sulfate and strontium concentrations in QSP waters are 333 and 181 µg/L, respectively, which are roughly equivalent to low-pH mine discharge.

Red Mountains and OPAM Acid-Sulfate Areas

Two large centers of acid-sulfate-altered and mineralized rock in the Red Mountains and OPAM areas (fig. 1) are related to high-level dacite intrusions emplaced at ≈23 Ma. Geologic and stable isotope studies indicate that alunite and pyrite within these systems formed contemporaneously from vapor-dominant, magmatic hydrothermal fluids with high H_2S:SO_4 ratios. The abundance and wide vertical range in which pyrite forms in these types of hydrothermal systems are important owing to the exposure of pyrite to weathering processes, regardless of erosion depth. The abundance of silver-bearing, copper-arsenic ores containing enargite, tetrahedrite-tennantite, as well as copper ores of chalcocite, bornite, and covellite, distinguishes the ores of the Red Mountains area from more typical polymetallic vein deposits within and outside the Red Mountains area. These distinctive ores are typically hosted in brecciated and highly silicified zones that resulted from processes related to the vapor-dominant, high-sulfidation fluids. Despite the similarity between the Red Mountains and OPAM acid-sulfate hydrothermal systems, silver- and copper-arsenic mineralization was apparently scarce in the OPAM area, as noted by the very limited production and small number of mines.

The acid-sulfate assemblages in the Red Mountains and OPAM areas are very deeply rooted (>300 m beneath the surface) and grade from quartz-alunite outward into quartz-pyrophyllite, dickite, and further into smectite, and (or) propylitically altered rock. Pervasive QSP-altered rock is commonly exposed up to the tops of many high ridges, as observed in the Red Mountains area, and grades laterally into a weak sericite-pyrite (WSP) alteration assemblage.

Background waters in the Red Mountains and OPAM areas have a wide range of chemical compositions that correspond to the degree of hydrothermally altered rock that they drain. Whereas pH values in waters draining AS and QSP altered rocks are similarly low (mean pH=3.54), mean calcium, magnesium, and manganese concentrations are at least four times less in AS versus QSP waters. These data reflect the near absence of acid-neutralizing mineral phases within the acid-sulfate altered rock due to highly effective dispersion of the vapor-dominant hydrothermal fluids; in contrast, remnants of more weakly altered rock remain in the QSP alteration zones, probably due to less efficient circulation by lower temperature hydrothermal waters. Although dissolved aluminum (2,060 µg/L mean), iron (852 µg/L mean), and sulfate (53 mg/L mean) reach relatively high concentrations in AS and QSP waters in these two areas, mean copper (14 µg/L mean) and zinc (67 µg/L mean) concentrations are low to moderately elevated relative to other background waters from combined Red Mountains and OPAM data sets.

Much of the acidity and high loadings of sulfate, aluminum, and iron in a well-studied drainage typical of the entire Red Mountains area (Prospect Gulch; see fig. 15) is derived from weathering of the pervasive AS and QSP alteration zones (Wirt and others, 2001). In contrast, the majority of zinc and copper loading is mostly attributable to mining-related sources. Low zinc concentrations in background waters in the Red Mountains area reflect the very low zinc abundance within the large expanse of altered rock in this area; in fact, the highest zinc values are associated with relatively unmineralized, propylitic rock (110 ppm mean). Only two background waters in the Red Mountains and OPAM areas—both spring sites—have zinc concentrations above 450 µg/L. Studies by Bove and others (2000) suggest that one of these springs (site CC129; database in Sole and others, this volume), which discharges near the mouth of Prospect Gulch (1,072 µg/L zinc) (fig. 15), may represent interaction of QSP waters with unmined, vein-related material. The other spring site (CC128), which is located in the upper reaches of Topeka Gulch area (998 µg/L zinc) (fig. 14), is more poorly understood. However, low abundances of zinc in rocks or dissolved in other background waters within this drainage suggest that zinc in this spring water may also have been largely derived from vein-related material. The low but detectable dissolved copper concentrations observed in background waters of the Red Mountains area may have been derived from acid-sulfate altered rock, which has the highest copper abundances of all alteration assemblages in this area (19 to 859 ppm, with a mean of 79 ppm). Drill core studies indicate that elevated copper abundances within these acid-sulfate zones are related to a trace to as much as several percent disseminated covellite and enargite, and rare mineralized veins or breccias with massive pyrite, enargite, and minor galena. The relatively low copper concentrations in these background waters may reflect weathering and oxidation to depths extending to 100 m beneath the ground surface, which left the rocks bleached and depleted of copper (fig. 6). Mass balance studies from the Prospect Gulch area (Bove and others, 2000) indicate that essentially no dissolved metals within these background waters were derived from the weathering of disseminated pyrite.

Compared to the other four mineralized areas, mine discharge (table 5) samples from the Red Mountains area show pronounced enrichments in copper (2,340 µg/L mean) and arsenic (103 µg/L mean) in association with highly elevated lead (177 µg/L mean) and zinc (10,600 µg/L mean). The recognition of these distinct geochemical signatures in seeps down gradient of mines in the upper Prospect Gulch area (copper >4,900 µg/L, arsenic >51 µg/L; zinc >9,770 µg/L; W.G. Wright, unpub. data, 2002) has helped to discriminate these waters from those dominated by non-mining-related source contributions, which are nearly devoid of dissolved arsenic (Bove and Knepper, 2000; Neubert, 2001) and have low copper and low to moderate zinc concentrations compared to mine discharge samples (table 6).

Although copper, lead, and zinc concentrations in OPAM mine discharge samples are moderately high compared to low-pH samples from the other mineralized areas, arsenic abundance is low. These data combined with the relatively low levels of arsenic within OPAM mine dumps confirm geologic reports citing the absence of enargite in all but a few mines in this area. Mine discharge samples from the OPAM area and those on the periphery of the Red Mountain system have appreciably higher manganese, strontium, and other base cation abundances than mine discharge samples from the core of the Red Mountains altered area. In OPAM samples and those peripheral to the Red Mountains area, this is most likely related to availability of calcite, plagioclase, and chlorite due to near proximity to large volumes of propylitically altered rock. In contrast, most mine discharge samples collected toward the interior of the Red Mountains area drain mineralized workings within acid-sulfate-dominant rock characterized by low manganese and other base-element abundances. Alternatively, anomalously high manganese concentration in OPAM mine water samples could be related to dissolution of huebnerite ($MnWO_4$), which is common in many mines in the corridor around Cement Creek.

Stable isotope studies focusing on sources of dissolved aqueous sulfate have perhaps proved most useful in the Red Mountains area. Results show that the dissolved sulfate in mining and background waters may be largely derived from sulfide mineral phases. The light $\delta^{34}S$ values of these waters are indicative of no to little interaction with isotopically heavier gypsum or anhydrite, which are present only beneath the upper deeply rooted, acid-sulfate alteration zones. These data combined with preliminary tritium studies (Bove and others, 2000; Wirt and others, 2001) suggest that these waters mostly represent recent, shallow-level recharge.

Eureka Graben Area

The Eureka Graben area (fig. 1) is characterized by polymetallic veins that formed along structures related to resurgence of the San Juan–Uncompahgre calderas. Many of the most economically important vein deposits within the study area are present here, such as the Sunnyside mine, historically one of the largest gold mines in the United States, having produced more than 800,000 ounces of gold and 14 million ounces of silver. Typical ores of the Sunnyside and related veins also contained as much as 2–3 percent lead and zinc, and as much as 0.3 percent copper. Similar veins in the Eureka Gulch, Treasure Mountain, and Placer Gulch areas, like the Sunnyside, were highly endowed in late-stage manganese ores, with weighted averages of 6 percent manganese over a 3-m wide vein. As shown in figure 19, manganese concentrations are highest near the Sunnyside-Mastodon vein systems and diminish variably in all directions away from this center.

As much as 75 percent of the rocks within the Eureka Graben area is propylitically altered. In contrast, QSP and WSP-altered areas make up only about 20 percent of the area. Vein-related QSP zones, which extend at most to two times the vein width, approximate nearly 5 percent of the area. The low pyrite abundance and high acid-neutralizing potential of these propylitic-dominant rocks explains the distribution of mostly higher pH in streams draining this area (Wright, Simon, and others, this volume, Chapter E10, fig. 10). However, the influence of mineralized veins on these propylitic waters is observed in a number of stream and spring samples. Vein-related background waters draining propylitic-dominant rocks (PROP-V, fig. 11) have a mean pH of 6.52 and measurable alkalinity but show markedly elevated zinc and a wide range in manganese concentrations. Water-quality data (table 8, this report; Kimball and others, this volume) suggest that Eureka graben background waters interacting with QSP-altered rock and large mineralized veins along their flow path produce low-pH and highly metal rich waters. Three such springs (V-QSP, fig. 11) discharging near the base of large QSP-altered zones in California Gulch, Houghton Mountain, and South Fork Eureka Gulch (fig. 17) have pH values <4.55 and concentrations of greater than 640 µg/L zinc (14,400 µg/L maximum) and 2,670 µg/L manganese (74,700 µg/L maximum) (table 8).

One of the more important questions regarding derivation of these low-pH and metal-rich waters is the initial water composition prior to reaction along their flow path with unexploited vein minerals. Because no water draining QSP-dominant rock was sampled in this area, we can only speculate that initial compositions may be analogous to QSP waters in the Mount Moly, Red Mountains, and OPAM areas (pH from 3.2 to 4.0 and zinc ranging from 100 to 300 µg/L) (table 5). Although these initial QSP waters were probably low in metals, their high acidity undoubtedly played an important role in promoting metal dissolution from the mineralized veins.

Mine discharge from the Eureka Graben area had the highest manganese concentrations (8,100 µg/L mean) of the five mineralized areas, reflecting the high percentage of manganese gangue minerals within these veins (fig. 19). These manganese-rich waters also ranked among the highest of the five areas in mean copper (633 µg/L), zinc (9,570 µg/L), and lead (170 µg/L) concentrations; however, due to the absence of enargite ores, arsenic concentrations were low (1 µg/L).

South Silverton Area

Ore deposits of the South Silverton area (fig. 1) mostly occur as low-grade and base-metal rich veins that filled simple fissures averaging 1–5 m in width. Veins were localized along two principal fracture systems (fig. 21). The first group, the "western shear system," includes a complex of mineralized northwest- and northerly-trending fractures that may be the southern continuation of a mineralized, northwest fracture zone west of the Red Mountains area (Yager and Bove, this volume, pl. 1). The second major group of fractures, or the "eastern shear system," is characterized by northwest-trending shear fractures and a set of "radial" fractures that trend normal to the margins of the Silverton and San Juan calderas. A vertical zoning from galena to silver-bearing tetrahedrite and gold-rich chalcopyrite with depth was recognized in some veins of the western shear system. Anglesite was abundant in the highest levels of the Shenandoah-Dives vein system and represents oxidation of ore above the upper limits of Pleistocene glacial downcutting. Several deposits of the eastern shear system contain both vein and carbonate replacement ores. The replacement deposits are present exclusively where large caldera-collapse blocks of Paleozoic-age carbonate rocks were intersected by metal-bearing veins. The replacement ore assemblage is very similar in bulk composition to the vein ores. Areas of hydrothermally altered rock are mostly confined to narrow zones surrounding the veins; more than 90 percent of the South Silverton area is characterized by regional propylitically altered rock.

Eleven of twelve mine discharge samples in the South Silverton area had relatively high pH and low mean concentrations of aluminum, iron, sulfate, and manganese compared to all other mine samples from the five mineralized areas. Although mean concentrations of lead, copper, and zinc rank among the lowest in the five mineralized areas, these metals were highly elevated in discharge from the Royal Tiger and Iowa mines (fig. 21), located in upper Arrastra Basin. The relatively high lead concentrations are somewhat unusual at the higher pH ranges of these waters. Factors that could contribute to these high dissolved lead concentrations are (1) the presence of oxidized lead ores such as anglesite, which are more soluble than lead sulfides at these higher pH ranges (Nordstrom and Alpers, 1999), (2) mixtures of metal-rich acidic waters and circumneutral waters within the mine, which had not reached equilibrium at the sample site, and (3) lack of iron oxyhydroxides due to low dissolved iron concentrations, which limits sorption effects and results in higher dissolved metal concentrations (Smith, 1999). The low alkalinity of the Royal Tiger and Iowa mine waters (<6 mg/L) suggests that metal complexing with carbonate anions was not a factor in the high dissolved lead concentrations.

The paucity of low-pH mine waters (table 5) distinguishes the South Silverton area from the other four areas in this report. The higher pH is probably controlled by an abundance of calcite in wallrock and vein-related gangue material. Greater than 90 percent of the rocks in this mineralized area have been affected by calcite-rich propylitic alteration, whereas pervasive zones of pyritic-bearing rock are relatively minor. As a result, the five propylitic-related water samples from this area have mean pH and alkalinities of 8.15 and 52.7 mg/L, respectively, and zinc concentrations less than 30 µg/L. Despite the high metal concentrations of some of these mine waters, mixing with high-pH background waters results in relatively high pH and low dissolved metal concentrations at the mouths of all mainstem streams that drain the South Silverton area (pH 7.51 to 8.1; zinc 10 to 300 µg/L) (Unpub. report to Colorado Water Quality Commission, ARSG, 2001; Wright, Simon, and others, this volume, fig. 10).

Acid-Neutralizing Potential (ANP) of Minerals and Relationship to Alteration Assemblages

All five mineralized areas discussed in this report were affected by a chlorite- and calcite-rich regional propylitic alteration assemblage that formed 5-15 million years prior to the major episodes of mineralization in the area. Propylitically altered rocks make up about 90 percent of the entire study area. As shown in a petrographic study of 16 regional propylitic samples (table 1), calcite content is highly variable, ranging from 0 to more than 20 volume percent of the rock (mean of 2 volume percent), whereas chlorite, with a minimum content of 7 volume percent, is much more homogeneously distributed (mean of 21 volume percent). Non-mining-affected streams and springs weathering propylitically altered rocks are characterized by generally good water quality with moderate to high pH values, measurable alkalinity, and low dissolved metal concentrations. These higher pH and metal-deficient waters are particularly prevalent in the Eureka Graben and South Silverton areas (fig. 1), which are underlain by about 70 and 90 percent propylitically altered rock, respectively. However, probably of greater importance—in contrast to the Mount Moly, Red Mountains, and OPAM areas—these two areas lack expanses of pervasively altered and highly pyritic rock that naturally weathers to produce low-pH water with high iron, aluminum, sulfate, and low to moderate metal concentrations (fig. 11).

Although calcite is well recognized for its strong acid-neutralizing potential (ANP) (Jambor and others, 2000), empirical data on chlinochlore—the dominant chlorite phase in the study area—suggests that it also has low to moderate acid-neutralizing potential when reacted with acidic solutions (Lawrence and Wang, 1997; Jambor and others, 2000). However, extrapolating these experimental results to the wide pH range of natural waters in the study area appears problematic. Despite the abundance of chlorite in regional propylitic and weak sericite-pyrite altered rocks (WSP), background water in the study area with pH higher than about 4.5 (for example WSP and PROP waters, table 8) has very low magnesium concentrations (fig. 22); higher magnesium concentrations would be expected if chlorite weathering was more prominent. These data along with inverse geochemical modeling studies (Bove and others, 2000; Mast and others, this volume) demonstrate that acid neutralization in these waters is mostly controlled by calcite, due to its abundance and high rates of dissolution; in contrast, the ANP role of chlorite in these higher pH ranges is limited because of its low kinetic rates of dissolution.

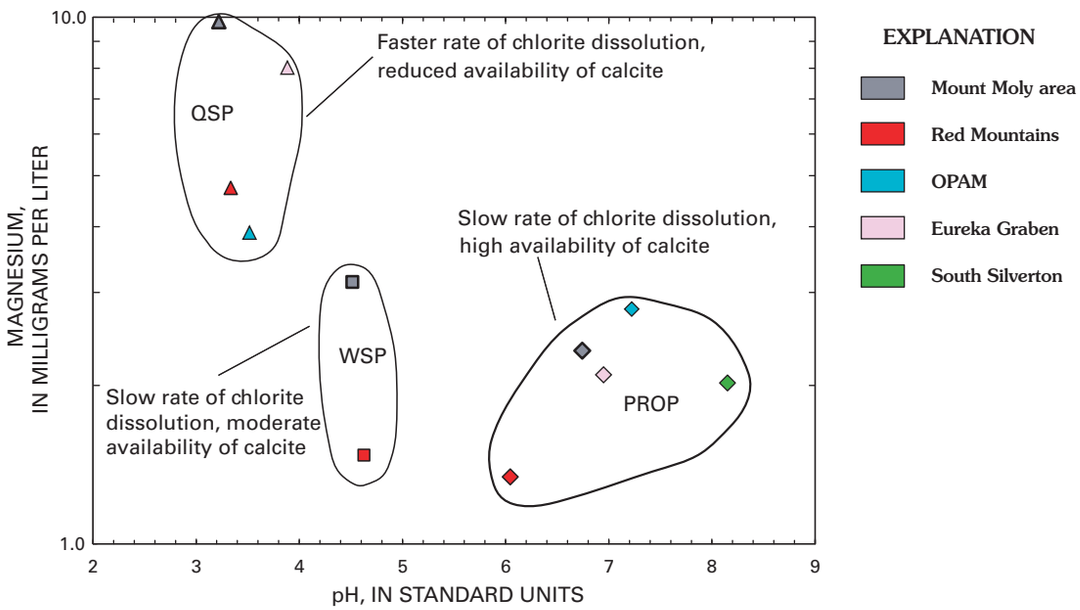

Figure 22. Mean values of dissolved magnesium versus pH from quartz-sericite-pyrite (QSP), weak sericite-pyrite (WSP), and propylitic (PROP) background waters from the five mineralized areas.

However, the degree of chlorite breakdown appears to increase during interaction with more acidic background waters (QSP waters, fig. 22), which confirms laboratory leach experiments (Lawrence and Wang, 1997; Jambor and others, 2000) documenting accelerated rates of chlorite dissolution in highly acidic solutions (pH <3.5). Although experimental data predict that chlorite dissolution in low-pH water has some potential to neutralize acidity (Lawrence and Wang, 1997; Jambor and others, 2000), the low pH of the QSP waters suggests that the degree of chlorite breakdown has done little to neutralize all the acid generated by pyrite oxidation. Although chlorite is commonly present in "islands" within and adjacent to these larger QSP alteration zones, calcite is generally absent and thus affords little to no ANP. The paucity of calcite in QSP-altered rocks is attributed to the low pH of the ancient hydrothermal fluids that formed this mineral assemblage (Rose and Burt, 1979; Ringrose, 1982).

Selected References

Bartos, P.J., 1993, Comparison of gold-rich and gold-poor quartz-base metal veins, western San Juan Mountains, Colorado—The Mineral Point area as an example: Society of Economic Geologists Newsletter, no. 15, 11 p.

Belser, Carl, 1956, Tungsten potential in the San Juan County area, Ouray, San Juan, and San Miguel Counties, Colorado: Bureau of Mines Information Circular, v. 7731, 18 p.

Bookstrom, A.A., 1989, The Climax-Alma granite batholith of Oligocene age and the porphyry molybdenum deposits of Climax, Colorado, U.S.A.: Engineering Geology, v. 27, p. 543–568.

Bove, D.J., Eberl, D.D., and McCarty, D.K., 2002, Characterization and modeling of illite crystal particles and growth mechanisms in a zoned hydrothermal deposit, Lake City, Colorado: American Mineralogist, v. 87, p. 1546–1556.

Bove, D.J., and Hon, Ken, 1992, Geology and alteration map and drill-core logs of the Red Mountain area, near Lake City, Hinsdale County, Colorado: U.S. Geological Survey Miscellaneous Investigations Map I–2286.

Bove, D.J., Hon, Ken, Budding, K.E., Slack, J.F., Snee, L.W., and Yeoman, R.A., 2001, Geochronology and geology of late Oligocene through Miocene volcanism and mineralization in the western San Juan Mountains, Colorado: U.S. Geological Survey Professional Paper 1642, 30 p.

Bove, D.J., and Knepper, D.H., Jr., 2000, Surface water data and geographic relation to Tertiary age intrusions and hydrothermal alteration in the Grand Mesa, Uncompahgre, and Gunnison National Forests (GMUG) and intervening Bureau of Land Management (BLM) lands, 2000: U.S. Geological Survey Open-File Report 99–347. URL http://pubs.usgs.gov/of/2000/ofr-00-0271/

Bove, D.J., Mast, M.A., Wright, W.G., Verplanck, P.L., Meeker, G.P., and Yager, D.B., 2000, Geologic control on acidic and metal-rich waters in the southeast Red Mountains area, near Silverton, Colorado, *in* ICARD 2000; Proceedings of the Fifth International Conference on Acid Rock Drainage, Volume 1: Society for Mining, Metallurgy, and Exploration, Inc., p. 523–535.

Bove, D.J., Rye, R.O., and Hon, Ken, 1990, Evolution of the Red Mountain alunite deposit: U.S. Geological Survey Open-File Report 90–0235, 30 p.

Bove, D.J., Wilson, A.B., Barry, T.H., Hon, K., Kurtz, J., Van Loenen, R.E., and Calkin, W.S., 1996, Geology, alteration, and rock and water chemistry of the Iron, Alum, and Bitter Creek areas, Upper Alamosa River, southwestern Colorado. U.S. Geological Survey Open-File Report 96–039, 34 p.

Bove, D.J., Wright, W.G., Mast, M.A., and Yager, D.B., 1998, Natural contributions of acidity and metals to surface waters of the upper Animas River watershed, Colorado, *in* von Guerard, P., and Nimick, D.A., eds., Science for watershed decisions on Abandoned Mine Lands; Review of Preliminary Results, Denver, Colorado: U.S. Geological Survey Open-File Report 98–0297.

Briggs, P.H., 1996, Forty elements by inductively coupled plasma-atomic emission spectrometry, *in* Arbogast, B.F., ed., Analytical methods manual for the Mineral Resource Surveys Program: U.S. Geological Survey Open-File Report 96–525, p. 77–94.

Burbank, W.S., 1933, Vein systems of the Arrastra Basin and regional geologic structure in the Silverton and Telluride quadrangles, Colorado: Proceedings of the Colorado Scientific Society, v. 13, p. 135–214.

Burbank, W.S., and Luedke, R.G., 1964, Geology of the Ironton quadrangle, Colorado: U.S. Geological Survey Quadrangle Map GQ–291, scale 1:24,000.

Burbank, W.S., and Luedke, R.G., 1969, Geology and ore deposits of the Eureka and adjoining districts San Juan Mountains, Colorado: U.S. Geological Survey Professional Paper 535, 73 p.

Casadevall, Thomas, and Ohmoto, Hiroshi, 1977, Sunnyside mine, Eureka mining district, San Juan County, Colorado; Geochemistry of gold and silver base metal deposition in a volcanic environment: Economic Geology, v. 72, p. 1285–1320.

Cunningham, C.G., Rye, R.O., Rockwell, B.W., Kunk, M.J., and Councell, T.B., 2005, Supergene destruction of a hydrothermal replacement alunite deposit at Big Rock Candy Mountain, Utah—Mineralogy, spectroscopic remote sensing, stable isotope and argon age evidences: Chemical Geology, v. 215, p. 317–337.

Dalton, J.B., King, T.V., Bove, D.J., Kokaly, R.F., Clark, R.N., Vance, J.S., and Swayze, G.A., 2000, Distribution of acid-generating and acid-buffering minerals in the Animas River watershed as determined by AVIRIS spectroscopy, *in* ICARD 2000; Proceedings of the Fifth International Conference on Acid Rock Drainage, Volume 2: Society for Mining, Metallurgy, and Exploration, Inc., p. 1541–1550.

Desborough, G.A., Briggs, P.H., Mazza, Nilah, and Driscoll, Rhonda, 1998, Acid-neutralization potential of minerals in intrusive rocks of the Boulder batholith in northern Jefferson County, Montana: U.S. Geological Survey Open-File Report 98–364, 21 p.

Desborough, G.A., Leinz, R.W., Smith, K.S., Hageman, P.L., Fey, D.L., and Nash, J.T., 1999, Acid generation and metal mobility of some metal-mining related wastes in Colorado: U.S. Geological Survey Open-File Report 99–322, 19 p.

Desborough, G.A., and Yager, D.B., 2000, Acid-neutralizing potential of minerals in intrusive bedrocks in the Animas River headwaters, San Juan County, Colorado: U.S. Geological Survey Open-File Report 00–0165, 14 p.

Eberl, D.D., Drits, V., Srodon, J., and Nüesch, R., 1996, MudMaster—A program for calculating crystallite size distributions and strain from the shapes of X-ray diffraction peaks: U.S. Geological Survey Open-File Report 96–171, 46 p.

Eberl, D.D., Nüesch, R., Sucha, V., and Tsipursky, S., 1998, Measurement of fundamental illite particle thickness by X-ray diffraction using PVP-10 intercalation: Clays and Clay Minerals, v. 46, p. 89–97.

Eberl, D.D., Srodon, J., Lee, M., Nadeau, P.H., and Northrup, H.R., 1987, Sericite from the Silverton caldera, Colorado—Correlation among structure, composition, origin, and particle thickness: American Mineralogist, v. 72, p. 914–934.

Fey, D.L., Nash, J.T., Yager, D.B., and Desborough, G.A., 2000, Analytical results for mine dump samples and leachate solutions, upper Animas River watershed, San Juan County, Colorado: U.S. Geological Survey Open-File Report 00–0338, 16 p.

Fisher, F.S., and Leedy, W.P., 1973, Geochemical characteristics of mineralized breccia pipes in the Red Mountain district, San Juan Mountains, Colorado: U.S. Geological Survey Bulletin 1381, 43 p.

Fournier, R.O., 1999, Hydrothermal processes related to movement of fluid from plastic into brittle rock in the magmatic environment: Economic Geology and the Society of Economic Geologists, v. 18, p. 486–497.

Giggenbach, W.F., 1997, The origin and evolution of fluids in magmatic-hydrothermal systems, *in* Barnes, H.L., ed., Geochemistry of hydrothermal ore deposits: New York, Wiley, p. 737–789.

Gilzean, M.N., 1984, Nature of a deep hydrothermal system, Red Mountain district, Colorado: Berkeley, Calif., University of California M.Sc. thesis, 104 p.

Goldstein, J.I., Newbury, D.E., Echlin, P., Joy, D.C., Romig, A.D., Jr., Lyman, C.E., Fiori, C., and Lifshin, E., 1992, Scanning electron microscopy and X-ray microanalysis: New York, Plenum Press, 820 p.

Grauch, V.J.S., 1987, Interpretive aeromagnetic map using the horizontal gradient—Lake City caldera area, San Juan Mountains, Colorado: U.S. Geological Survey Geophysical Investigations Map GP–974.

Gray, J.E., and Coolbaugh, M.F., 1994, Geology and geochemistry of Summitville, Colorado—An epithermal acid-sulfate deposit in a volcanic dome: Economic Geology, v. 89, p. 1906–1923.

Hardwick, J.F., 1984, Epithermal vein and carbonate replacement mineralization related to caldera development, Cunningham Gulch, Silverton, Colorado: Austin, Tex., University of Texas M.S. thesis, 130 p.

Hildreth, Wes, 1979, The Bishop Tuff—Evidence for the origin of compositional zonation in silicic magma chambers, *in* Chapin, C.E., and Elston, W.E., eds., Ash flow tuffs: Geological Society of America Special Paper 180, p. 43–75.

Hillebrand, J.R., and Kelley, V.C., 1959, Mines and ore deposits from Red Mountain Pass to Ouray, Ouray County, Colorado, *in* New Mexico Geological Society Guidebook, 8th Annual Field Conference, Southwestern San Juan Mountains, Colorado, 1959: p. 188–199.

Hurlburt, E.B., 1894, On alunite from Red Mountain, Ouray County, Colorado: American Journal of Science, v. 48, p. 130–131.

Hon, Ken, 1986, Emplacement and cooling zonation of the intracaldera Sunshine Peak Tuff, Lake City caldera, Colorado, U.S.A.: International Volcanological Congress Abstracts, New Zealand, February 1986, p. 48.

Hon, Ken, 1987a, Geologic, alteration, and vein maps of the Redcloud Peak (Lake City caldera) and Handies Peak Wilderness Study Areas, Hinsdale County, Colorado: U.S. Geological Survey Miscellaneous Field Studies Map MF–1949.

Hon, Ken, 1987b, Geologic and petrologic evolution of the Lake City caldera, San Juan Mountains, Colorado: Boulder, Colo., University of Colorado Ph. D. thesis, 244 p.

Hon, Ken, Bove, D.J., and Grauch, V.J.S., 1986, Geology and mineral deposits of the region surrounding the American Flats Wilderness Study Area, western San Juan Mountains, Colorado: U.S. Geological Survey Open-File Report 86–431, 36 p.

Hon, Ken, and Lipman, P.W., 1989, Oligocene-Miocene San Juan volcanic field, Colorado: New Mexico Bureau of Mines and Mineral Resources Memoir, v. 46, p. 303–380.

Jambor, J.L., Dutrizac, J.E., and Chen, T.T., 2000, Contribution of specific minerals to the neutralization potential in static tests, *in* ICARD 2000; Proceedings of the Fifth International Conference on Acid Rock Drainage, Volume 1: Society for Mining, Metallurgy, and Exploration, Inc., p. 551–565.

Johnston, D.A., and Naeser, C.W., 1976, Timing and duration of episodes of andesitic volcanism, northwestern San Juan Mountains, Colorado: Geological Society of America Abstracts with Programs, v. 8, p. 593–594.

Kelley, V.C., 1946, Geology, ore deposits, and mines of the Mineral Point, Poughkeepsie, and Upper Uncompahgre districts, Ouray, San Juan, and Hinsdale Counties, Colorado: Colorado Scientific Society Proceedings, v. 14, no. 7, p. 289–466.

Kirkham, R., Lovekin, J.R., and Sares, M.A., 1995, Sources of acidity and heavy metals in the Alamosa River Basin outside of the Summitville mining area, Colorado, *in* Posey, H.H., Pendleton, J.A., and Van Zyl, D., eds., Proceedings—Summitville Forum '95: Colorado Geological Survey Special Publication 38, p. 42–56.

Koch, B.C., 1990, Origin of the Gold King–Davis epithermal gold lode, Silverton caldera, Colorado: Golden, Colo., Colorado School of Mines Ph. D. thesis, 291 p.

Krouse, H.R., Gould, W.D., McCready, R.L., and Rajan, S., 1991, ^{18}O incorporation into sulphate during the bacterial oxidation of sulfide minerals and the potential for oxygen isotope exchange between O_2, H_2O and oxidized sulphur intermediates: Earth and Planetary Science Letters, v. 107, p. 90–94.

Lamothe, P.J., Meier, A.L., and Wilson, Steve, 1999, The determination of forty-four elements in aqueous samples by inductively coupled plasma–mass spectrometry: U.S. Geological Survey Open-File Report OF–99–0151, 14 p.

Langston, D.A., 1978, The geology and geochemistry of the northeasterly gold veins, Sunnyside mine, San Juan County, Colorado: Golden, Colo., Colorado School of Mines Ph. D. thesis, 163 p.

Lawrence, R.W., and Wang, Y., 1997, Determination of neutralization potential in the prediction of acid rock drainage, *in* Proceedings Fourth International Conference on Acid Rock Drainage, MEND: Natural Resources Canada, Ottawa, v. 1, p. 451–464.

Lipman, P.W., 1984, The roots of ash flow calderas in western North America; Windows into the tops of granitic batholiths, *in* Lipman, P.W., Self, S.S., and Heiken, G., eds., Introduction to calderas special issue: Journal of Geophysical Research, v. 89, p. 8801–8841.

Lipman, P.W., Bethke, P.M., Casadevall, T.J., and Steven, T.A., 1982, Relationship of mineralization to volcanic eruption of the San Juan Mountains, Colorado: Society of Economic Geologists Field Trip Guide, San Juan Mountains Field Conference, Sept. 19–24, 1982, 53 p.

Lipman, P.W., Doe, B.R., Hedge, C.E., and Steven, T.A., 1978, Petrologic evolution of the San Juan volcanic field, southwestern Colorado; Pb and Sr isotope evidence: Geological Society of America Bulletin, v. 89, p. 59–82.

Lipman, P.W., Fisher, F.S., Mehnert, H.H., Naeser, C.W., Luedke, R.G., and Steven, T.A., 1976, Multiple ages of mid-Tertiary mineralization and alteration in the western San Juan Mountains, Colorado: Economic Geology, v. 71, p. 571–588.

Lipman, P.W., Steven, T.A., Luedke, R.G., and Burbank, W.S., 1973, Revised volcanic history of the San Juan, Uncompahgre, Silverton, and Lake City calderas in the western San Juan Mountains, Colorado: U.S. Geological Survey Journal of Research, v. 1, p. 627–642.

Lipman, P.W., Steven, T.A., and Mehnert, H.H., 1970, Volcanic history of the San Juan Mountains, Colorado, as indicated by potassium-argon dating: Geological Society of America Bulletin, v. 81, p. 2329–2352.

Ludington, Steve, 1981, The Redskin Granite; Evidence for thermogravitational diffusion in a Precambrian granite batholith: Journal of Geophysical Research, v. 86, p. 10423–10430.

Luedke, R.G., and Burbank, W.S., 1989, Geologic map of the Handies Peak quadrangle, San Juan, Hinsdale, and Ouray Counties, Colorado: U.S. Geological Survey Quadrangle Map GQ–1595.

Luedke, R.G., and Burbank, W.S., 2000, Geologic maps of the Silverton and Howardsville quadrangles, San Juan, Hinsdale, and Ouray Counties, Colorado: U.S. Geological Survey Miscellaneous Investigations Series Map I–2681, scale 1:24,000.

Mast, M.A., Evans, J.B., Leib, K.J., and Wright, W.G., 2000, Hydrologic and water-quality data at selected sites in the upper Animas River watershed, southwestern Colorado, 1997–1999: U.S. Geological Survey Open-File Report 00–53, 20 p.

Mast, M.A., Verplanck, P.L., Yager, D.B., Wright, W.G., and Bove, D.J., 2000, Natural sources of metals to surface waters in the upper Animas River watershed, *in* ICARD 2000; Proceedings of the Fifth International Conference on Acid Rock Drainage, Volume 1: Society for Mining, Metallurgy, and Exploration, Inc., p. 513–522.

McCusker, R.T., 1982, Mount Moly progress report, 1979–1980, Drill holes 1-6: Amax Exploration, Inc. report, 24 p.

McCusker, R.T., 1983, Precious metal evaluation of the Mount Moly prospect, San Juan County, Colorado: Amax Exploration, Inc. report, 23 p.

Miller, W.R., 1999, Geochemical baselines and maps showing acid-neutralizing capacity and potential release of total dissolved solids of stream and spring waters from different rock compositional types from mountainous watersheds in the Gunnison, Uncompahgre, and Grand Mesa National Forest, Colorado: U.S. Geological Survey Open-File Report 99–0580, 107 p.

Miller, W.R., and McHugh, J.B., 1994, Natural acid drainage from altered areas within and adjacent to the upper Alamosa River basin, Colorado: U.S. Geological Survey Open-File Report 94–0144, 47 p.

Moore, D.M., and Reynolds, R.C., Jr., 1989, X-ray diffraction and the identification of clay minerals: New York, Oxford, 322 p.

Nash, J.T., 1975, Fluid-inclusion study of vein, breccia pipe, and replacement ores, northwestern San Juan Mountains, Colorado: Economic Geology, v. 70, p. 1038–1040.

Neubert, J.T., 2000, Naturally degraded surface waters associated with hydrothermally altered terrane in Colorado: Colorado Geological Survey Open-File Report 00–16, CDROM publication.

Nordstrom, D.K., and Alpers, C.N., 1999, Geochemistry of acid mine waters, *in* Plumlee, G.S., and Logsdon, M.J., eds., The environmental geochemistry of mineral deposits—Part B, Case studies and research topics: Society of Economic Geologists, Reviews in Economic Geology, v. 6B, p. 133–160.

Nordstrom, D.K., and Ball, J.W., 1986, The geochemical behavior of aluminum in acidified surface waters: Science, v. 232, p. 54–56.

Pallister, J.S., Hoblitt, R.P., and Reyes, A.G., 1992, A basalt trigger for the 1991 eruptions of Pinatubo volcano: Nature, v. 356, p. 426–428.

Plumlee, G.S., 1999, The environmental geology of mineral deposits, *in* Plumlee, G.S., and Logsdon, M.J., eds., The environmental geochemistry of mineral deposits—Part A, Processes, techniques, and health issues: Society of Economic Geologists, Reviews in Economic Geology, v. 6A, p. 71–116.

Plumlee, G.S., and Logsdon, M.J., 1999, An earth-system science toolkit for environmentally friendly mineral resource development, *in* Plumlee, G.S., and Logsdon, M.J., eds., The environmental geochemistry of mineral deposits—Part A, Processes, techniques, and health issues: Society of Economic Geologists, Reviews in Economic Geology, v. 6A, p. 1–27.

Plumlee, G.S., Smith, K.S., Montour, M.R., Ficklin, W.H., and Mosier, E.L., 1999, Geologic controls on the composition of natural waters and mine waters draining diverse mineral-deposit types, *in* Filipek, L.H., and Plumlee, G.S., eds., The environmental geochemistry of mineral deposits—Part B, Case studies and research topics: Society of Economic Geologists, Reviews in Economic Geology, v. 6B, p. 373–432.

Ransome, F.L., 1901, A report on the economic geology of the Silverton quadrangle, Colorado: U.S. Geological Survey Bulletin 182, 265 p.

Ringrose, C.R., 1982, Geology, geochemistry, and stable isotope studies of a porphyry-style hydrothermal system west Silverton district, San Juan Mountains, Colorado: Aberdeen, Scotland, University of Aberdeen Doctoral dissertation, 257 p.

Ringrose, C.R., Harmon, R.S., Jackson, S.E., and Rice, C.M., 1986, Stable isotope geochemistry of a porphyry-style hydrothermal system, West Silverton District, San Juan Mountains, Colorado, U.S.A.: Applied Geochemistry, v. 1, p. 357–373.

Rose, A.W., and Burt, D.M., 1979, Hydrothermal alteration, *in* Barnes, H.L., ed., Geochemistry of hydrothermal ore deposits, Second Edition: New York, John Wiley, 798 p.

Rye, R.O., Bethke, P.M., and Wasserman, M.D., 1992, The stable isotope geochemistry of acid sulfate alteration: Economic Geology, v. 87, p. 225–262.

Schwarz, T.E., 1883, Remarks on occurrences of ore in mines near Silverton: Colorado Scientific Society Proceedings, v. 1, p. 134–144.

Slack, J.F., 1976, Hypogene zoning and multistage vein mineralization in the Lake City area, western San Juan Mountains, Colorado: Stanford, Calif., Stanford University Ph. D. thesis, 327 p.

Smith, K.S., 1999, Metal sorption on mineral surfaces, *in* Filipek, L.H., and Plumlee, G.S., eds., The environmental geochemistry of mineral deposits—Part B, Case studies and research topics: Society of Economic Geologists, Reviews in Economic Geology, v. 6B, p. 161–176.

Smith, K.S., and Huyck, Holly, 1999, An overview of the abundance, relative mobility, bioavailability, and human toxicity of metals, *in* Filipek, L.H., and Plumlee, G.S., eds., The environmental geochemistry of mineral deposits—Part B, Case studies and research topics: Society of Economic Geologists, Reviews in Economic Geology, v. 6B, p. 29–64.

Srodon, J., and Eberl, D.D., 1984, Illite, *in* Bailey, S.W., ed., Micas: Mineralogical Society of America, Reviews in Mineralogy, v. 13, p. 495–544.

Standen, A.R., and Kyle, J.R., 1985, Geologic characteristics of the Scotia-Vanderbilt vein, Silverton, Colorado; implications for epithermal precious metal exploration in volcanic settings, *in* Park, W.C., Hausen, D.M., and Hagni, R.D., eds., Applied mineralogy: The Second International Congress on Applied Mineralogy in the Minerals Industry, Los Angeles, Calif., Feb. 22–25, 1984, p. 1051–1063.

Steven, T.A., Hon, Ken, and Lanphere, M.A., 1999, Neogene geomorphic evolution of the central San Juan Mountains near Creede, Colorado: U.S. Geological Survey Miscellaneous Investigations Series Map I–2504, scale 1:100,000.

Steven, T.A., and Lipman, P.W., 1976, Calderas of the San Juan volcanic field, southwestern Colorado: U.S. Geological Survey Professional Paper 958, 35 p.

Steven, T.A., Lipman, P.W., Fisher, F.S., Bieniewski, C.L., Meeves, H.C., Popenoe, Peter, and Luedke, R.G., 1977, Mineral resources of study areas contiguous to the Uncompahgre Primitive Area, San Juan Mountains, southwestern Colorado, with a section on interpretation of aeromagnetic data: U.S. Geological Survey Bulletin 1391–E, 126 p.

Steven, T.A., Luedke, R.G., and Lipman, P.W., 1974, Relation of mineralization to calderas in the San Juan volcanic field, southwestern Colorado: U.S. Geological Survey Journal of Research, v. 2, p. 405–409.

Stoffregen, R.E., 1987, Genesis of acid sulfate alteration and Au-Cu-Ag mineralization at Summitville, Colorado: Economic Geology, v. 82, p. 1575–1591.

Stoffregen, R.E., and Alpers, C.N., 1987, Svanbergite and woodhouseite in hydrothermal ore deposits—Implications for apatite destruction during advanced argillic alteration: Canadian Mineralogist, v. 25, p. 201–212.

Stoffregen, R.E., Rye, R.O., and Wasserman, M.D., 1994, Experimental studies of alunite—I, 18O-16O and D-H fractionation factors between alunite and water at 250°–450°C: Geochimica et Cosmochimica Acta, v. 58, p. 903–916.

Taylor, H.P., 1997, Oxygen and hydrogen stable isotope relationships in hydrothermal mineral deposits, *in* Barnes, H.L., ed., Geochemistry of hydrothermal ore deposits: New York, Wiley, p. 229–300.

Varnes, D.J., 1963, Geology and ore deposits of the south Silverton mining area, San Juan County, Colorado: U.S. Geological Survey Professional Paper 378–A, 56 p.

Waegli, J.A., 1979, Geology and mineralization of the Uncle Sam vein and surrounding area, San Juan County, Colorado: Golden, Colo., Colorado School of Mines M.S. thesis, 127 p.

Wasserman, M.D., Rye, R.O., Bethke, P.M., and Arribas, Antonio, Jr., 1992, Methods for separation and total stable isotope analysis of alunite: U.S. Geological Survey Open-File Report 92–9, 20 p.

White, A.F., and Brantley, S.L., 1995, Chemical weathering rates of silicate minerals, *in* White, A.F., and Brantley, S.L., eds., Reviews in Mineralogy: v. 31, p. 1–22.

White, W.W., Bookstrom, A.A., Kamilli, R.J., Ganster, M.J., Smith, R.P., Ranta, D.E., and Steininger, R.C., 1981, Character and origin of Climax-type molybdenum deposits, *in* Skinner, B.J., ed., Economic Geology, 75th Anniversary Volume: p. 270–316.

Wirt, Laurie, Leib, K.J., Bove, D.J., Mast, M.A., Evans, J.B., and Meeker, G.P., 1999, Determination of chemical constituent loads during base-flow and storm runoff conditions near historical mines in Prospect Gulch, upper Animas River watershed, southwestern Colorado: U.S. Geological Survey Open-File Report 99–159, 39 p.

Wirt, Laurie, Leib, K.J., Bove, D.J., and Melick, R., 2001, Metal loading assessment of point and non-point sources in a small alpine sub-basin characterized by acid drainage—Prospect Gulch, upper Animas River watershed, Colorado: U.S. Geological Survey Open-File Report 01–0258, 36 p.

Young, W.E., 1966, Manganese occurrences in the Eureka–Animas Forks area of the San Juan Mountains, San Juan County, Colorado: U.S. Bureau of Mines Information Circular IC–8303, 51 p.

Zielinski, R.A., Lipman, P.W., and Millard, H.T., 1977, Minor-element abundances in obsidian, perlite, and felsite of calc-alkaline rhyolites: American Mineralogist, v. 62, p. 426–437.